iScience

CellPress
OPEN ACCESS

Article

Light-Driven Metal-Free Direct Deoxygenation of Alcohols under Mild Conditions

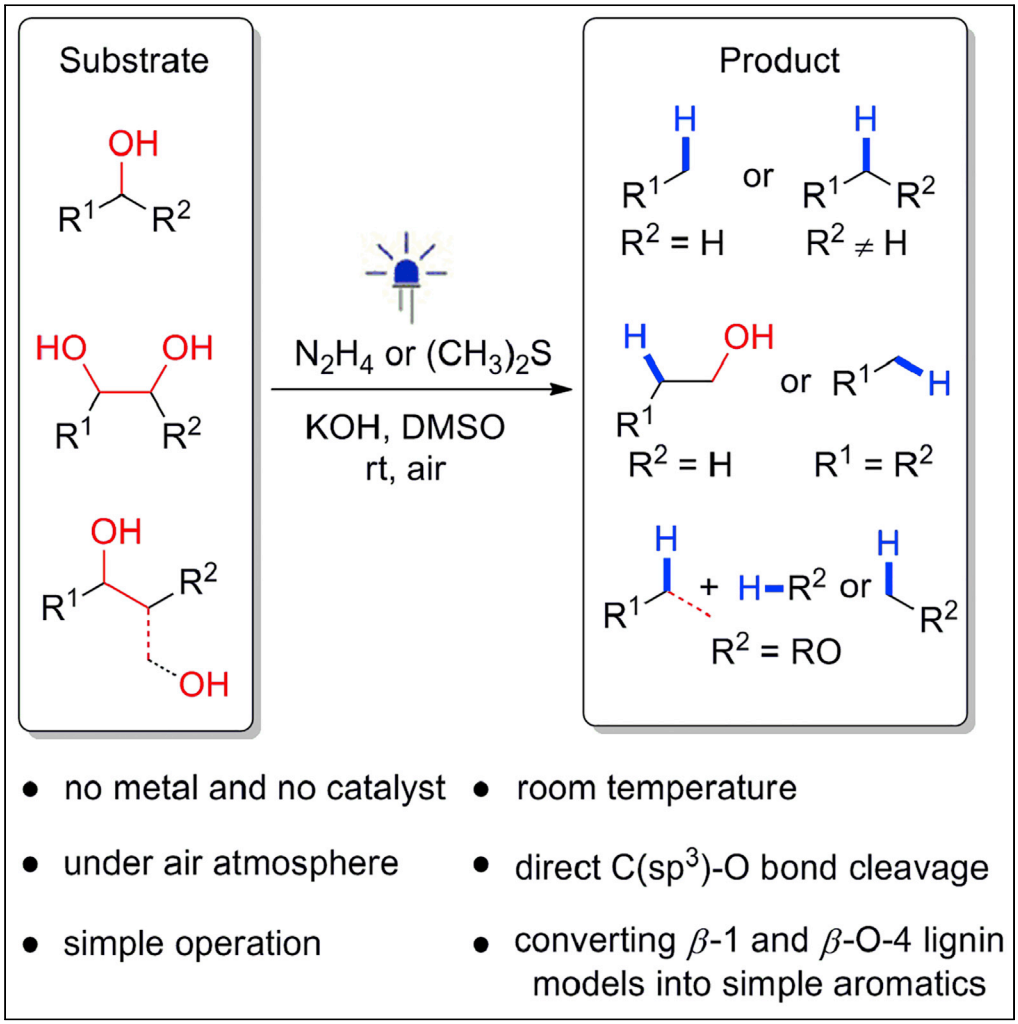

Dawei Cao, Zhangpei Chen, Leiyang Lv, Huiying Zeng, Yong Peng, Chao-Jun Li

cj.li@mcgill.ca

HIGHLIGHTS

Metal-free direct deoxygenation of alcohols enabled by light

Traceless non-toxic N_2 and H_2 as by-products

Broad substrate scope and wide functional group compatibility

Converting lignin models into simple aromatics

Cao et al., iScience *23*, 101419 August 21, 2020
https://doi.org/10.1016/j.isci.2020.101419

iScience

CellPress
OPEN ACCESS

Article

Light-Driven Metal-Free Direct Deoxygenation of Alcohols under Mild Conditions

Dawei Cao,[1,2,3] Zhangpei Chen,[1] Leiyang Lv,[1] Huiying Zeng,[3] Yong Peng,[2] and Chao-Jun Li[1,4,*]

SUMMARY

Hydroxyl is widely found in organic molecules as functional group and its deprivation plays an inevitable role in organic synthesis. However, the direct cleavage of Csp^3-O bond in alcohols with high selectivity and efficiency, especially without the assistance of metal catalyst, has been a formidable challenge because of its strong bond dissociation energy and unfavorable thermodynamics. Herein, an efficient metal-free strategy that enables direct deoxygenation of alcohols has been developed for the first time, with hydrazine as the reductant induced by light. This protocol features mild reaction conditions, excellent functional group tolerance, and abundant and easily available starting materials, rendering selective deoxygenation of a variety of 1° and 2° alcohols, vicinal diols, and β-1 and even β-O-4 models of natural wood lignin. This strategy is also highlighted by its "traceless" and non-toxic by-products N_2 and H_2, as readily escapable gases. Mechanistic studies demonstrated dimethyl sulfide being a key intermediate in this transformation.

INTRODUCTION

In view of the diminishing oil reserves and the ongoing climate change, improving the energy and utilization efficiency of natural resources is a key task to achieve future chemical sustainability (He et al., 2013; Li, 2016). Therefore, direct and selective transformation of naturally abundant functional groups is very important to increase efficiency in organic synthesis (Palacios et al., 2007; Veitch et al., 2007). In particular, the deoxygenation reaction provides an enabling tool for future biorefinery concepts through the cleavage of C-O bonds (Ruppert et al., 2012; Li et al., 2020; Schwob et al., 2019; Volkov et al., 2015; Wang et al., 2018), which allows the conversion of biomass-based readily available alcohols and polyols into platform chemicals and fuels (Bozell and Petersen, 2010; Corma et al., 2007; Dam and Hanefeld, 2011). The common methods for the deoxygenation of alcohols are divided into two categories: indirect and direct C–O bond cleavages. A well-known indirect protocol is the Barton-McCombie deoxygenation procedure, which involves first converting the alcohols into reactive xanthate intermediates that are subsequently reduced easily with stannane (Barton and McCombie, 1975; Crich and Quintero, 1989; Hartwig, 1983; Robins et al., 1983). Later, other active derivatives such as benzoyl ester and phosphite variants are also used in the radical deoxygenation process (Scheme 1, **1a**) (Jordan and Miller, 2012; Lam and Markó, 2008, 2009, 2011; Saito et al., 1986; Zhang and Koreeda, 2004). Another indirect deoxygenation protocol is the ionic process that converts the hydroxyl group into more easily leaving groups, such as OTs, OMs, and halogens (Masamune et al., 1973, 1974; Nguyen et al., 2013) (Scheme 1, **1b**). However, these methods suffered from multistep conversions that resulted in poor step efficiency and atom efficiency. The more desirable direct deoxygenation of aliphatic alcohols is a great challenge owing to the strong C-O bond dissociation energy (332.6–468.6 kJ/mol) (Haynes, 2012).

To overcome these issues, single-step direct deoxygenation strategies for alcohols have been developed, catalyzed by transition metals such as Ti, Pd, Ir, Ru, and Mn (Bauer et al., 2017; Ciszek and Fleischer, 2018; Dai and Li, 2016; Diéguez et al., 2010; Huang et al., 2013; Sawadjoon et al., 2013). (Scheme 1, **2a**) However, the requirement of relatively high temperature (>80°C) and the cost of some precious metal catalysts have greatly limited their broad applicability. Alternatively, Doyle developed a photoredox catalysis strategy that could enable the direct C−O bond cleavage of alcohols at room temperature via the phosphorus radical intermediates (Stache et al., 2018). Nevertheless, it still requires the use of expensive iridium

[1]Department of Chemistry and FRQNT Centre for Green Chemistry and Catalysis, McGill University, 801 Sherbrooke St. West, Montreal, QC H3A 0B8, Canada

[2]Key Laboratory of Magnetism and Magnetic Materials of the Ministry of Education, School of Physical Science and Technology and Electron Microscopy Centre, Lanzhou University, Lanzhou 730000, P. R. China

[3]The State Key Laboratory of Applied Organic Chemistry, Lanzhou University, Lanzhou 730000, P. R. China

[4]Lead Contact

*Correspondence: cj.li@mcgill.ca

https://doi.org/10.1016/j.isci.2020.101419

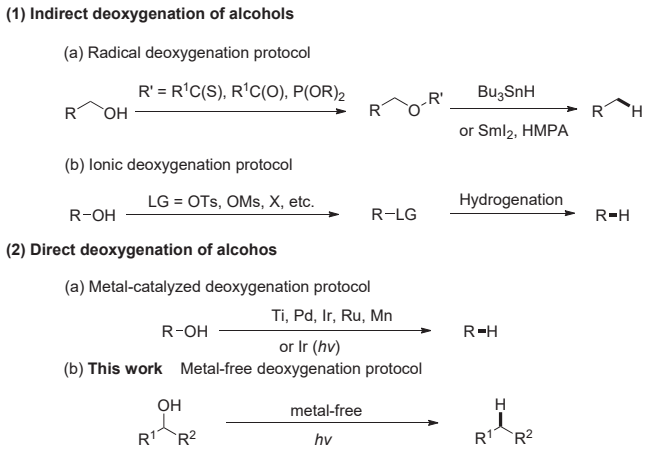

Scheme 1. Strategies for the Deoxygenation of Alcohols

photoredox catalyst in this protocol. Therefore, the development of mild and efficient direct deoxygenation in a single step, especially without using precious metals, is still highly desirable.

Inspired by our previous work on using N_2H_4 as traceless mediator for homo- and cross-aryl couplings (Lv et al., 2018), and as non-metallic hydrogen-atom-transfer (HAT) reductant for pinacol couplings enabled by light (Qiu et al., 2019), we postulate to use N_2H_4 as clean reductant for the direct deoxygenation of alcohols. In this transformation, N_2 and H_2 are generated as gaseous nontoxic by-products, making the deoxygenation process dramatically clean and easy to handle. We herein disclose the first light-driven metal-free direct deoxygenation of alcohols with hydrazine through Csp^3-O bond cleavage (Scheme 1, **2b**).

RESULTS AND DISCUSSION

To validate our hypothesis, the direct deoxygenation of (3,4,5-trimethoxyphenyl)methanol (**1L**) with hydrazine (**2**) was initially carried out under *hv* (254 nm) irradiation with DMSO as solvent and KOH as base under air at room temperature. Gratifyingly, the desired product **3l** was obtained in 63% yield after 24 h (Table 1, entry 1). However, other conditions including blue light emitting diode (LED), compact fluorescent lamps (CFL), or without light showed poor activities for this conversion (Table 1, entries 2–4). Next, a variety of bases, including NaOH, *t*-BuOK, and K_2CO_3, were further evaluated (Table 1, entries 5–7). Disappointingly, the efficiency of this transformation did not improve. The reaction showed poor activity when using other solvents such as MeCN, H_2O, and 1,4-dioxane, which indicated that the solvent played an important role in the reaction (Table 1, entries 8–10). The influence of the amount of hydrazine was also investigated, and 4 equiv. of hydrazine was found to be the best choice (Table 1, entries 11–14). In addition, the effluence of reaction time was also studied (Table 1, entries 15–16). When the reaction time was reduced to 18 h, there was no obvious effect on the reaction, whereas the yield was significantly lower when the time was reduced to 12 h. Finally, only 20% of the product was obtained when the reaction was carried out under argon atmosphere, indicating that the presence of O_2 facilitated this reaction (Table 1, entry 17).

With the optimized reaction conditions in hand, the substrate scope of primary benzyl alcohols was investigated as shown in Table 2. To our delight, different benzyl alcohols with electron-donating or electron-withdrawing groups were successfully deoxygenated to afford the corresponding aromatics (**3a**-**3h**) in moderate to good yields. 4-(Hydroxymethyl)phenol bearing free hydroxyl could also be smoothly deoxygenated to generate the desired product **3d** in 40% yield. The NO_2 group is reduced during the deoxygenation process, as shown for (4-nitrophenyl)methanol, which was converted to (4-aminophenyl)methanol (**3f**) in 55% yield. Primary alcohols bearing multisubstituted phenyl group were also effective in this transformation to provide the products (**3i**-**3m**) in 62%–95% yields. Benzyl alcohols bearing polycyclic (hetero-) aromatic substituents such as indene, dioxole, naphthalene, phenanthrene, benzothiophene, pyridine, and quinolone units could be well tolerated in the reaction (**3n–3u**). Moreover, easy removal of both hydroxyl groups in *o*-dibenzyl alcohol was achieved, leading to 1,2,4-trimethylbenzene (**3v**) in 62% yield when hydrazine was increased to 0.6 mmol. However, benzyl alcohols bearing other electron-withdrawing groups (e.g., 4-CF_3, 4-F, 4-CN) were investigated, showing poor reactivity in this transformation (**3w**-**3y**). Various

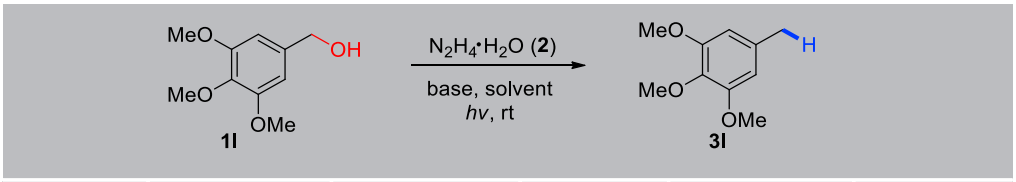

Entry[a]	*hv*	$N_2H_4 \cdot H_2O$	Base	Solvent	3l Yield[b]/%
1	*hv* (254 nm)	2	KOH	DMSO	63
2	Blue LED	2	KOH	DMSO	n.p.
3	CFL	2	KOH	DMSO	n.p.
4	Dark	2	KOH	DMSO	n.p.
5	*hv* (254 nm)	2	NaOH	DMSO	44
6	*hv* (254 nm)	2	t-BuOK	DMSO	48
7	*hv* (254 nm)	2	K_2CO_3	DMSO	Trace
8	*hv* (254 nm)	2	KOH	MeCN	Trace
9	*hv* (254 nm)	2	KOH	H_2O	n.p.
10	*hv* (254 nm)	2	KOH	1,4-dioxane	Trace
11	*hv* (254 nm)	0	KOH	DMSO	8
12	*hv* (254 nm)	1	KOH	DMSO	33
13	*hv* (254 nm)	4	KOH	DMSO	93
14	*hv* (254 nm)	5	KOH	DMSO	92
15[c]	*hv* (254 nm)	4	KOH	DMSO	93(89)
16[d]	*hv* (254 nm)	4	KOH	DMSO	62
17[e]	*hv* (254 nm)	4	KOH	DMSO	20

Table 1. Optimization of the Reaction Conditions

[a]General conditions: **1l** (0.1 mmol), **2** (x equiv.), base (0.2 mmol), and solvent (1 mL) at rt for 24 h under air.

[b]Yields were determined by ^{1}HNMR with 1,3,5-trimethoxybenzene as internal standard and isolated yields in brackets.

[c]18 h.

[d]12 h.

[e]Under Ar.

secondary benzyl alcohols were then examined to expand the generality of this system. 1-Phenylethanol and phenylethanols bearing methoxy at different positions all reacted smoothly with hydrazine to afford the corresponding products (**3z–3ab**). 1-Phenylheptan-1-ol and 1,2-diphenylethanol were also competent substrates, delivering the corresponding products (**3ac**, **3ad**) in excellent yields. Additionally, the deoxygenation of various diaryl alcohols including symmetrical and unsymmetrical substrates proceeded well and gave compounds **3ae–3ag** smoothly. When a bromine-containing substrate was used, the product diphenylmethane (**3ae**) could be obtained by simultaneous cleavages of C–Br and C-O bonds, which was consistent with previous reported results (Cao et al., 2019). The substrates with other aromatic (hetero-) rings such as indene, chroman, and xanthene also tolerated in this reaction to generate the desired products **3ah–3aj**.

The conversion of vicinal diols via C-O cleavage to realize the stoichiometric removal of all (or most) of the oxygen content is greatly significant in organic synthesis because of its prevalence in medicines, agrochemical chemicals, and biomass, especially carbohydrates and lignins. Up to now, a range of reductive deoxygenation methods such as hydrodeoxygenation, hydrogenolysis, decarbonylation, and decarboxylation have been developed (Dethlefsen and Fristrup, 2015). However, these approaches suffer from poor deoxygenation selectivity, resulting in the possibility of forming a mixture of products. To our delight, the

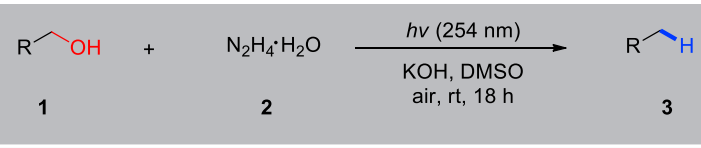

1° alcohols[a]				
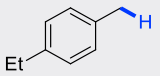	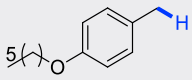	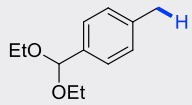	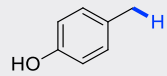	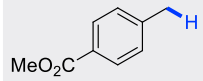
3a 80%[b]	3b 86%	3c 92%	3d 40%[c]	3e 45%, 36 h
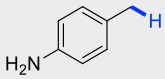	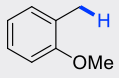	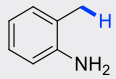	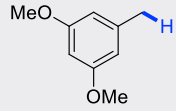	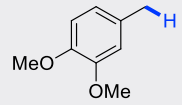
3f 55%[d]	3g 68%	3h 92%	3i 70%	3j 72%
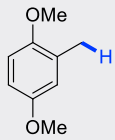	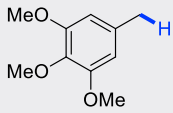	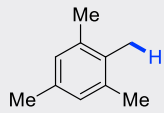	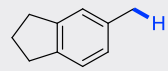	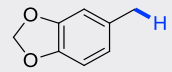
3k 92%	3l 89%	3m 62%	3n 86%	3o 91%
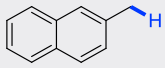	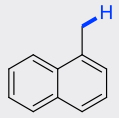	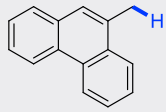	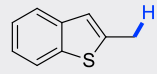	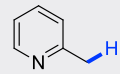
3p 82%	3q 61%	3r 60%	3s 95%	3t 96%[b]
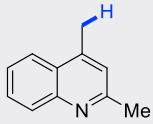	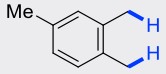	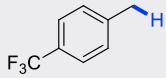	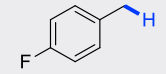	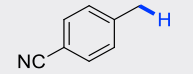
3u 80%	3v 62%, 36 h[e]	3w trace 36 h	3x trace 36 h	3y n.p. 36 h
2° alcohols[a]				
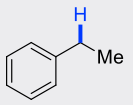	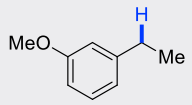	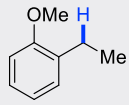	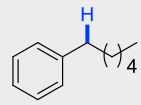	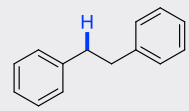
3z 50%, 36 h[b]	3aa 62%, 36 h	3ab 36%, 36 h	3ac 93%, 36 h	3ad 96%, 36 h
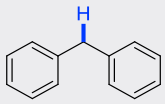	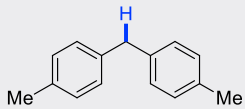	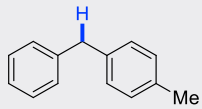	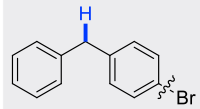	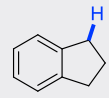
3ae 52%, 36 h	3af 95%, 36 h	3ag 90%, 36 h	3ae 48%, 36 h[f]	3ah 57%, 36 h

Table 2. Substrate Scope of 1° and 2° Alcohols

(Continued on next page)

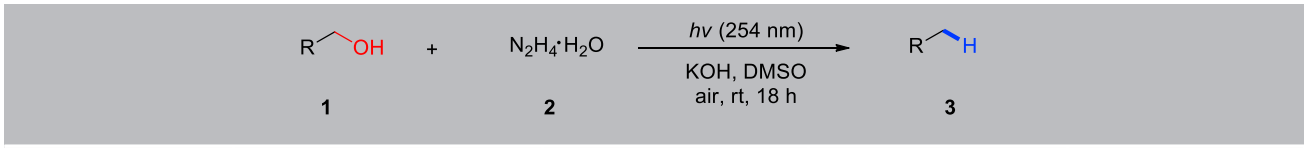

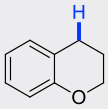	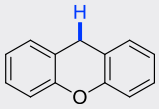			
3ai 89%, 36 h	3aj 62%, 36 h			

Table 2. Continued

[a]General conditions: **1** (0.1 mmol), **2** (0.4 mmol), KOH (0.2 mmol) in DMSO (1 mL) at room temperature for 18 h under air and isolated yield based on **1**.
[b]Yield was determined by GC-MS.
[c]KOH (0.4 mmol).
[d](4-Nitrophenyl)methanol was used as substrate.
[e]**2** (0.6 mmol) and KOH (0.4 mmol) were used.
[f]Debromination product **3ab** was obtained.

selective deoxygenation occurred at the benzyl position to give 2-phenylethanol (Table 3, **3ak**) when 1-phenylethane-1,2-diol was tested. To our surprise, when diaryl pinacols were used as the substrates, the simultaneous C-O and C-C bonds both cleavage products (Table 3, **3al**, **3am**, **3ae**) were obtained in good to high yields under the current catalytic system.

The conversion of bio-renewable lignin into sustainable aromatic compounds has attracted widespread attention owing to its natural abundance and the rapid reduction of non-renewable fossil resources (Ragauskas et al., 2014; Singh et al., 2015; Verma et al., 2016; Xu et al., 2014). To evaluate the application potentials of direct deoxygenation reaction, β-1 and β-O-4 model compounds—as important family of natural wood lignin—were tested under the standard reaction conditions (Table 4). Aromatic products including 1-methoxy-4-methylbenzene (**3al**) and 1,2-dimethoxy-4-methylbenzene (**3j**) can be obtained in moderate yields through both C-O and C-C bonds cleavage of β-1 lignin model substrates. Interestingly, the corresponding aromatic (**3z**, **3an, 3al**) and phenol (**4a, 4b**) compounds were obtained when β-O-4 lignin model compounds were used as substrates.

In order to gain the mechanistic insights of this transformation, some control experiments were performed (Scheme 2). First, considering that the deoxygenation reaction could only occur with DMSO as the solvent and also an unpleasant odor was sensed when opening the reaction tube, we suspected that dimethyl sulfide gas, generated during the reaction, might have a certain effect on the reaction. Therefore, we used dimethyl sulfide instead of N_2H_2 as the reducing agent for this deoxygenation reaction, and the desired product was obtained in 81% yield. The result indicated that dimethyl sulfide intermediate may be produced from DMSO in the presence of hydrazine, which played a crucial role in the reduction process. Second, we performed the reaction with $N_2D_4 \cdot D_2O$ under the standard conditions, and the deoxygenation product ***d*-3l** was obtained in 90% yield with about 65% deuteration at benzyl position. Third, free radical trap experiments were performed: when 1 or 3 equiv. of TEMPO (2,2,6,6-tetramethyl-1-piperidinyloxy) were added into the reaction system under standard conditions, the reaction still could deliver 76% and 62% yields of the deoxygenation products, demonstrating an unlikely radical pathway in this transformation. Finally, with 3,4,5-trimethoxybenzaldehyde as raw material, only a small amount of the corresponding product was obtained in the presence of hydrazine or dimethyl sulfide, whereas by-products **8** and **9** were generated in 65% and 78% yields, showing that aldehyde may not be an intermediate in this reaction.

Based on the mechanistic studies above, we proposed a plausible reaction mechanism as shown in Scheme 3. Initially, dimethyl sulfide is *in situ* generated from the reaction of DMSO with hydrazine under the promotion of light, meanwhile releasing N_2, H_2, and H_2O (Kim and Lee, 2018; Smit et al., 2008). Considering the importance of O_2 in this reaction and in view of previous studies (Ishiguro et al., 1996; Liang et al., 1983), dimethyl sulfide then interacts with light-excited O_2 to form intermediate **A**, which reacts with alcohols **1** in the presence of base to provide the species **B**. The release of O_2 and DMSO from **B** results in the

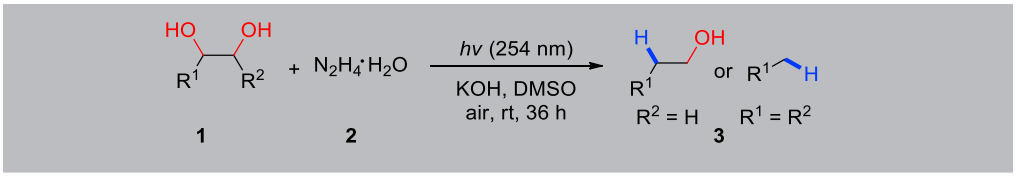

Substrate 1	Product 3	Yield (%)[a]
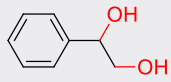	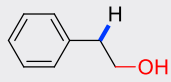	3ak 76
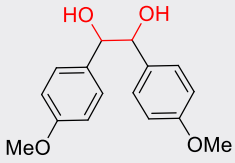	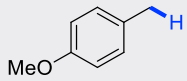	3al 126[b]
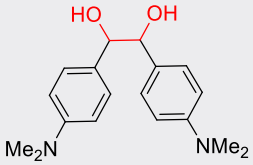	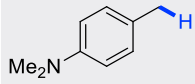	3am 122[b]
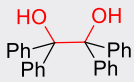	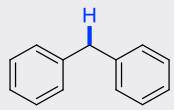	3ae 160[b]

Table 3. Substrate Scope of Vicinal Diols

[a]General conditions: **1** (0.1 mmol), **2** (0.8 mmol), KOH (0.4 mmol) in DMSO (1 mL) at room temperature for 36 h under air and isolated yield based on **1**.

[b]Symmetrical substrate, total yield doubles.

carbanion intermediate **C**. Finally, hydrogen proton abstraction from H_2O by carbanion **C** gives the deoxygenation product **3**.

It is particularly noteworthy for the unprecedented role of dimethylsulfide in this novel alcohol deoxygenation reaction. On the other hand, the amount of dimethyl sulfide generated from the oceans and microorganisms is about 38–40 million metric tons per annum (Chasteen and Bentley, 2004). Moreover, dimethyl sulfide is a by-product of many reactions such as the Kornblum oxidation, the Moffatt oxidation, the Parikh-Doering oxidation, and the Swern oxidation. Thus, we wondered the possibility of using dimethyl sulfide for alcohol deoxygenation. Indeed, we found that a simple and generally applicable methodology for the direct deoxygenation of alcohols (0.1 mmol) can be achieved with dimethyl sulfide (2 equiv.) in DMSO (1 mL) enabled by light at room temperature under air. Different alcohols including primary and secondary benzyl alcohols (Table 5) all gave the products of Csp^3-O bond cleavage in good yields. The reactions of dimethyl sulfide as reducing agent are ongoing in our laboratory and will be reported in due course.

Conclusions

In conclusion, we described a photo-induced metal-free direct deoxygenation of alcohols with hydrazine at room temperature under air atmosphere. The fundamental innovation of this strategy is that traceless nontoxic N_2 and H_2 are generated as by-products, making the direct deoxygenation dramatically clean. This protocol is functional-group tolerant and selective for 1°, 2° alcohols and vicinal diols. Importantly, β-1 and β-O-4 lignin model compounds displayed exceptional reactivity, producing the corresponding aromatics and phenols through C-O/C-C bonds cleavage, which provides a potential method for converting lignin and its model compounds into useful chemicals. Moreover, we successfully used dimethyl sulfide

Substrate 1	Product 3	Yield (%)[a]	Product 4	Yield (%)[a]
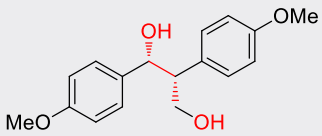	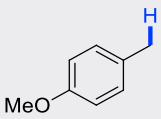	3al 86[b]		
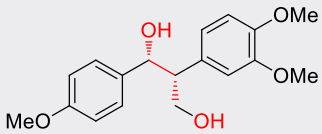	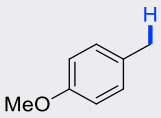	3al 45	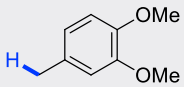	3j 30
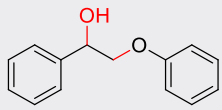	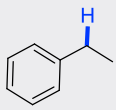	3z 41[c]	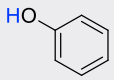	4a 46
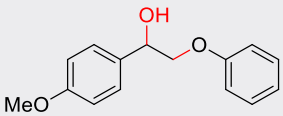	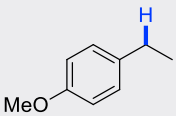	3an 43	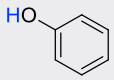	4a 47
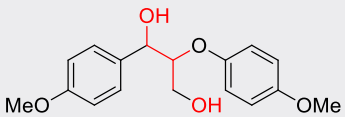	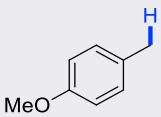	3al 32	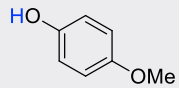	4b 44

Table 4. Substrate Scope of β-1 and β-O-4 Lignin Model Compounds

[a]General conditions: **1** (0.1 mmol), **2** (0.8 mmol), KOH (0.4 mmol) in DMSO (1 mL) at room temperature for 36 h under air and isolated yield based on **1**.

[b]Substrate with the same substituent on both aromatic rings, double product yield.

[c]Yield was determined by GC-MS.

instead of hydrazine as the reducing agent for such alcohol deoxygenation reaction. Further studies on the mechanism and synthetic applications of this protocol are undergoing in our laboratory.

Limitations of the Study

Our direct deoxygenation of alcohols works well for most of the tested substrates; however, primary benzyl alcohols bearing electron-withdrawing groups (e.g., 4-CF_3, 4-F, 4-CN) showed poor reactivity in this transformation. In addition, the detailed mechanism of simultaneous C-O and C-C bonds cleavage process is still not clear.

Resource Availability

Lead Contact

Further information and requests for resources and reagents should be directed to and will be fulfilled by the Lead Contact, Chao-Jun Li (cj.li@mcgill.ca).

Materials Availability

All unique/stable reagents generated in this study are available from the Lead Contact without restriction.

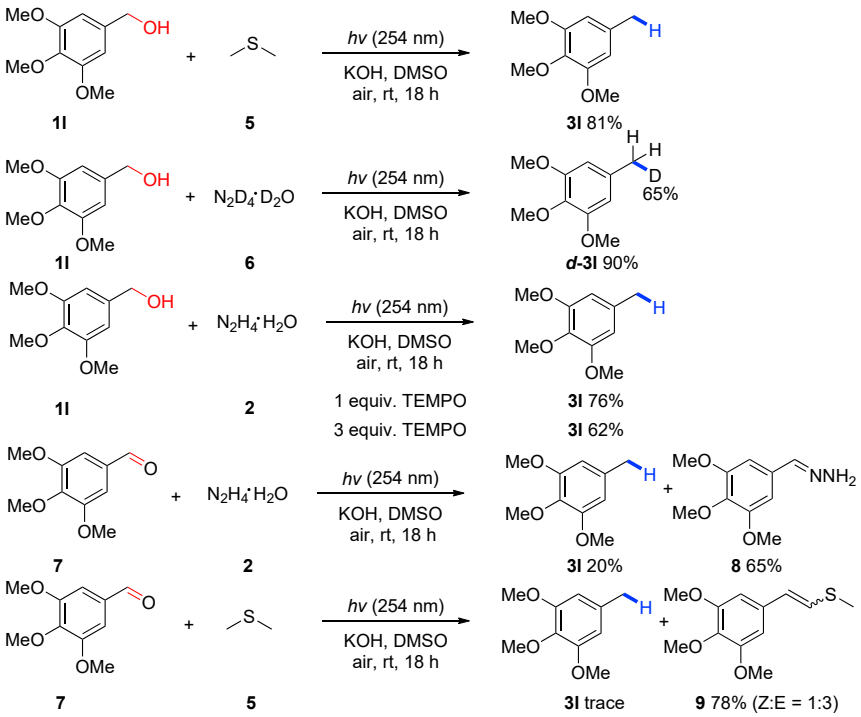

Scheme 2. Control Experiments

Data and Code Availability

All relevant data supporting the findings of this study are available within the paper and its Supplemental Information files. Additional data are provided upon reasonable request.

METHODS

All methods can be found in the accompanying Transparent Methods supplemental file.

SUPPLEMENTAL INFORMATION

Supplemental Information can be found online at https://doi.org/10.1016/j.isci.2020.101419.

ACKNOWLEDGMENTS

We thank NSERC, CFI, FQRNT and Canada Research Chair (to CJL), and Lanzhou University for support of our research. We also thank Dr. Shumei Xia (Nankai University, China) for her advice on the manuscript and Dr. Pan Pan (Lanzhou University, China) for reproducing the compound **3l** in Table 5.

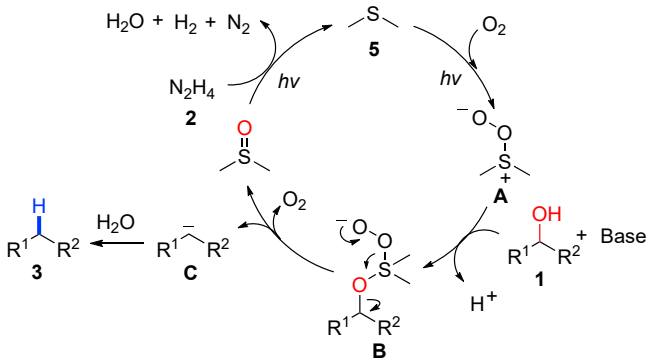

Scheme 3. The Plausible Mechanism for the Direct Dehydroxylation of Alcohols

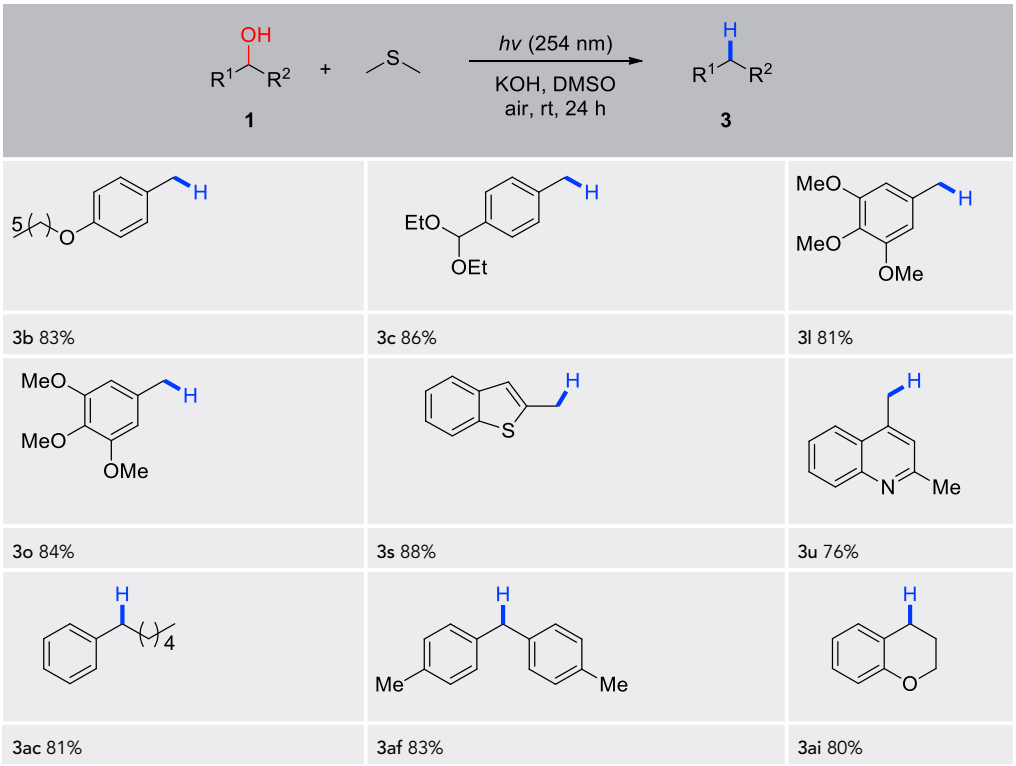

Table 5. Substrate Scope of Alcohols with Dimethyl Sulfide

General conditions: **1** (0.1 mmol), $(CH_3)_2S$ (0.2 mmol), KOH (0.2 mmol) in DMSO (1 mL) at room temperature for 24 h under air. Isolated yield based on **1**.

AUTHOR CONTRIBUTIONS

D.C., Y.P., and C.-J.L. conceived and designed the project. D.C. conducted the experiments, analyzed the data, and composed the manuscript. Z.C., L.L., H.Z., and Y.P. discussed the experimental results and commented on the manuscript. C.-J.L. conducted general guidance, project directing, and manuscript revisions.

DECLARATION OF INTERESTS

The authors declare no competing interests.

Received: May 18, 2020
Revised: July 2, 2020
Accepted: July 24, 2020
Published: August 21, 2020

REFERENCES

Barton, D.H.R., and McCombie, S.W. (1975). A new method for the deoxygenation of secondary alcohols. JCS Perkin. *1975*, 1574–1585.

Bauer, J.O., Chakraborty, S., and Milstein, D. (2017). Manganese-catalyzed direct deoxygenation of primary alcohols. ACS Catal. *7*, 4462–4466.

Bozell, J.J., and Petersen, G.R. (2010). Technology development for the production of biobased products from biorefinery carbohydrates—the US Department of Energy's "Top 10" revisited. Green Chem. *12*, 539–554.

Cao, D., Yan, C., Zhou, P., Zeng, H., and Li, C.-J. (2019). Hydrogen bonding promoted simple and clean photo-induced reduction of C–X bond with isopropanol. Chem. Commun. (Camb.) *55*, 767–770.

Chasteen, T.G., and Bentley, R. (2004). Volatile organic sulfur compounds of environmental interest: dimethyl sulfide and methanethiol. An introductory overview. J. Chem. Educ. *81*, 1524–1528.

Ciszek, B., and Fleischer, I. (2018). Homogeneous palladium-catalyzed transfer hydrogenolysis of benzylic alcohols using formic acid as reductant. Chem. Eur. J. *24*, 12259–12263.

Corma, A., Iborra, S., and Velty, A. (2007). Chemical routes for the transformation of biomass into chemicals. Chem. Rev. *107*, 2411–2502.

Crich, D., and Quintero, L. (1989). Radical chemistry associated with the thiocarbonyl group. Chem. Rev. *89*, 1413–1432.

Dai, X.-J., and Li, C.-J. (2016). En route to a practical primary alcohol deoxygenation. J. Am. Chem. Soc. *138*, 5433–5440.

Dam, J., and Hanefeld, U. (2011). Renewable chemicals: dehydroxylation of glycerol and polyols. ChemSusChem *4*, 1017–1034.

Dethlefsen, J.R., and Fristrup, P. (2015). Rhenium-catalyzed deoxydehydration of diols and polyols. ChemSusChem *8*, 767–775.

Diéguez, H.R., López, A., Domingo, V., Arteaga, J.F., Dobado, J.A., Herrador, M.M., Quílez del Moral, J.F., and Barrero, A.F. (2010). Weakening C−O bonds: Ti(III), a new reagent for alcohol deoxygenation and carbonyl coupling olefination. J. Am. Chem. Soc. *132*, 254–259.

Hartwig, W. (1983). Modern methods for the radical deoxygenation of alcohols. Tetrahedron *39*, 2609–2645.

Haynes, W.M. (2012). Handbook of Chemistry and Physics, 93rd edn (CRC Press).

He, M., Sun, Y., and Han, B. (2013). Green carbon science: scientific basis for integrating carbon resource processing, utilization, and recycling. Angew. Chem. Int. Ed. *52*, 9620–9633.

Huang, J.-L., Dai, X.-J., and Li, C.-J. (2013). Iridium-catalyzed direct dehydroxylation of alcohols. Eur. J. Org. Chem. *2013*, 6496–6500.

Ishiguro, K., Hayashi, M., and Sawaki, Y. (1996). Mechanism of sulfone formation in the reaction of sulfides and singlet oxygen: Intermediacy of S-hydroperoxysulfonium ylide. J. Am. Chem. Soc. *118*, 7265–7271.

Jordan, P.A., and Miller, S.J. (2012). An approach to the site-selective deoxygenation of hydroxy groups based on catalytic phosphoramidite transfer. Angew. Chem. Int. Ed. *51*, 2907–2911.

Kim, K.D., and Lee, J.H. (2018). Visible-light photocatalyzed deoxygenation of *N*-heterocyclic *N*-oxides. Org. Lett. *20*, 7712–7716.

Lam, K., and Markó, I.E. (2011). Novel electrochemical deoxygenation reaction using diphenylphosphinates. Org. Lett. *13*, 406–409.

Lam, K., and Markó, I.E. (2009). Organic electrosynthesis using toluates as simple and versatile radical precursors. Chem. Commun. (Camb.) *2009*, 95–97.

Lam, K., and Markó, I.E. (2008). Using toluates as simple and versatile radical precursors. Org. Lett. *10*, 2773–2776.

Li, C.-J. (2016). Exploration of new chemical reactivities for sustainable molecular transformations. Chem. *1*, 423–437.

Li, H., Gao, Z., Lei, L., Liu, H., Han, J., Hong, F., Luo, N., and Wang, F. (2020). Photocatalytic transfer hydrogenolysis of aromatic ketones using alcohols. Green Chem. *22*, 3802–3808.

Liang, J.J., Gu, C.L., Kacher, M.L., and Foote, C.S. (1983). Chemistry of singlet oxygen. 45. Mechanism of the photooxidation of sulfides. J. Am. Chem. Soc. *105*, 4717–4721.

Lv, L., Qiu, Z., Li, J., Liu, M., and Li, C.-J. (2018). N_2H_4 as traceless mediator for homo- and cross-aryl coupling. Nat. Commun. *9*, 4739.

Masamune, S., Bates, G.S., and Georghiou, P.E. (1974). Reactions of lithium alkyl and alkynyl cuprates. Selective removal of halo and mesyloxy groups and reduction of .alpha.,.beta.-unsaturated ketones. J. Am. Chem. Soc. *96*, 3686–3688.

Masamune, S., Rossy, P.A., and Bates, G.S. (1973). Reductive removal of halo and mesyloxy groups with a copper(I) complex. J. Am. Chem. Soc. *95*, 6452–6454.

Nguyen, J.D., Reiß, B., Dai, C., and Stephenson, C.R.J. (2013). Batch to flow deoxygenation using visible light photoredox catalysis. Chem. Commun. (Camb.) *49*, 4352–4354.

Palacios, D.S., Anderson, T.M., and Burke, M.D. (2007). A Post-PKS oxidation of the amphotericin B skeleton predicted to be critical for channel formation Is not required for potent antifungal activity. J. Am. Chem. Soc. *129*, 13804–13805.

Qiu, Z., Pham, H.D.M., Li, J., Li, C.-C., Castillo-Pazos, D.J., Khaliullin, R.Z., and Li, C.-J. (2019). Light-enabled metal-free pinacol coupling by hydrazine. Chem. Sci. *10*, 10937–10943.

Ragauskas, A.J., Beckham, G.T., Biddy, M.J., Chandra, R., Chen, F., Davis, M.F., Davison, B.H., Dixon, R.A., Gilna, P., Keller, M., et al. (2014). Lignin valorization: improving lignin processing in the biorefinery. Science *344*, 1246843.

Robins, M.J., Wilson, J.S., and Hansske, F. (1983). Nucleic acid related compounds. 42. A general procedure for the efficient deoxygenation of secondary alcohols. Regiospecific and stereoselective conversion of ribonucleosides to 2′-deoxynucleosides. J. Am. Chem. Soc. *105*, 4059–4065.

Ruppert, A.M., Weinberg, K., and Palkovits, R. (2012). Hydrogenolysis goes bio: from carbohydrates and sugar alcohols to platform chemicals. Angew. Chem. Int. Ed. *51*, 2564–2601.

Saito, I., Ikehira, H., Kasatani, R., Watanabe, M., and Matsuura, T. (1986). Photoinduced reactions. 167. Selective deoxygenation of secondary alcohols by photosensitized electron-transfer reaction. A general procedure for deoxygenation of ribonucleosides. J. Am. Chem. Soc. *108*, 3115–3117.

Sawadjoon, S., Lundstedt, A., and Samec, J.S.M. (2013). Pd-catalyzed transfer hydrogenolysis of primary, secondary, and tertiary benzylic alcohols by formic acid: a mechanistic atudy. ACS Catal. *3*, 635–642.

Schwob, T., Kunnas, P., de Jonge, N., Papp, C., Steinrück, H.P., and Kempe, R. (2019). General and selective deoxygenation by hydrogen using a reusable earth-abundant metal catalyst. Sci. Adv. *5*, 3680–3688.

Singh, A.K., Jang, S., Kim, J.Y., Sharma, S., Basavaraju, K.C., Kim, M.-G., Kim, K.-R., Lee, J.S., Lee, H.H., and Kim, D.-P. (2015). One-pot defunctionalization of lignin-derived compounds by dual-functional $Pd_{50}Ag_{50}/Fe_3O_4$/*N*-rGO catalyst. ACS Catal. *5*, 6964–6972.

Smit, C., Fraaije, M.W., and Minnaard, A.J. (2008). Reduction of carbon−carbon double bonds using organocatalytically generated diimide. J. Org. Chem. *73*, 9482–9485.

Stache, E.E., Ertel, A.B., Rovis, T., and Doyle, A.G. (2018). Generation of phosphoranyl radicals via photoredox catalysis enables voltage–independent activation of strong C–O bonds. ACS Catal. *8*, 11134–11139.

Veitch, G.E., Beckmann, E., Burke, B.J., Boyer, A., Maslen, S.L., and Ley, S.V. (2007). Synthesis of azadirachtin: a long but successful journey. Angew. Chem. Int. Ed. *46*, 7629–7632.

Verma, S., Nasir Baig, R.B., Nadagouda, M.N., and Varma, R.S. (2016). Visible light mediated upgrading of biomass to biofuel. Green Chem. *18*, 1327–1331.

Volkov, A., Gustafson, K.P.J., Tai, C.-W., Verho, O., Bäckvall, J.-E., and Adolfsson, H. (2015). Mild deoxygenation of aromatic ketones and aldehydes over Pd/C using polymethylhydrosiloxane as the reducing agent. Angew. Chem. Int. Ed. *54*, 5122–5126.

Wang, S., Zhou, P., Jiang, L., Zhang, Z., Deng, K., Zhang, Y., Zhao, Y., Li, J., Bottle, S., and Zhu, H. (2018). Selective deoxygenation of carbonyl groups at room temperature and atmospheric hydrogen pressure over nitrogen-doped carbon supported Pd catalyst. J. Catal. *368*, 207–216.

Xu, C., Arancon, R.A.D., Labidi, J., and Luque, R. (2014). Lignin depolymerisation strategies: towards valuable chemicals and fuels. Chem. Soc. Rev. *43*, 7485–7500.

Zhang, L., and Koreeda, M. (2004). Radical deoxygenation of hydroxyl groups via phosphites. J. Am. Chem. Soc. *126*, 13190–13191.

iScience, Volume *23*

Supplemental Information

Light-Driven Metal-Free Direct Deoxygenation of Alcohols under Mild Conditions

Dawei Cao, Zhangpei Chen, Leiyang Lv, Huiying Zeng, Yong Peng, and Chao-Jun Li

Supplemental Information

Light-Driven Metal-Free Direct Deoxygenation of Alcohols under Mild Conditions

Dawei Cao, Zhangpei Chen, Leiyang Lv, Huiying Zeng, Yong Peng and Chao-Jun Li

Supplemental Figures for NMR spectra:

Figure S1. ^{1}H NMR spectrum of compound **1-(hexyloxy)-4-methylbenzene** (**3b**), related to **Table 2**, **Table 5**.

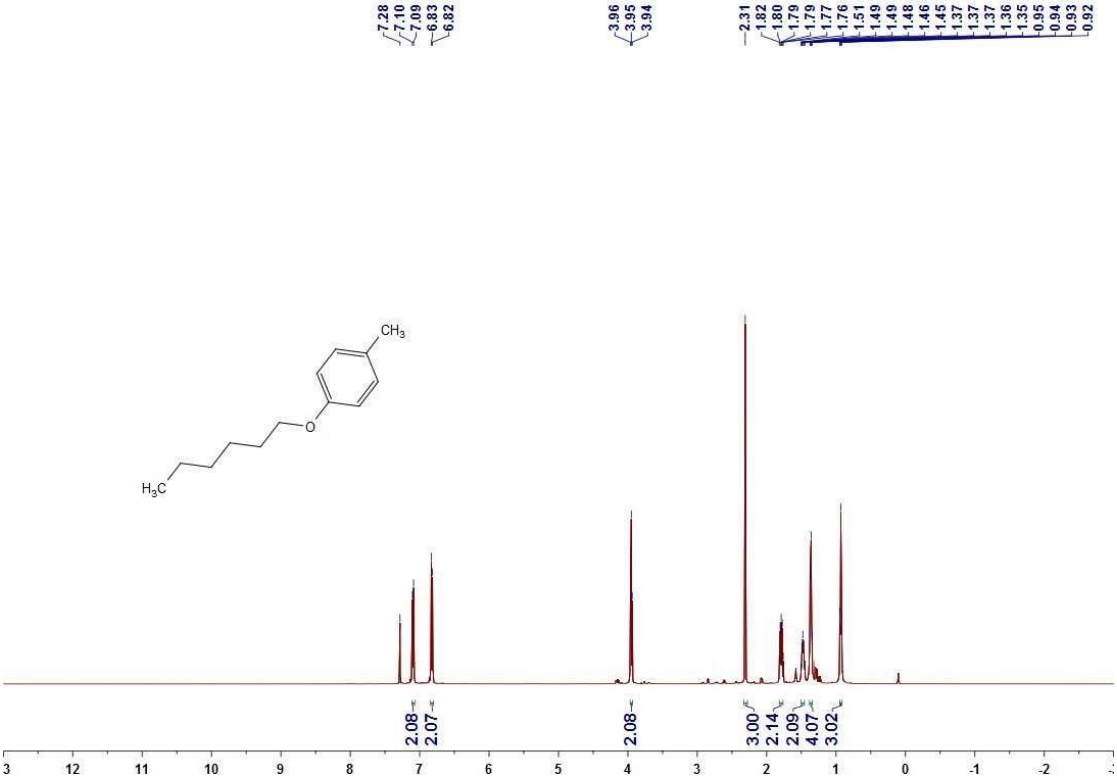

Figure S2. ^{13}C NMR spectrum of compound **1-(hexyloxy)-4-methylbenzene** (**3b**), related to **Table 2**, **Table 5**.

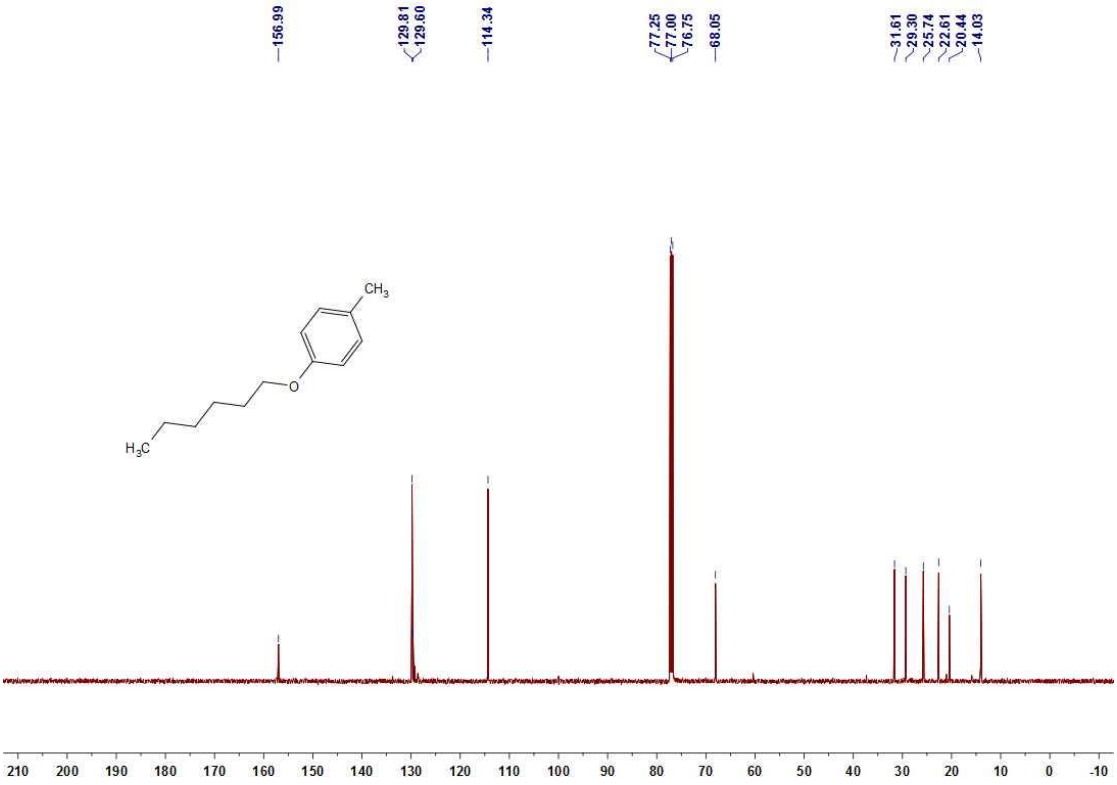

Figure S3. ^{1}H NMR spectrum of compound **1-(diethoxymethyl)-4-methylbenzene (3c),** related to **Table 2**, **Table 5**.

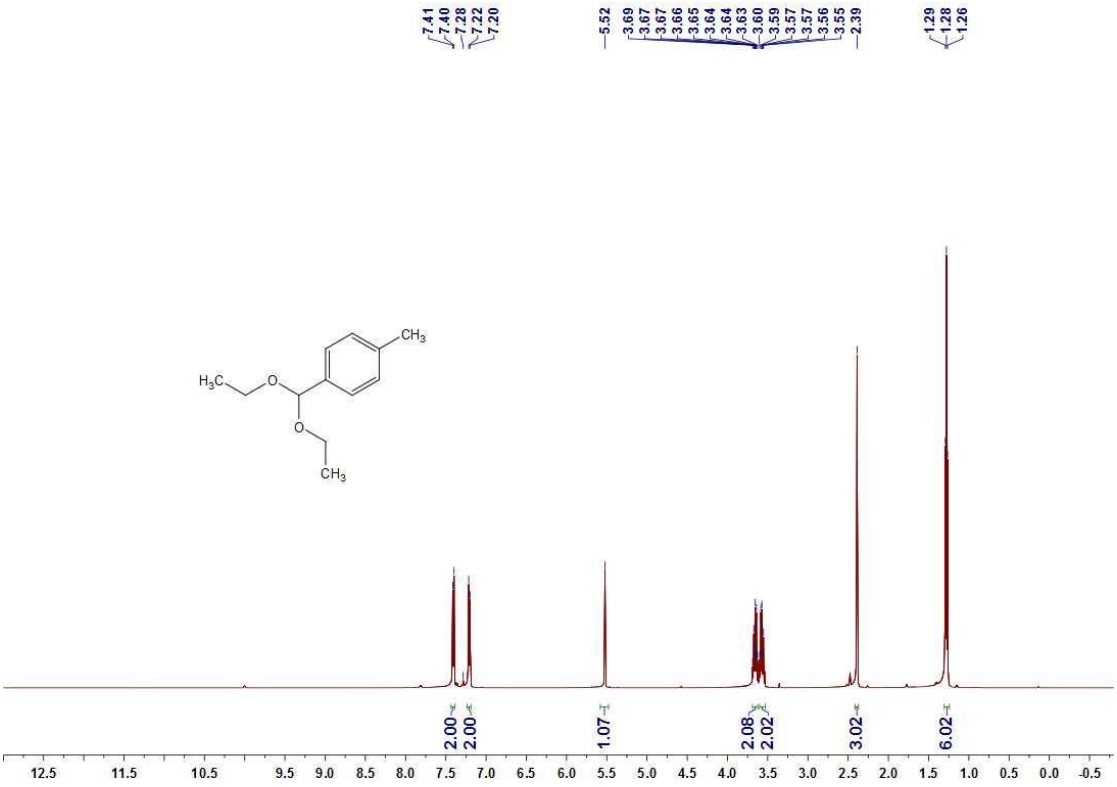

Figure S4. ^{13}C NMR spectrum of compound **1-(diethoxymethyl)-4-methylbenzene (3c),** related to **Table 2**, **Table 5**.

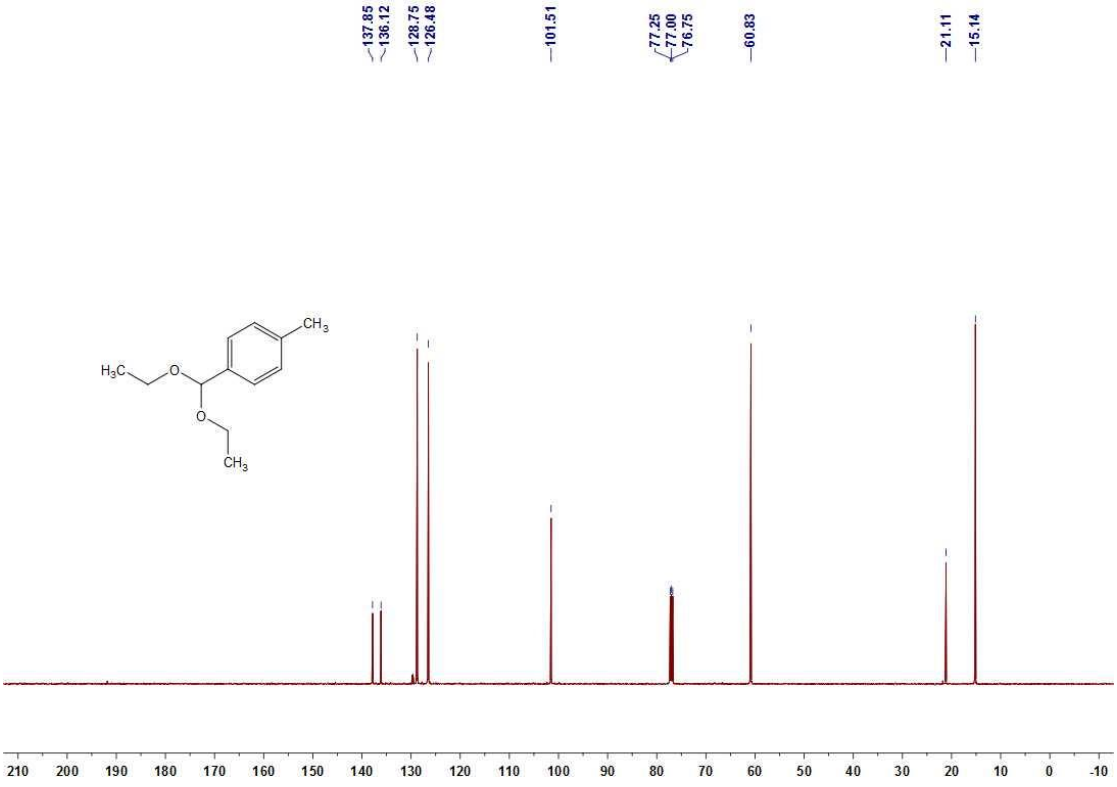

Figure S5. ^{1}H NMR spectrum of compound ***p*-cresol (3d),** related to **Table 2**.

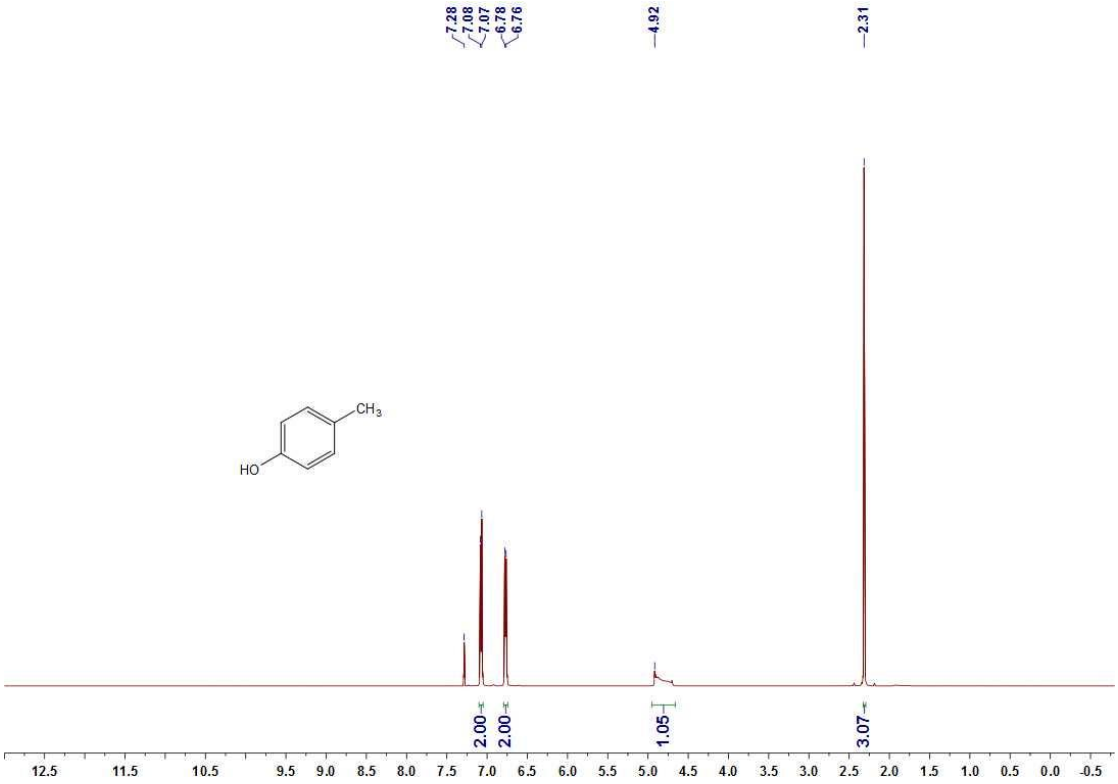

Figure S6. ^{13}C NMR spectrum of compound ***p*-cresol (3d),** related to **Table 2**.

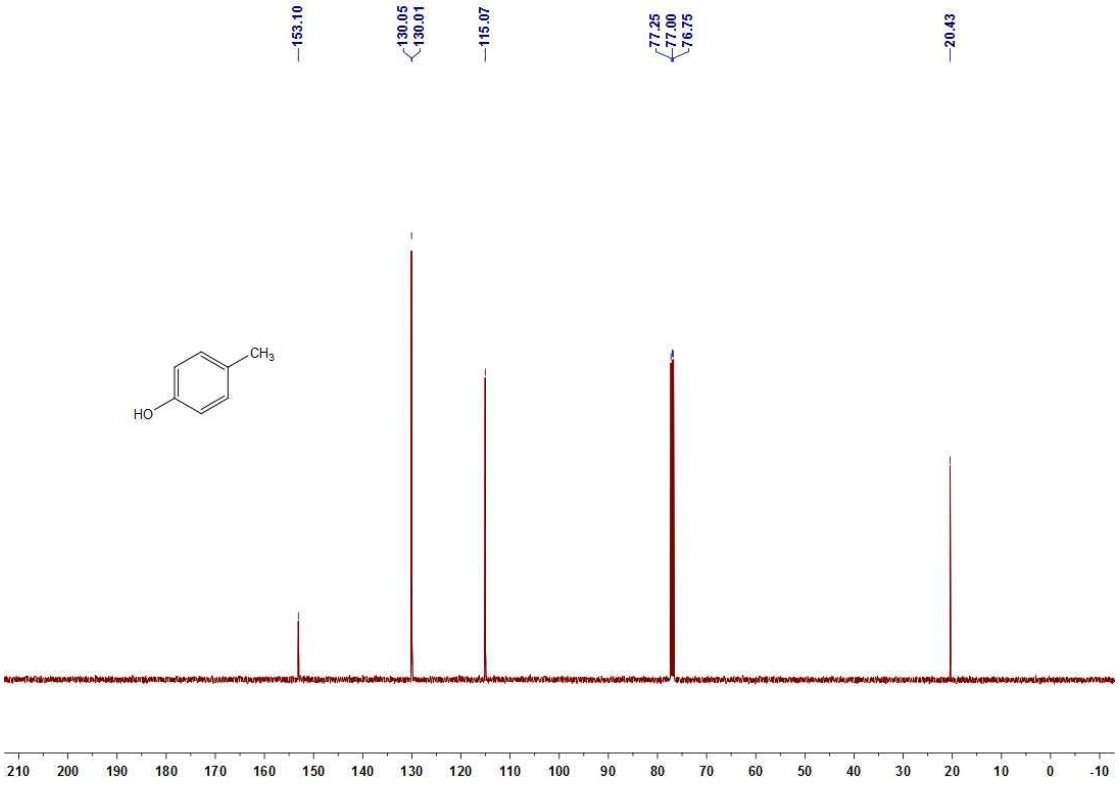

Figure S7. ^{1}H NMR spectrum of compound **methyl 4-methylbenzoate (3e) ,** related to **Table 2**.

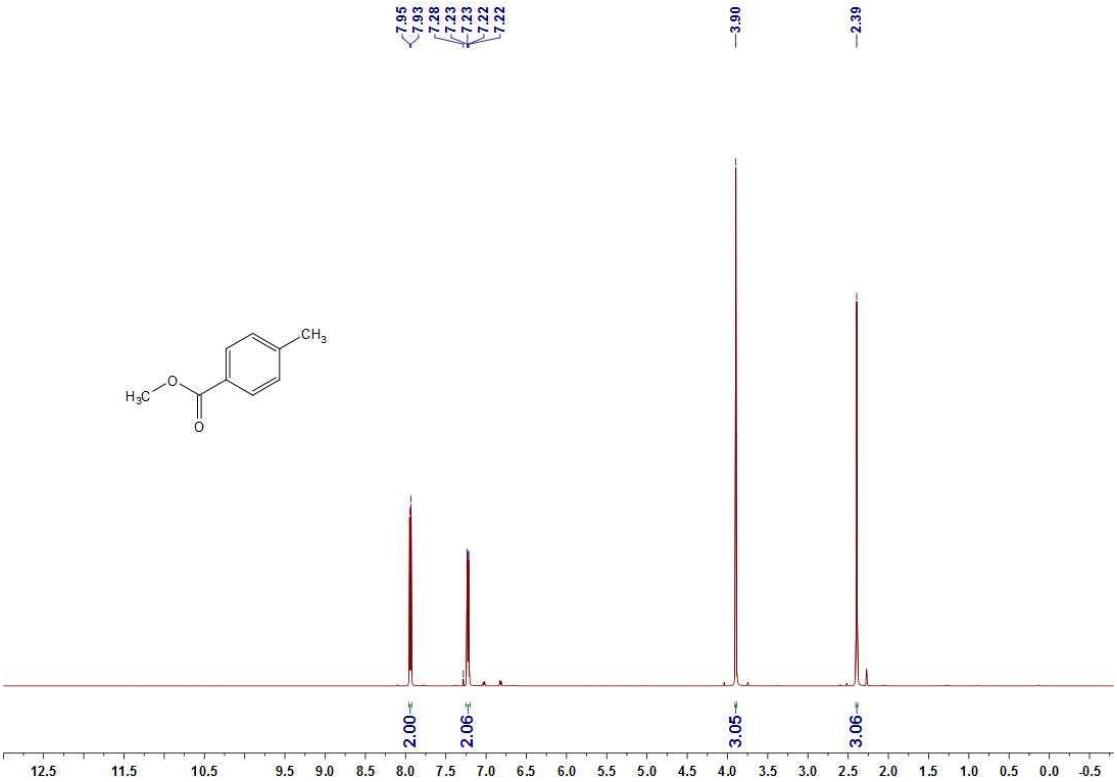

Figure S8. ^{13}C NMR spectrum of compound **methyl 4-methylbenzoate (3e),** related to **Table 2**.

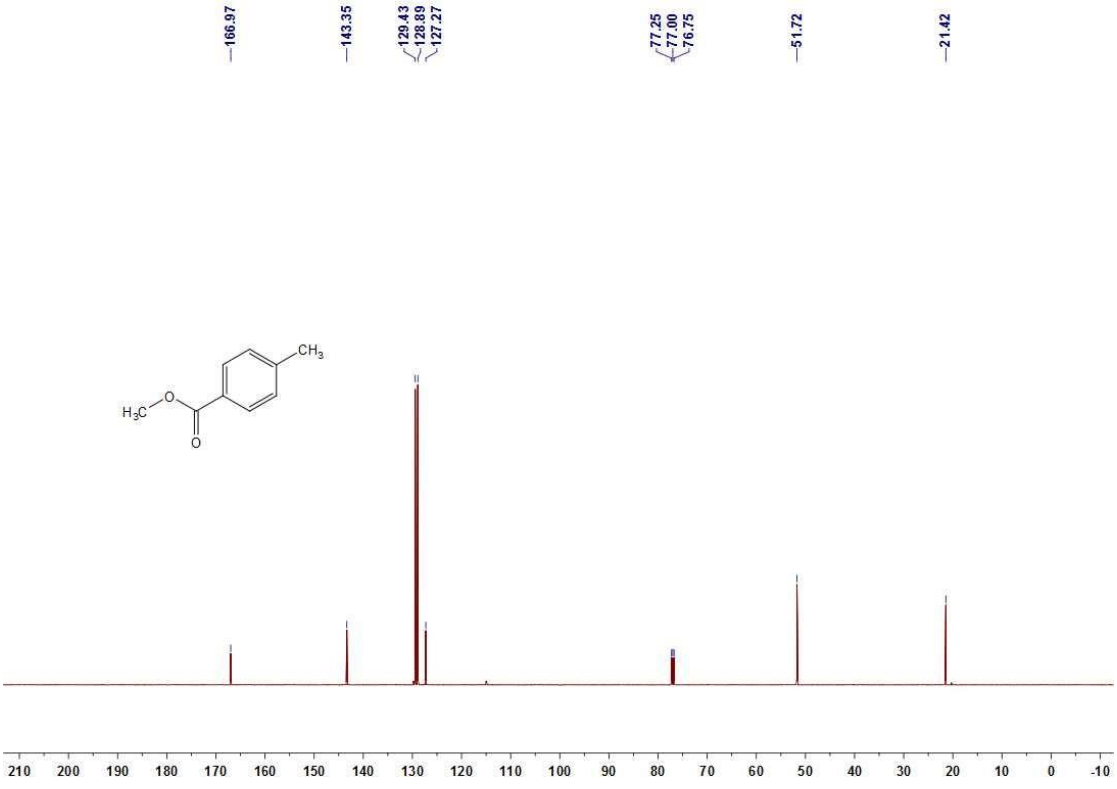

Figure S9. ^{1}H NMR spectrum of compound ***p*-toluidine (3f),** related to **Table 2**.

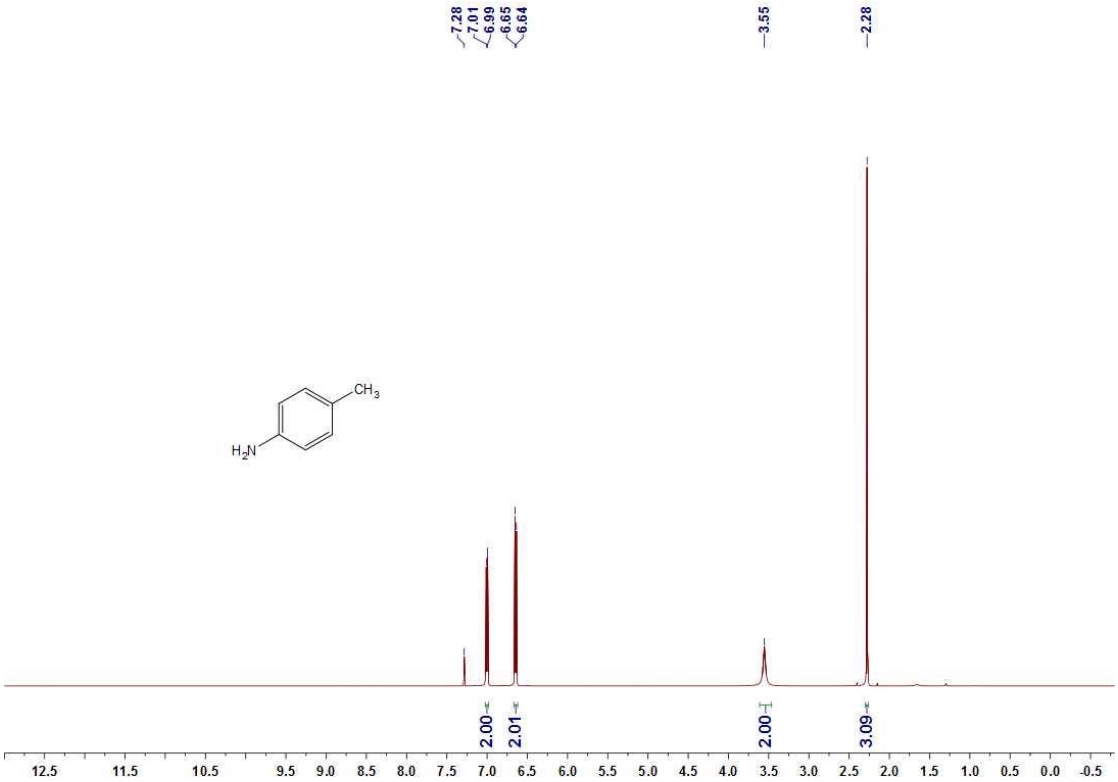

Figure S10. ^{13}C NMR spectrum of compound ***p*-toluidine (3f),** related to **Table 2**.

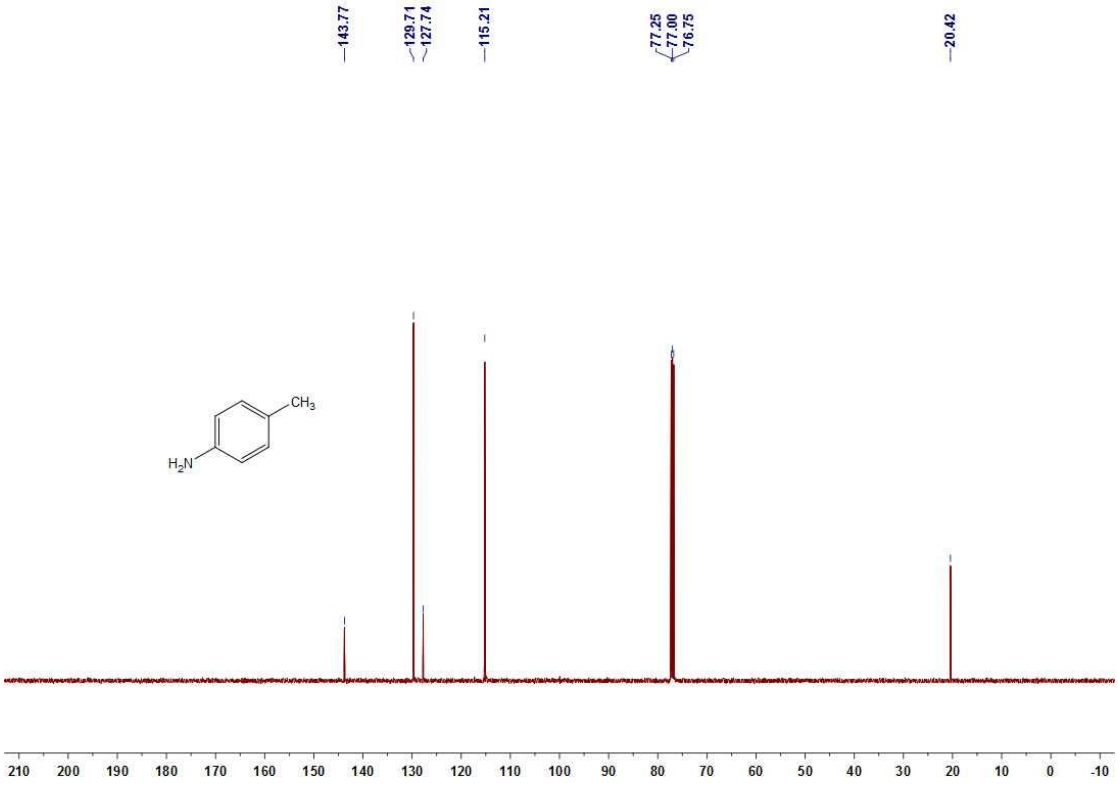

Figure S11. ^{1}H NMR spectrum of compound **1-methoxy-2-methylbenzene (3g),** related to **Table 2**.

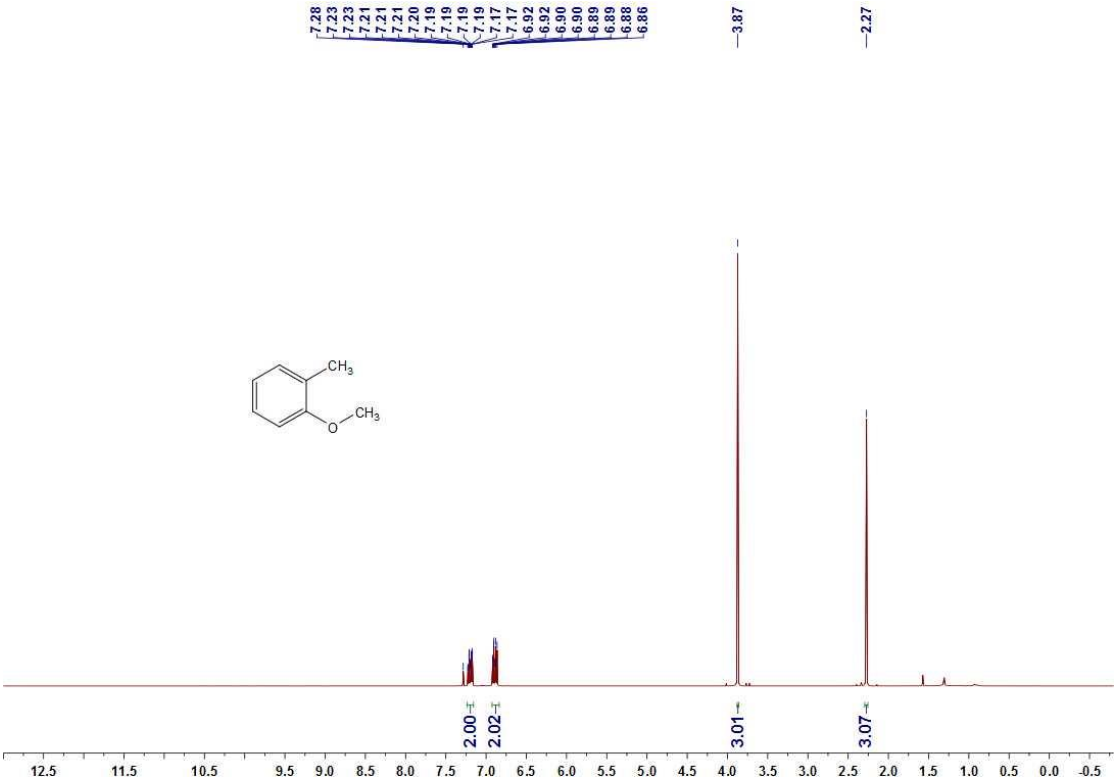

Figure S12. ^{13}C NMR spectrum of compound **1-methoxy-2-methylbenzene (3g),** related to **Table 2**.

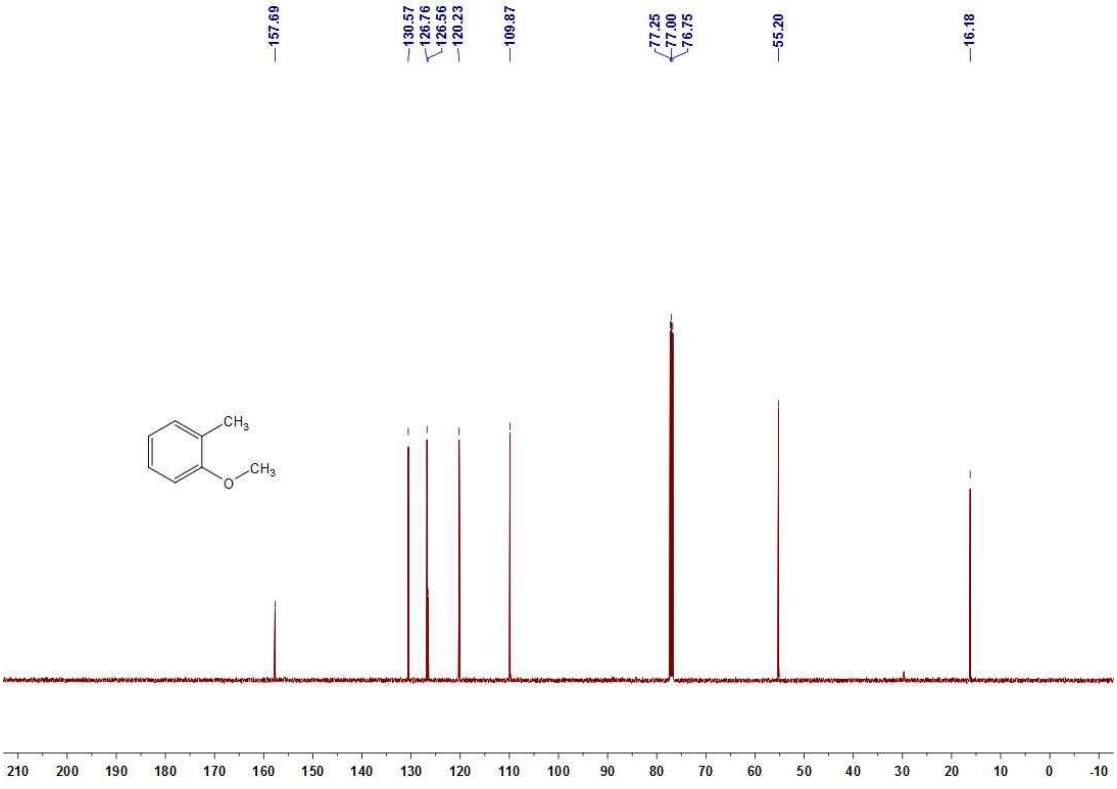

Figure S13. ^{1}H NMR spectrum of compound ***o*-toluidine (3h),** related to **Table 2**.

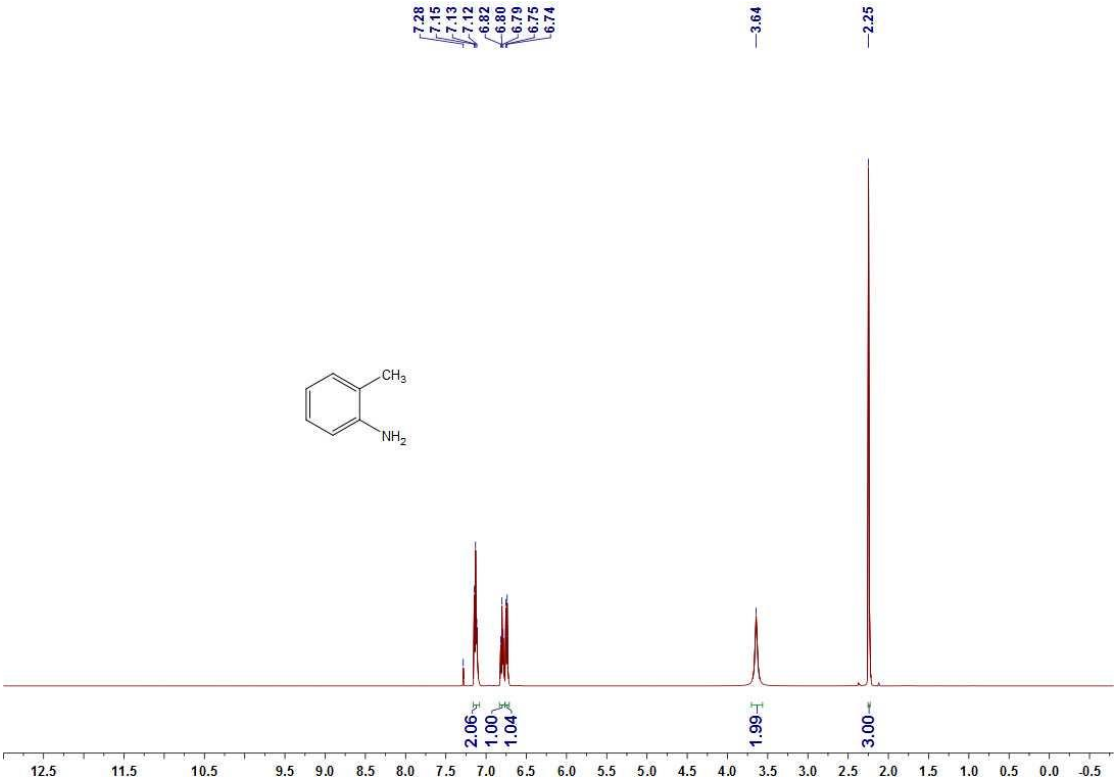

Figure S14. ^{13}C NMR spectrum of compound ***o*-toluidine (3h),** related to **Table 2**.

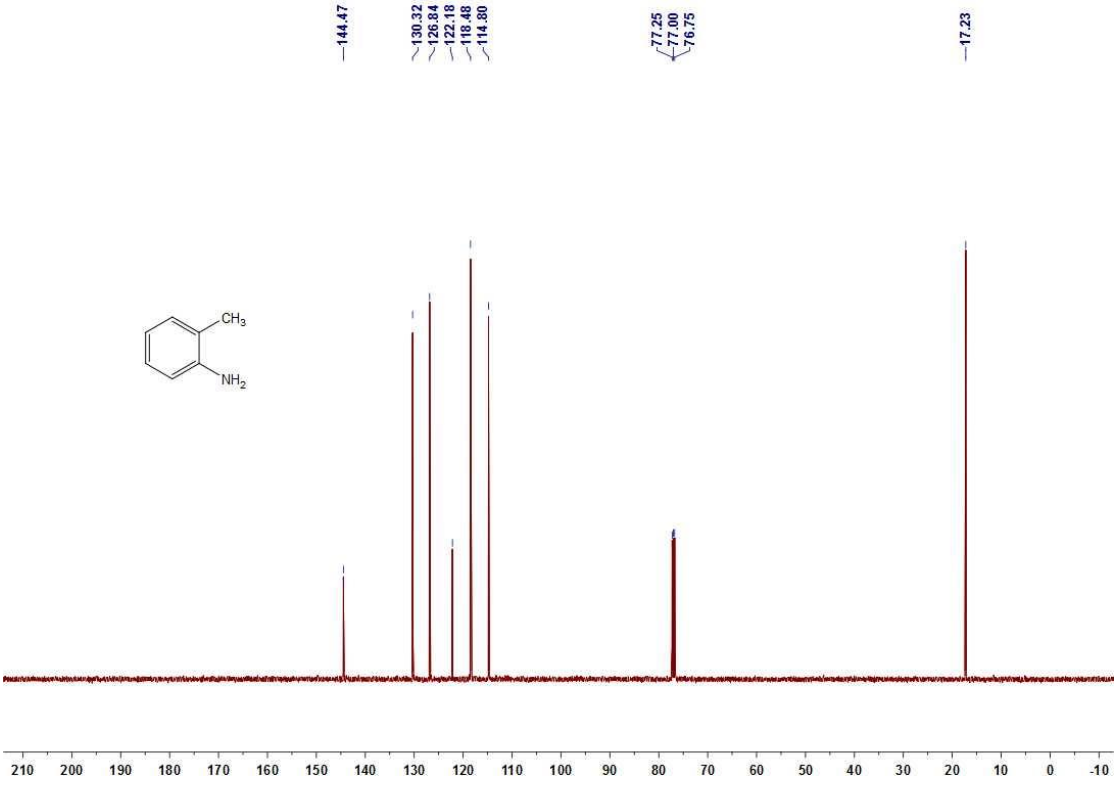

Figure S15. ^{1}H NMR spectrum of compound **1,3-dimethoxy-5-methylbenzene (3i),** related to **Table 2**.

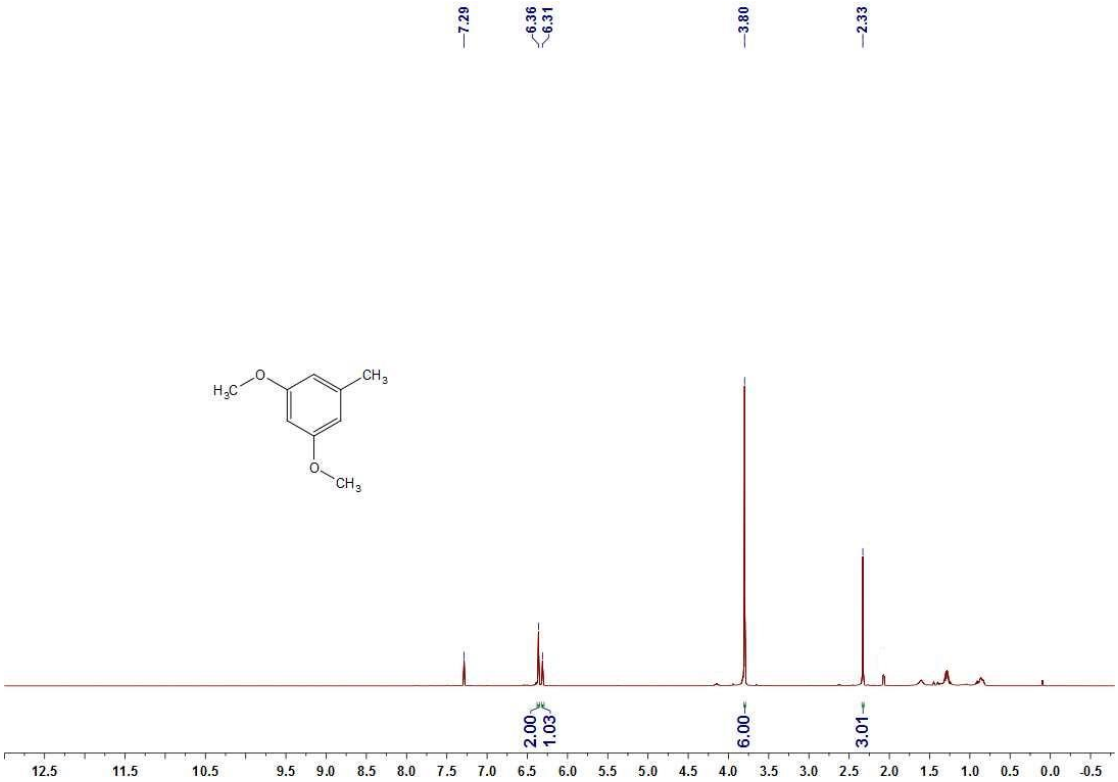

Figure S16. ^{13}C NMR spectrum of compound **1,3-dimethoxy-5-methylbenzene (3i),** related to **Table 2**.

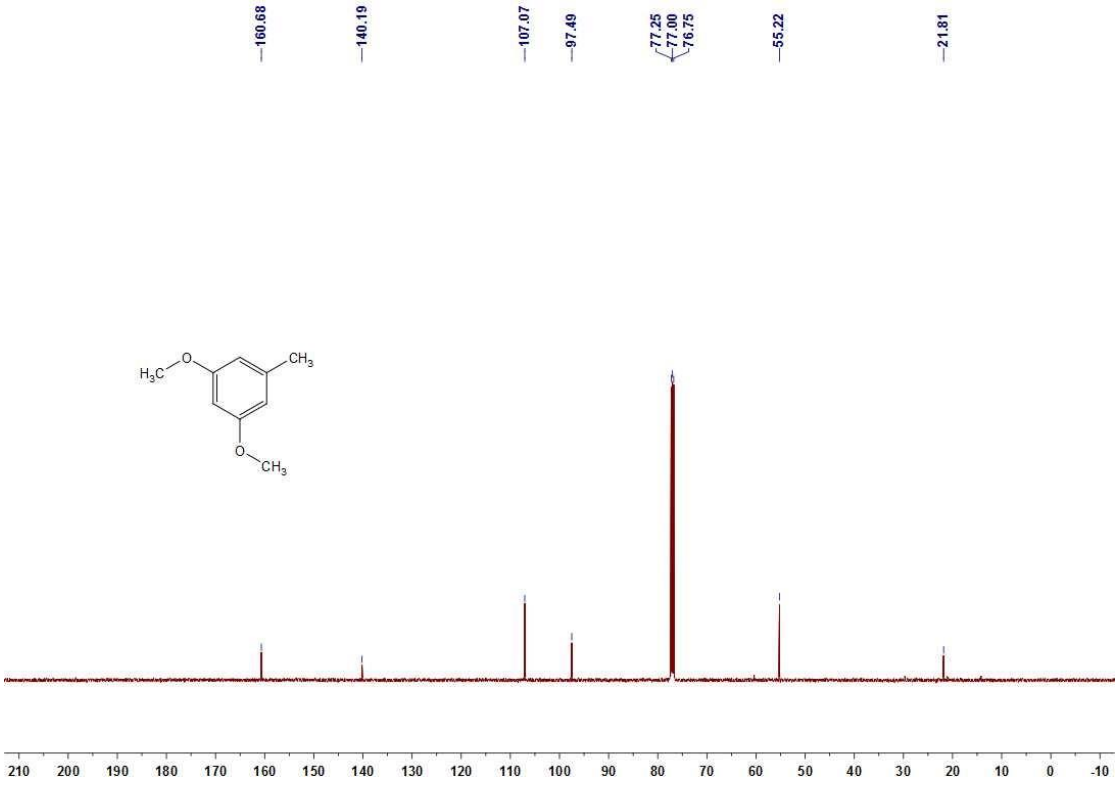

Figure S17. ^{1}H NMR spectrum of compound **1,2-dimethoxy-4-methylbenzene (3j),** related to **Table 2**.

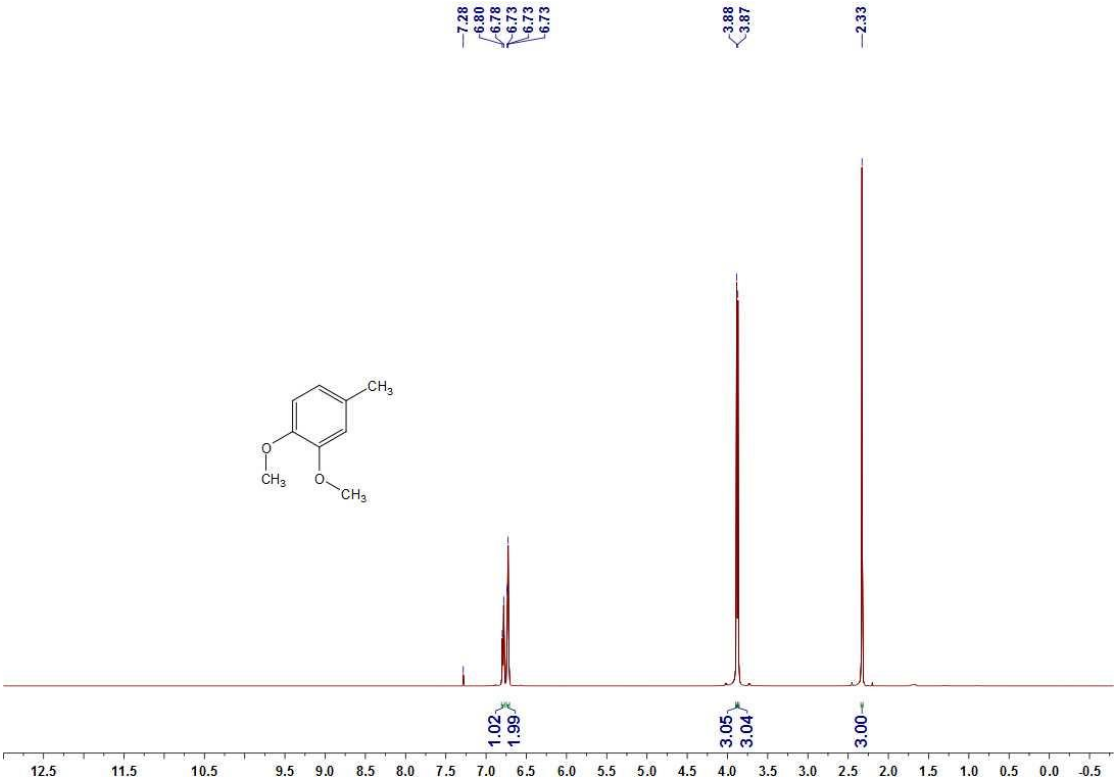

Figure S18. ^{13}C NMR spectrum of compound **1,2-dimethoxy-4-methylbenzene (3j),** related to **Table 2**.

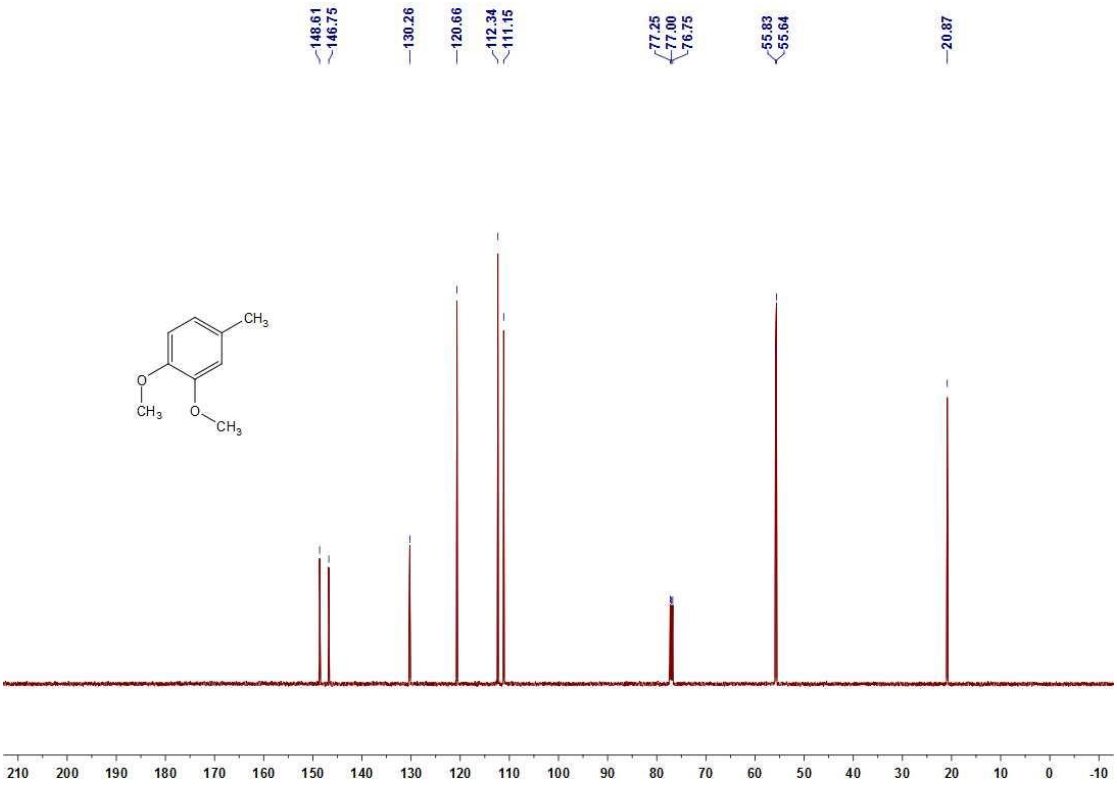

Figure S19. ^{1}H NMR spectrum of compound **1,4-dimethoxy-2-methylbenzene (3k),** related to **Table 2**.

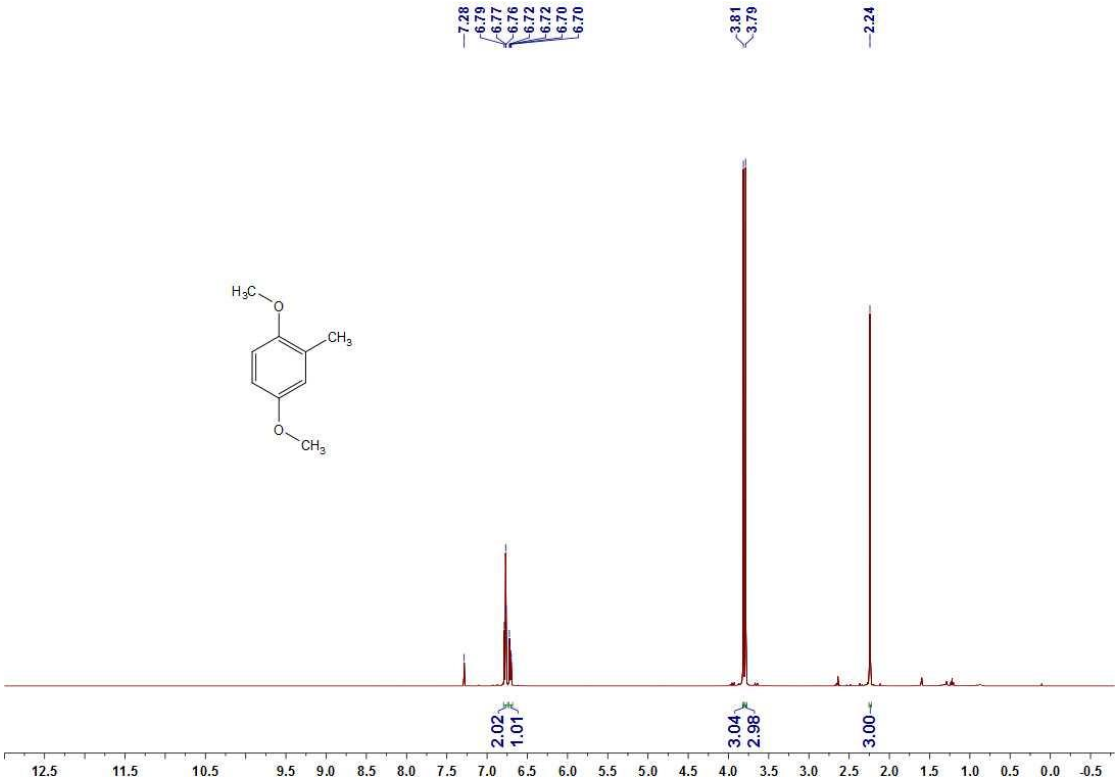

Figure S20. ^{13}C NMR spectrum of compound **1,4-dimethoxy-2-methylbenzene (3k),** related to **Table 2**.

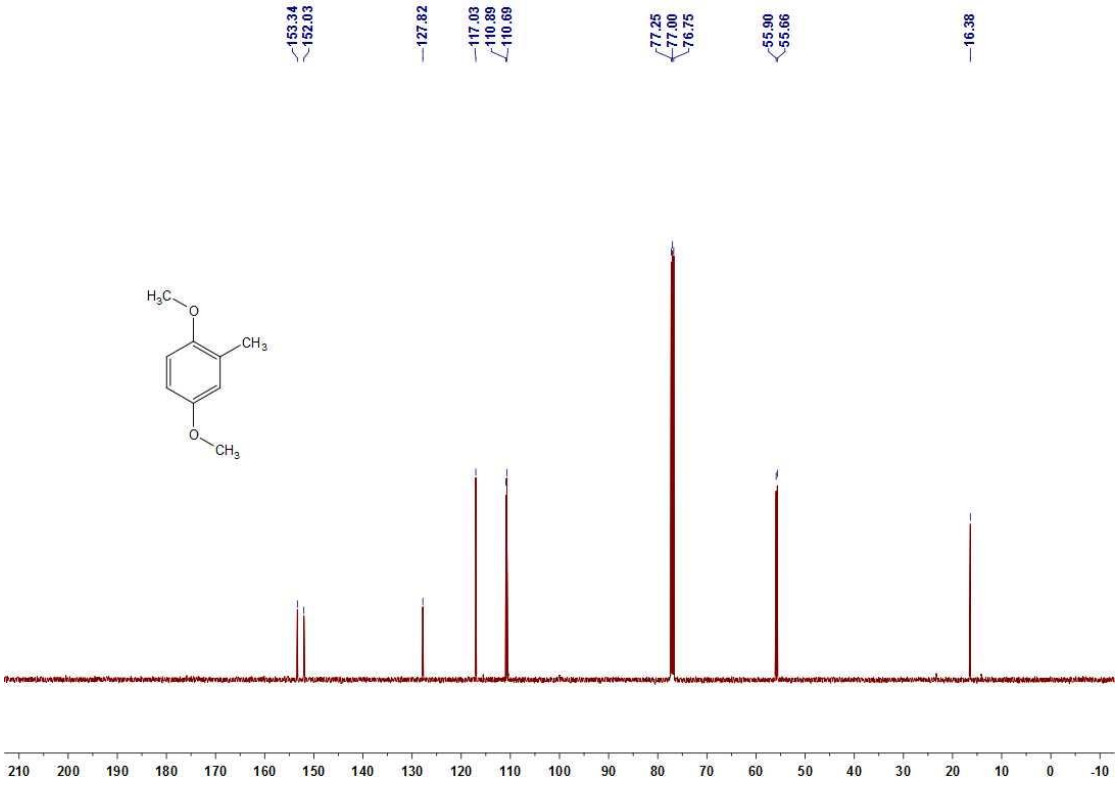

Figure S21. ^{1}H NMR spectrum of compound **1,2,3-trimethoxy-5-methylbenzene (3l),** related to **Table 1**, **Table 2**, **Table 5**.

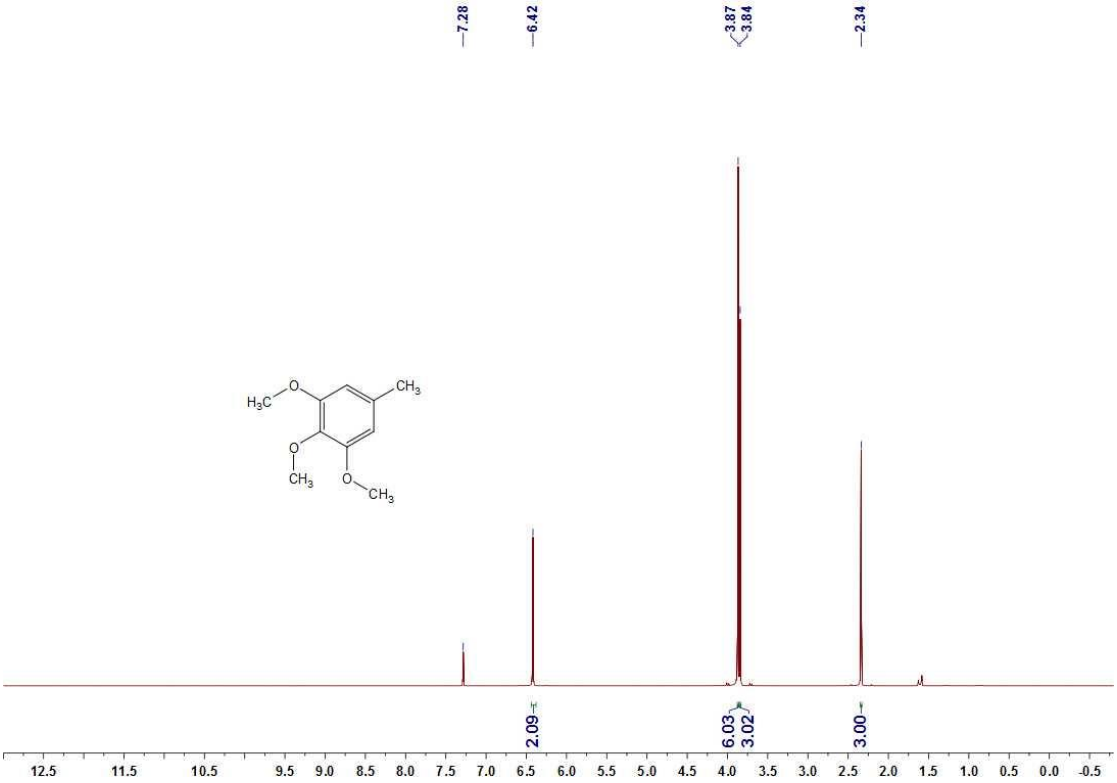

Figure S22. ^{13}C NMR spectrum of compound **1,2,3-trimethoxy-5-methylbenzene (3l),** related to **Table 1**, **Table 2**, **Table 5**.

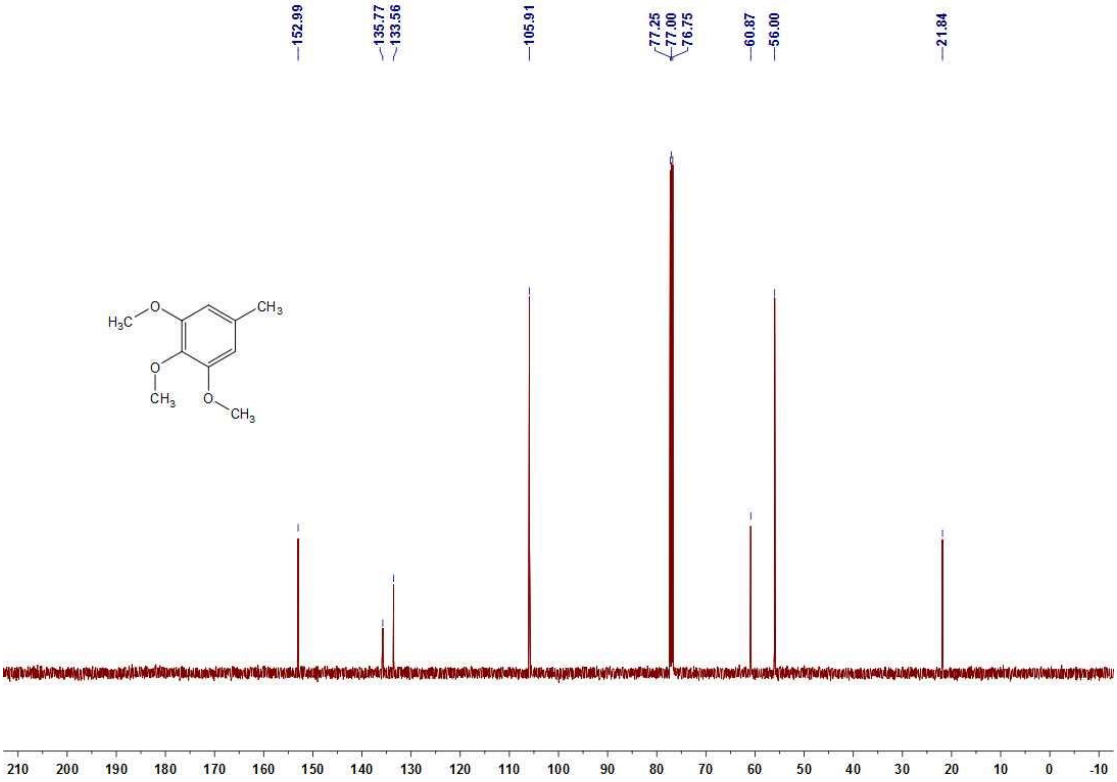

Figure S23. ^{1}H NMR spectrum of compound **1,2,3,5-tetramethylbenzene (3m),** related to **Table 2**.

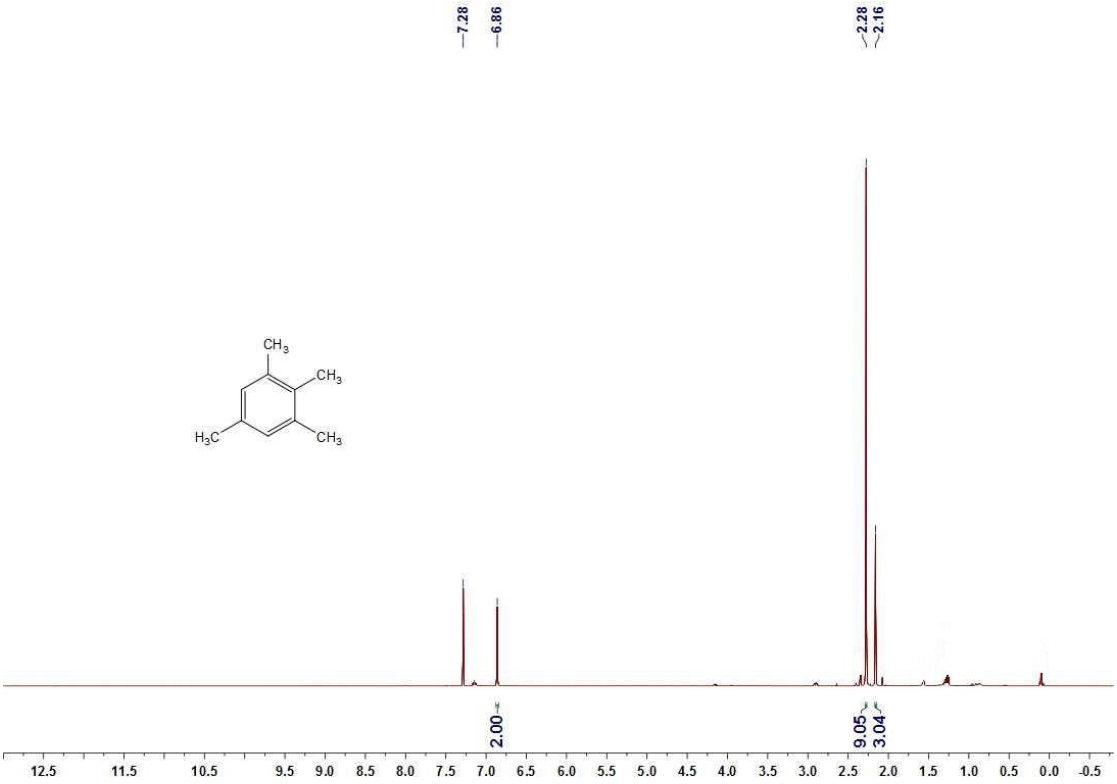

Figure S24. ^{13}C NMR spectrum of compound **1,2,3,5-tetramethylbenzene (3m),** related to **Table 2**.

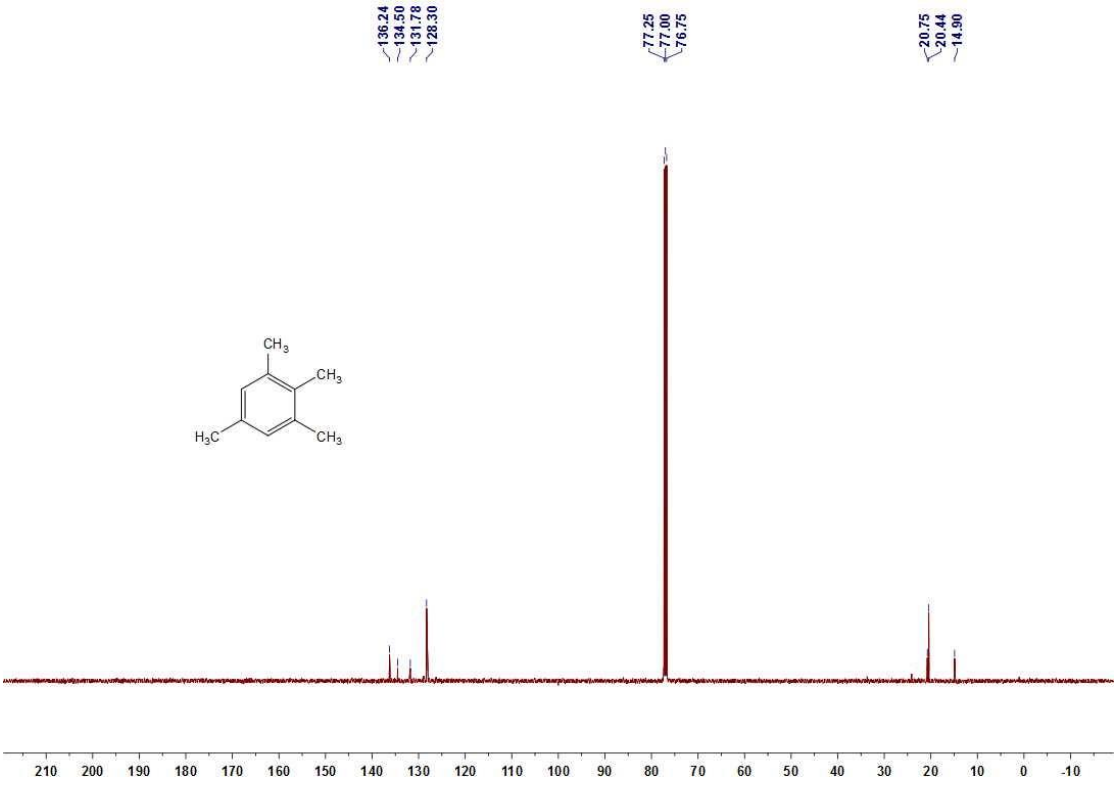

Figure S25. ^{1}H NMR spectrum of compound **5-methyl-2,3-dihydro-1*H*-indene (3n),** related to **Table 2**.

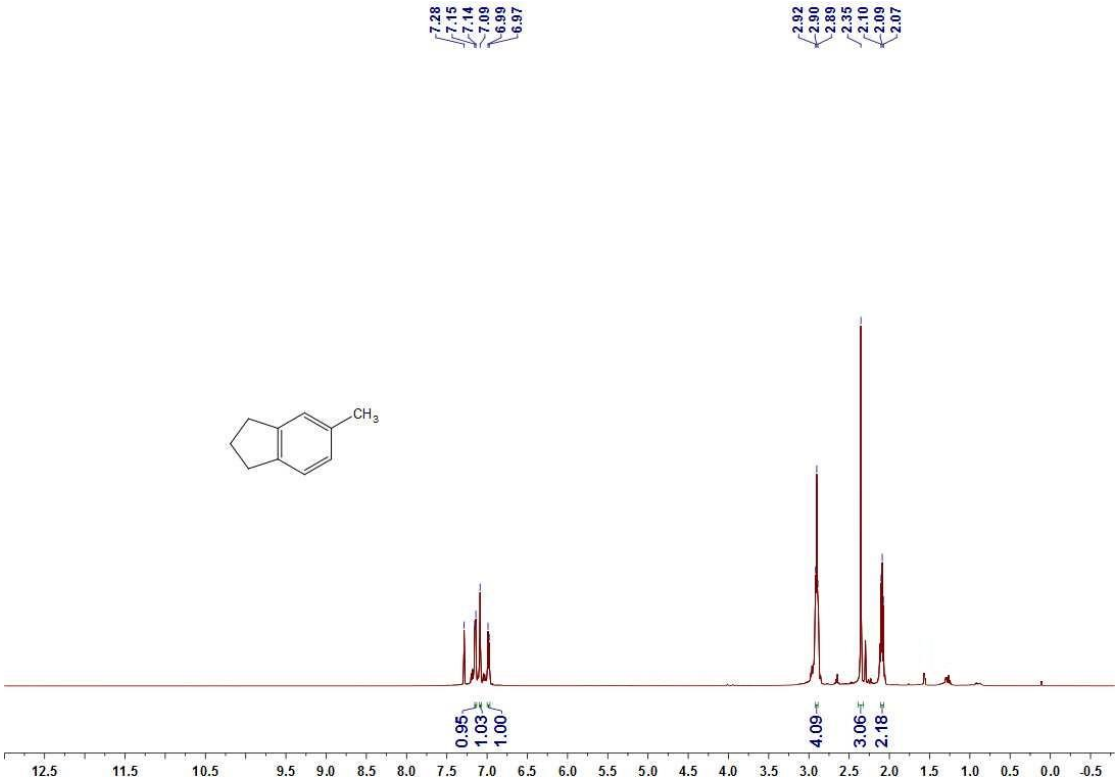

Figure S26. ^{13}C NMR spectrum of compound **5-methyl-2,3-dihydro-1*H*-indene (3n),** related to **Table 2**.

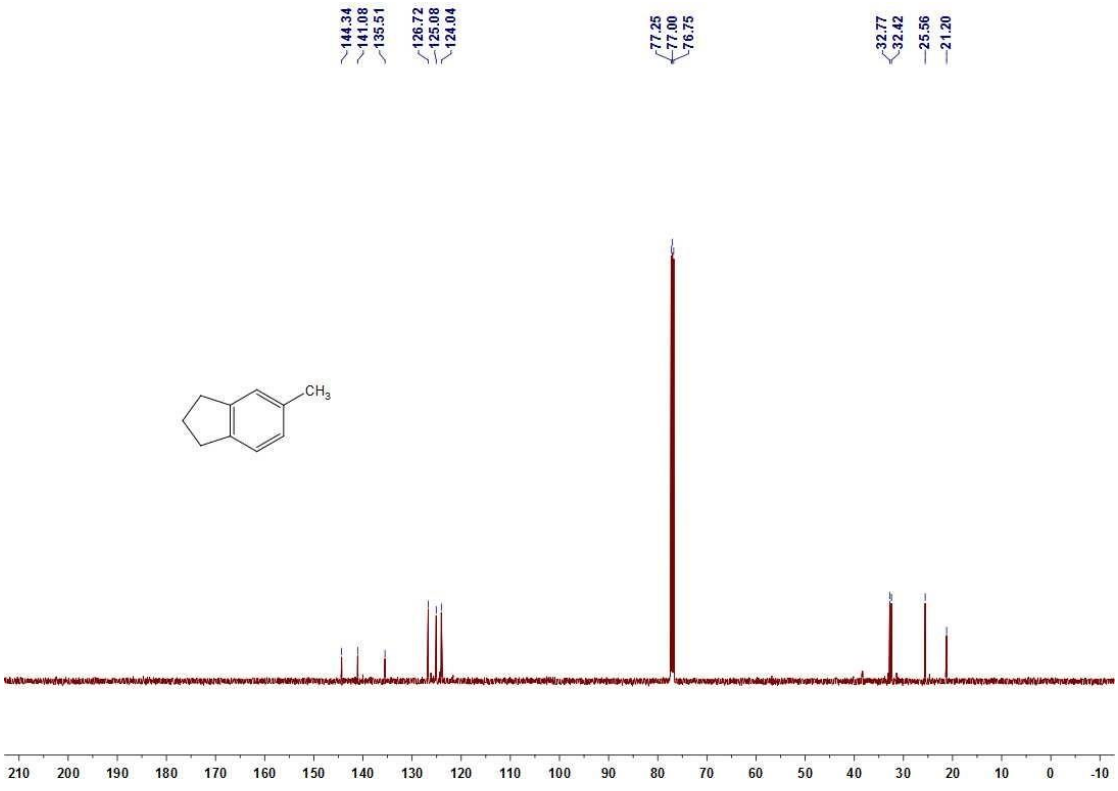

Figure S27. ^{1}H NMR spectrum of compound **5-methylbenzo[*d*][1,3]dioxole (3o),** related to **Table 2, Table 5**.

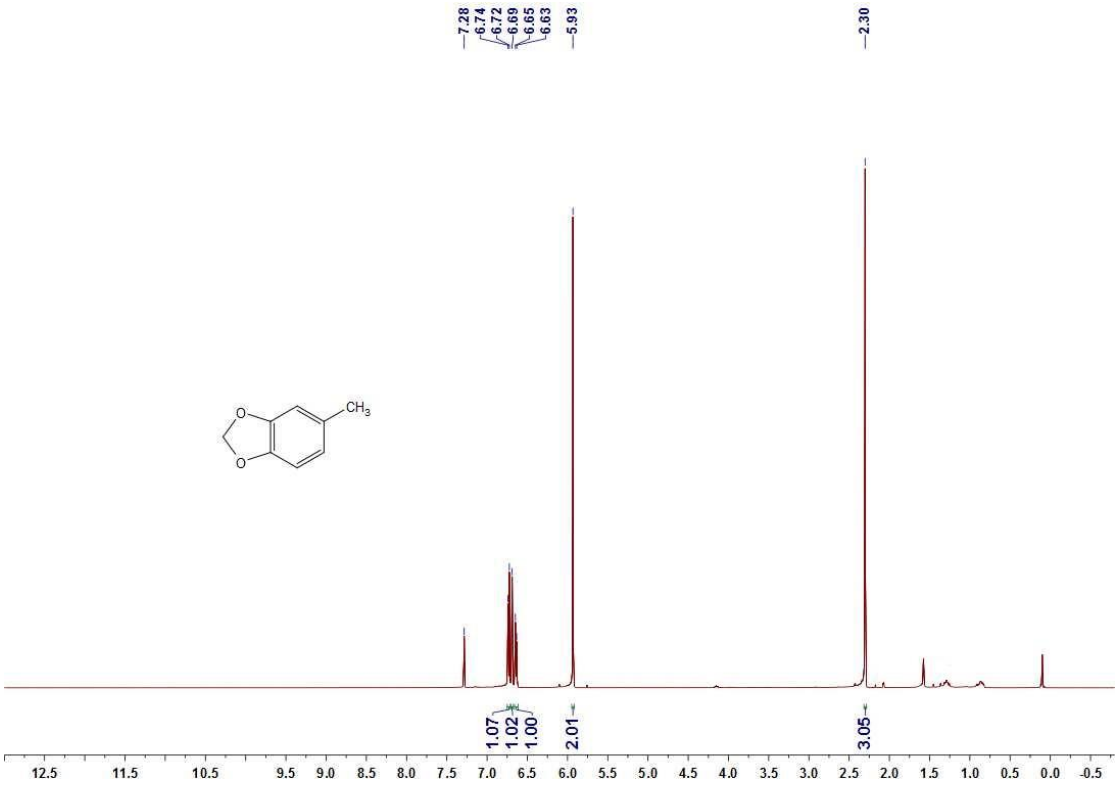

Figure S28. ^{13}C NMR spectrum of compound **5-methylbenzo[*d*][1,3]dioxole (3o),** related to **Table 2, Table 5**.

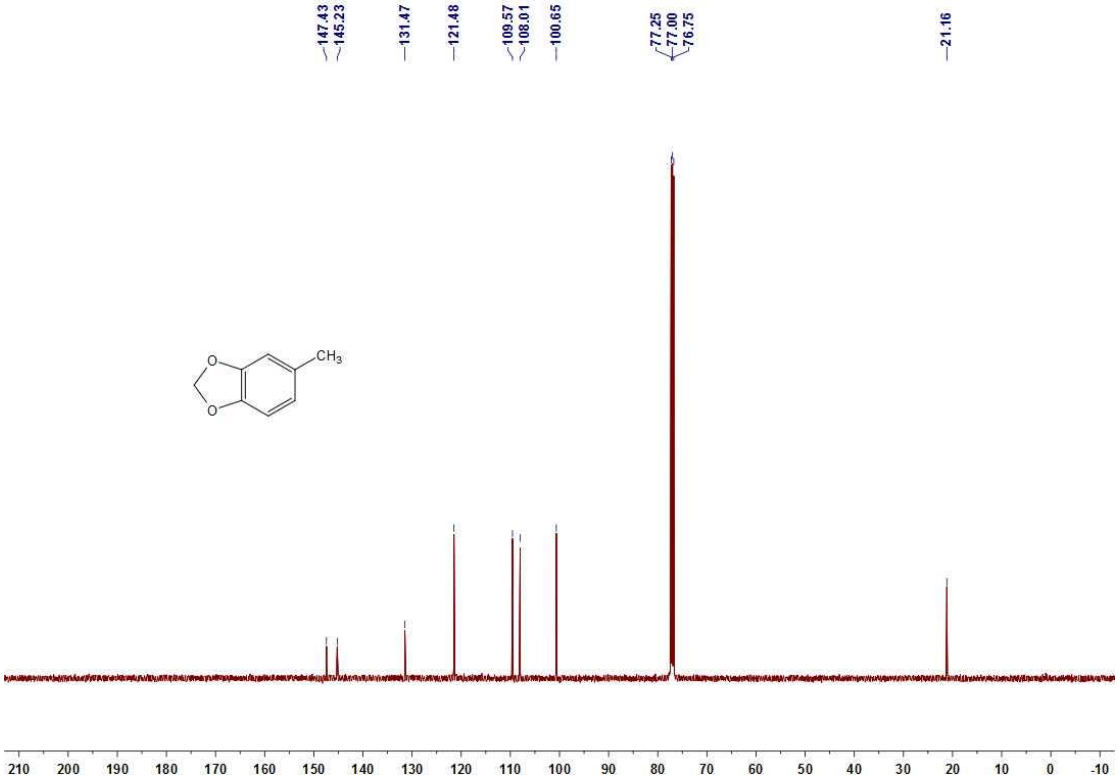

Figure S29. ^{1}H NMR spectrum of compound **2-methylnaphthalene (3p),** related to **Table 2.**

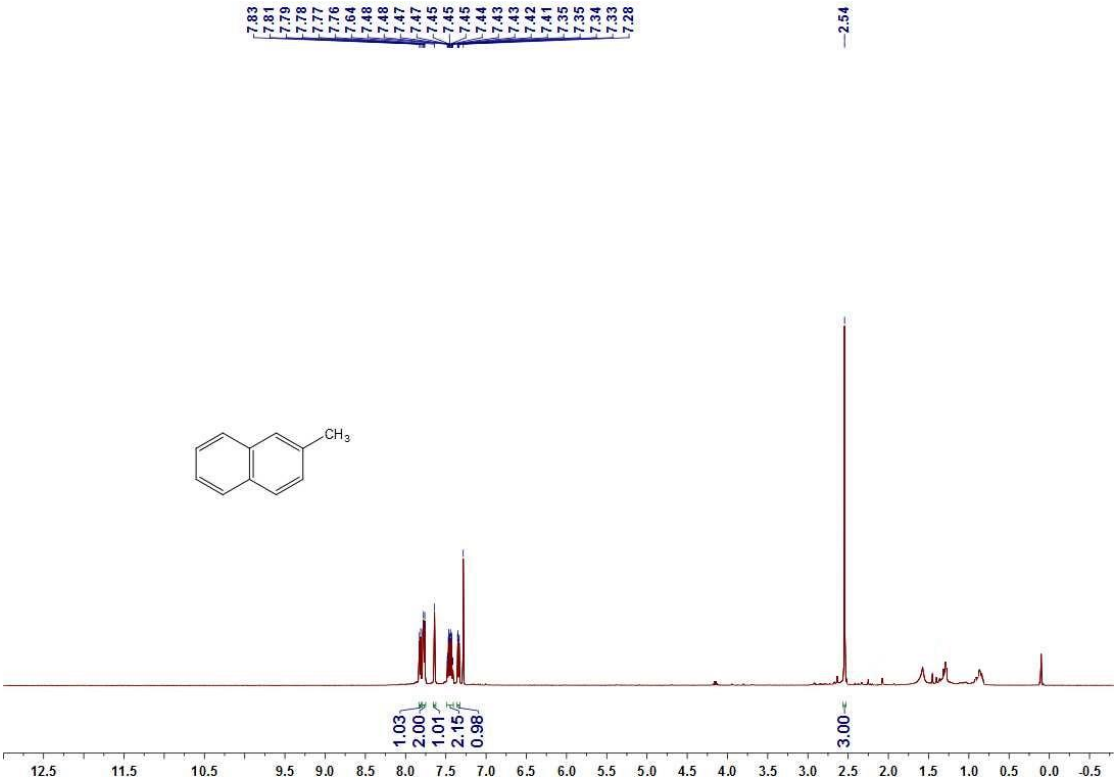

Figure S30. ^{13}C NMR spectrum of compound **2-methylnaphthalene (3p),** related to **Table 2.**

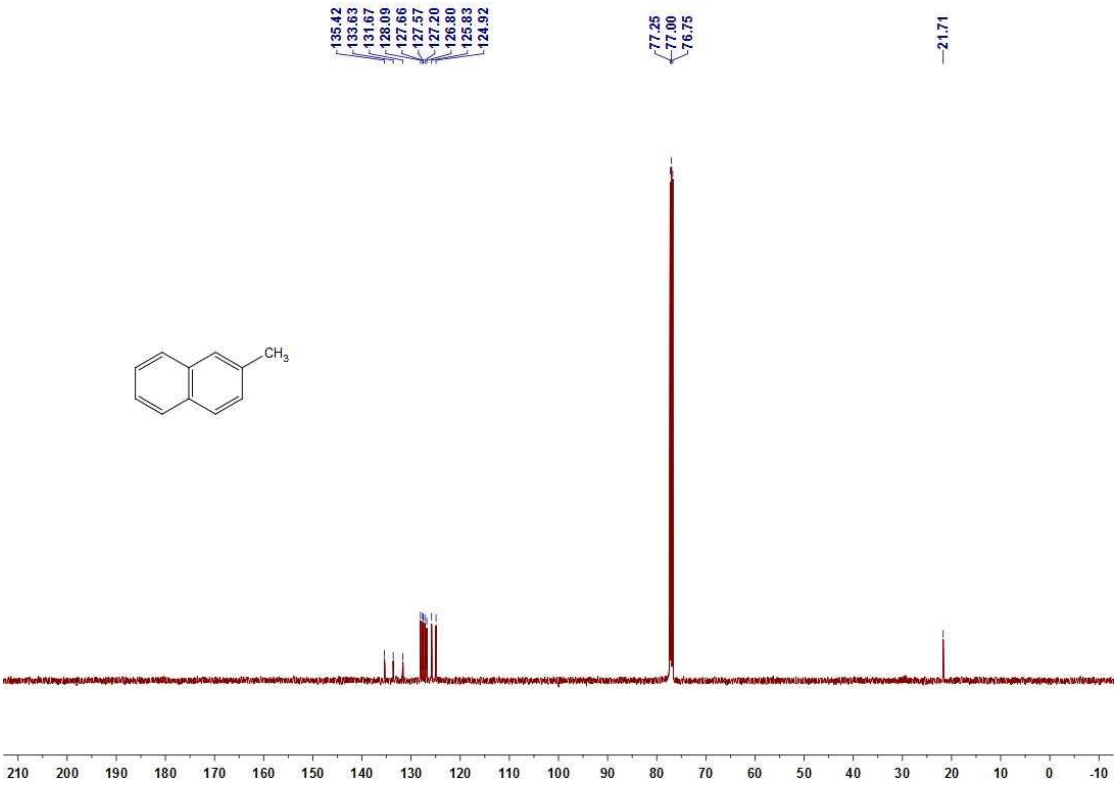

Figure S31. ^{1}H NMR spectrum of compound **1-methylnaphthalene (3q),** related to **Table 2.**

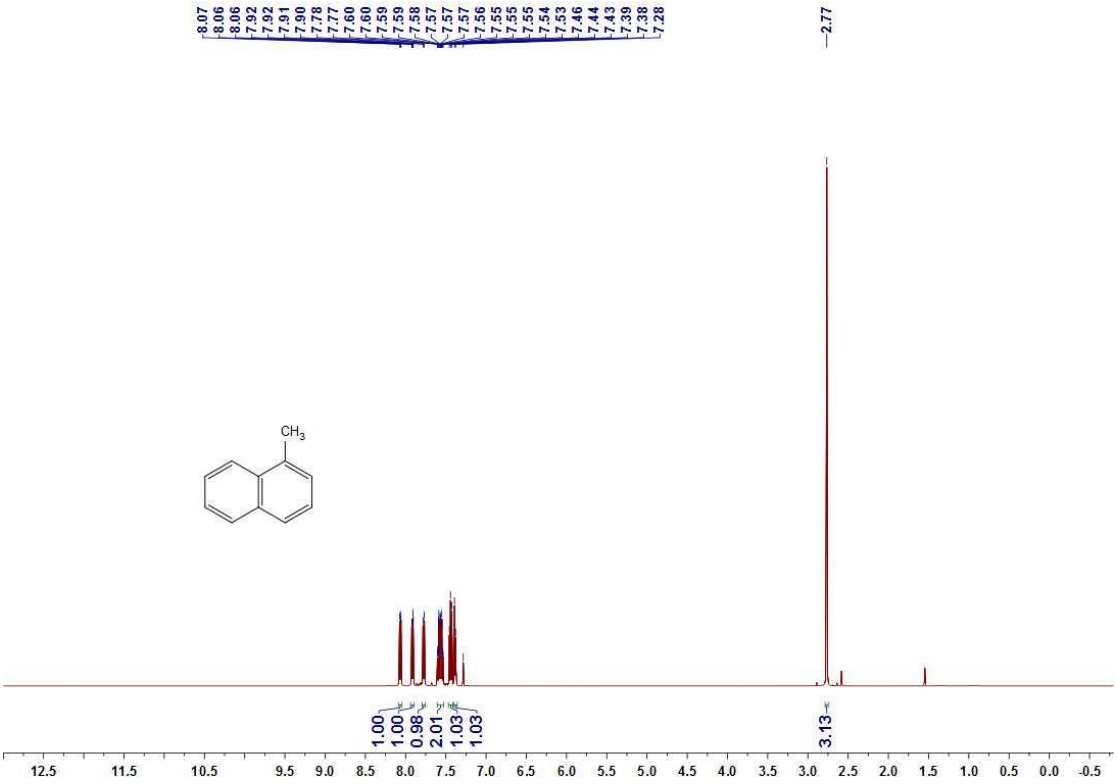

Figure S32. ^{13}C NMR spectrum of compound **1-methylnaphthalene (3q),** related to **Table 2.**

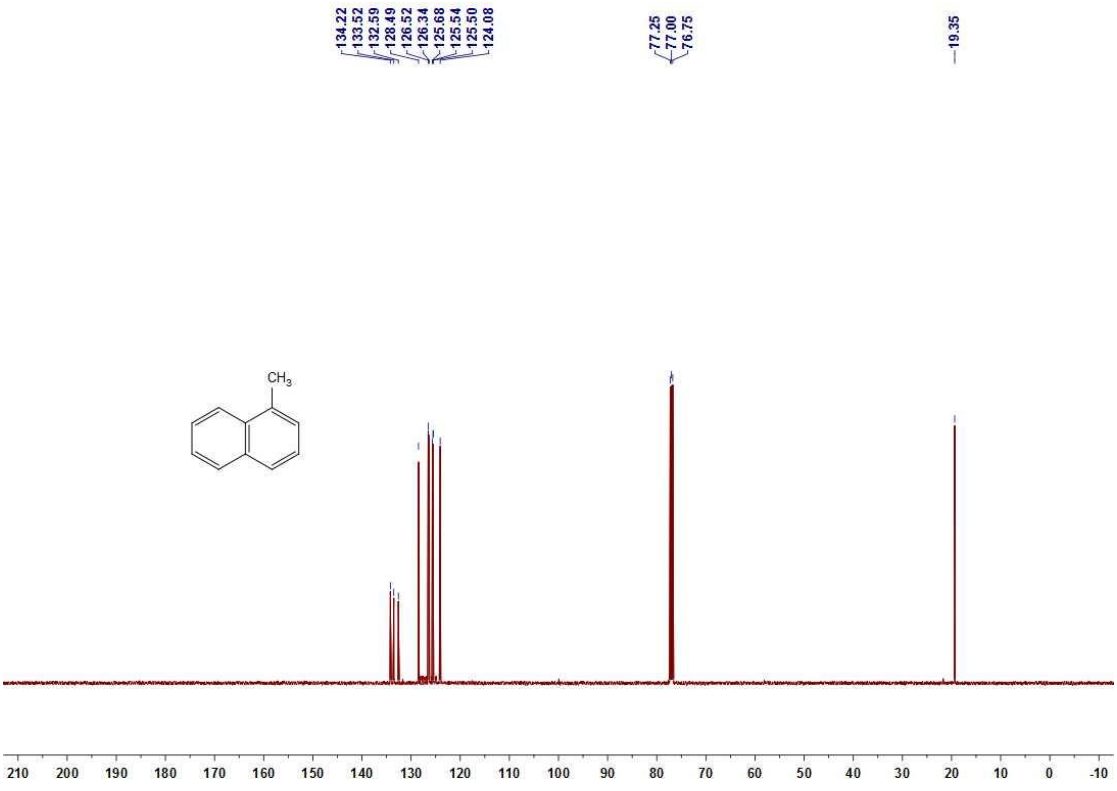

Figure S33. ^{1}H NMR spectrum of compound **9-methylphenanthrene (3r),** related to **Table 2.**

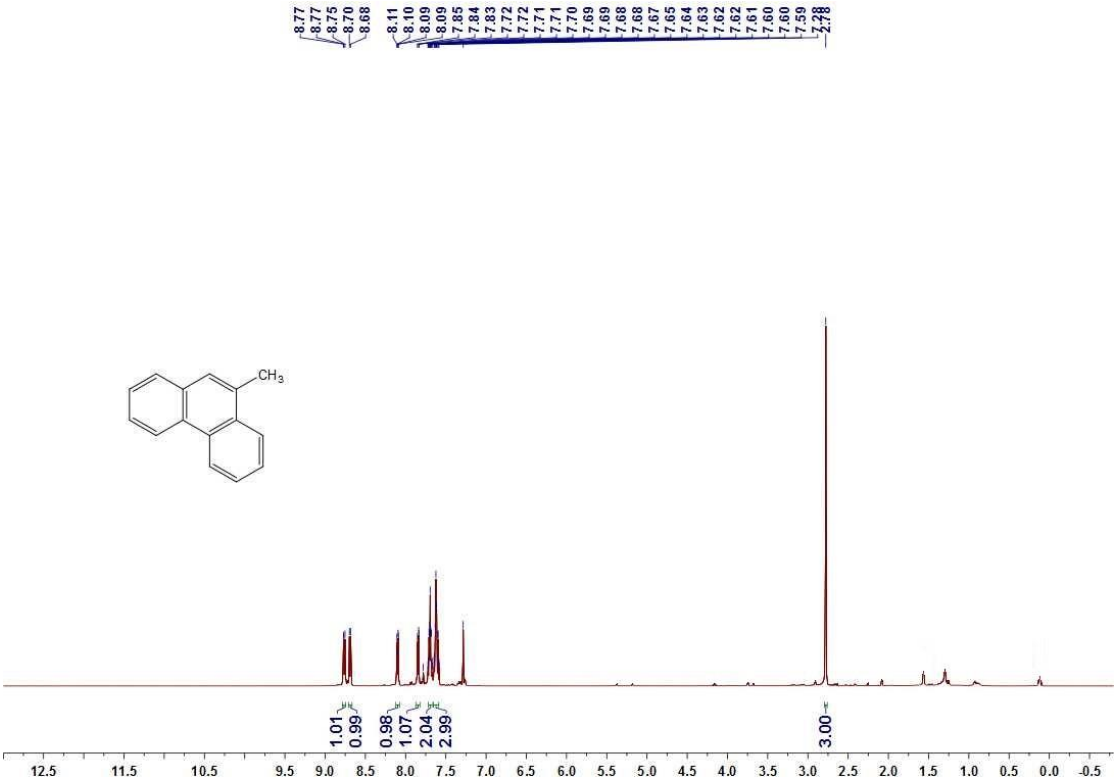

Figure S34. ^{13}C NMR spectrum of compound **9-methylphenanthrene (3r),** related to **Table 2.**

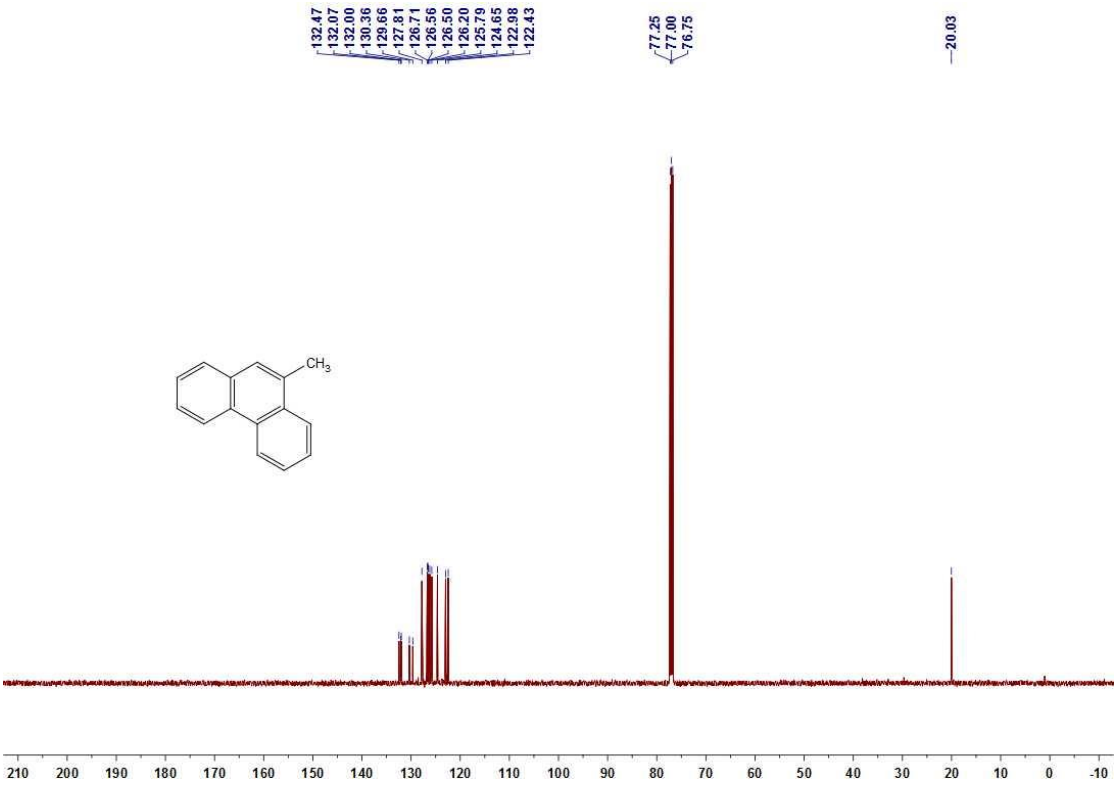

Figure S35. ^{1}H NMR spectrum of compound **2-methylbenzo[*b*]thiophene (3s),** related to **Table 2, Table 5.**

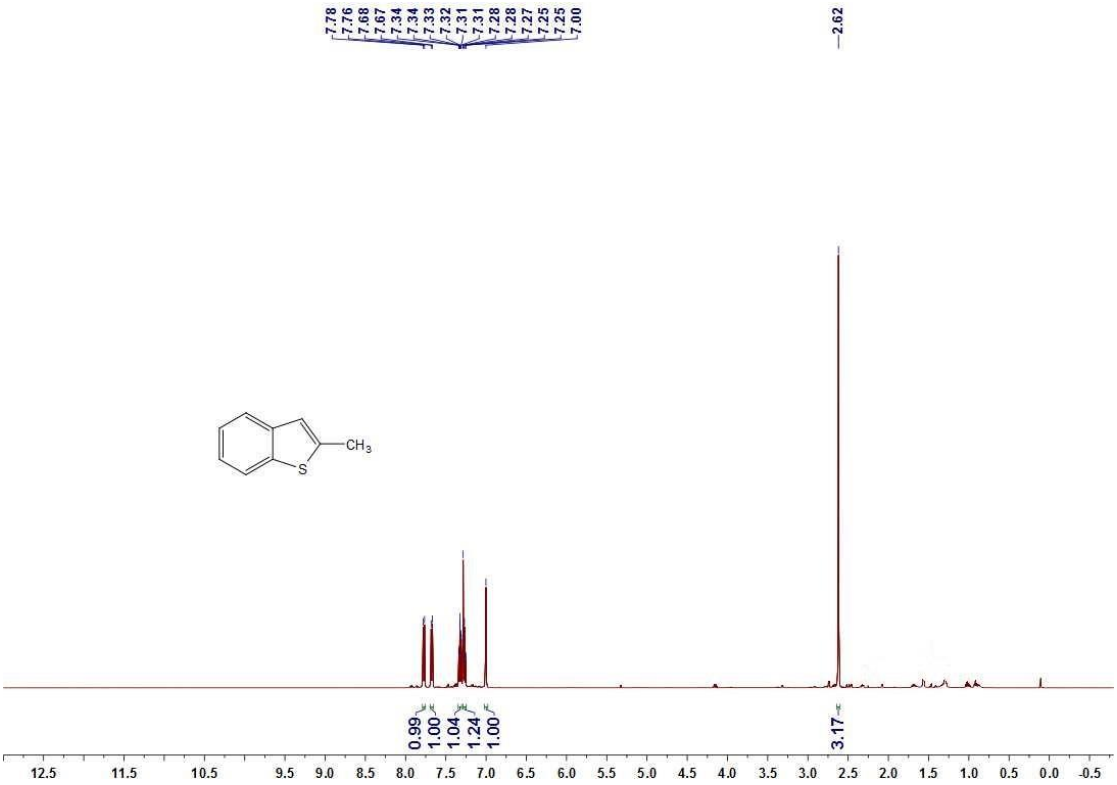

Figure S36. ^{13}C NMR spectrum of compound **2-methylbenzo[*b*]thiophene (3s),** related to **Table 2, Table 5.**

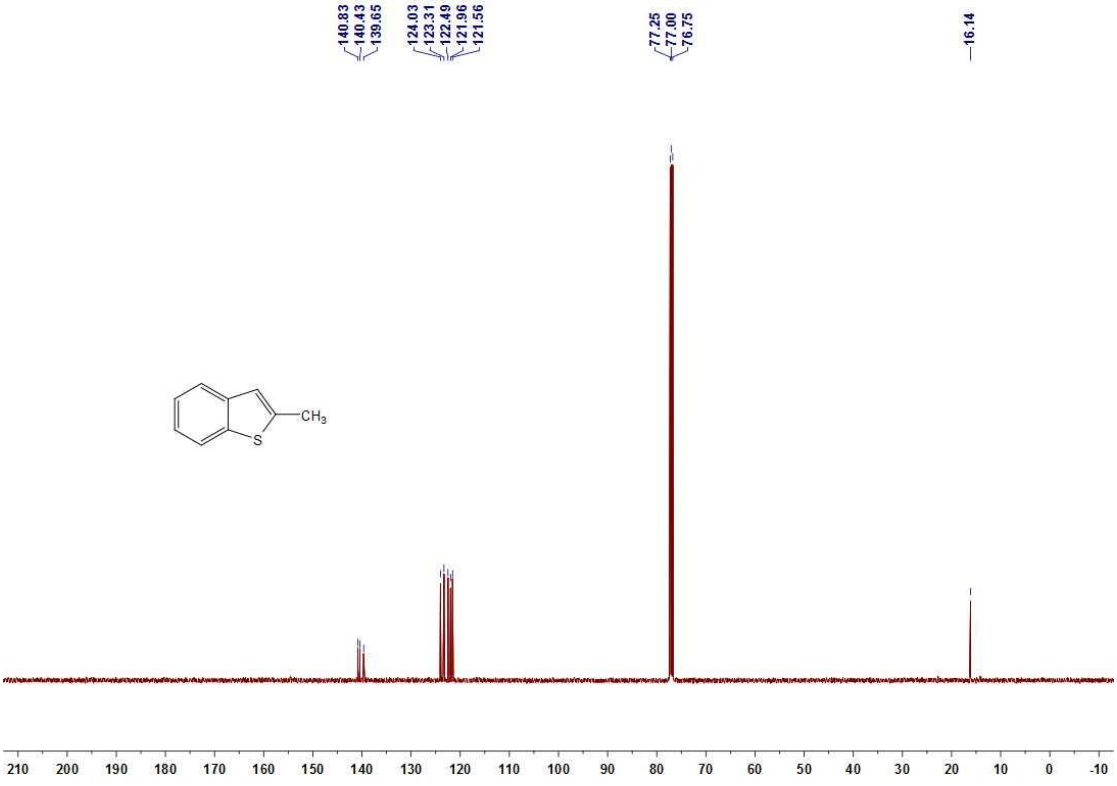

Figure S37. ^{1}H NMR spectrum of compound **2,4-dimethylquinoline (3u),** related to **Table 2, Table 5.**

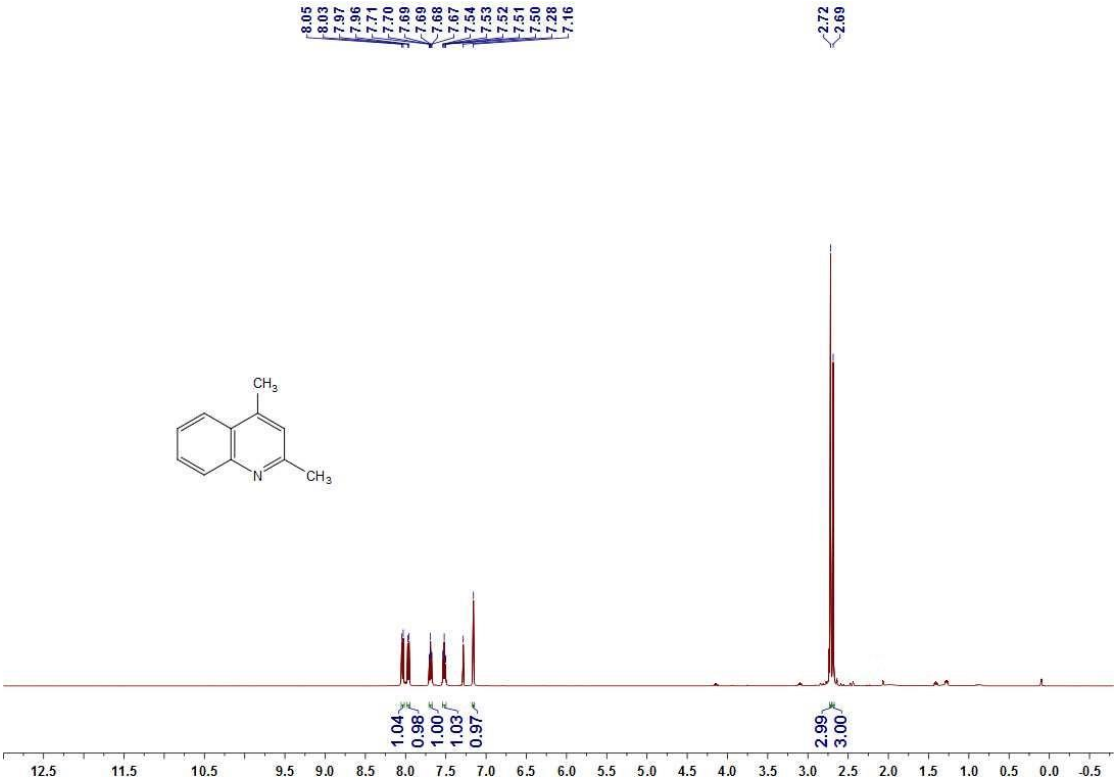

Figure S38. ^{13}C NMR spectrum of compound **2,4-dimethylquinoline (3u),** related to **Table 2, Table 5.**

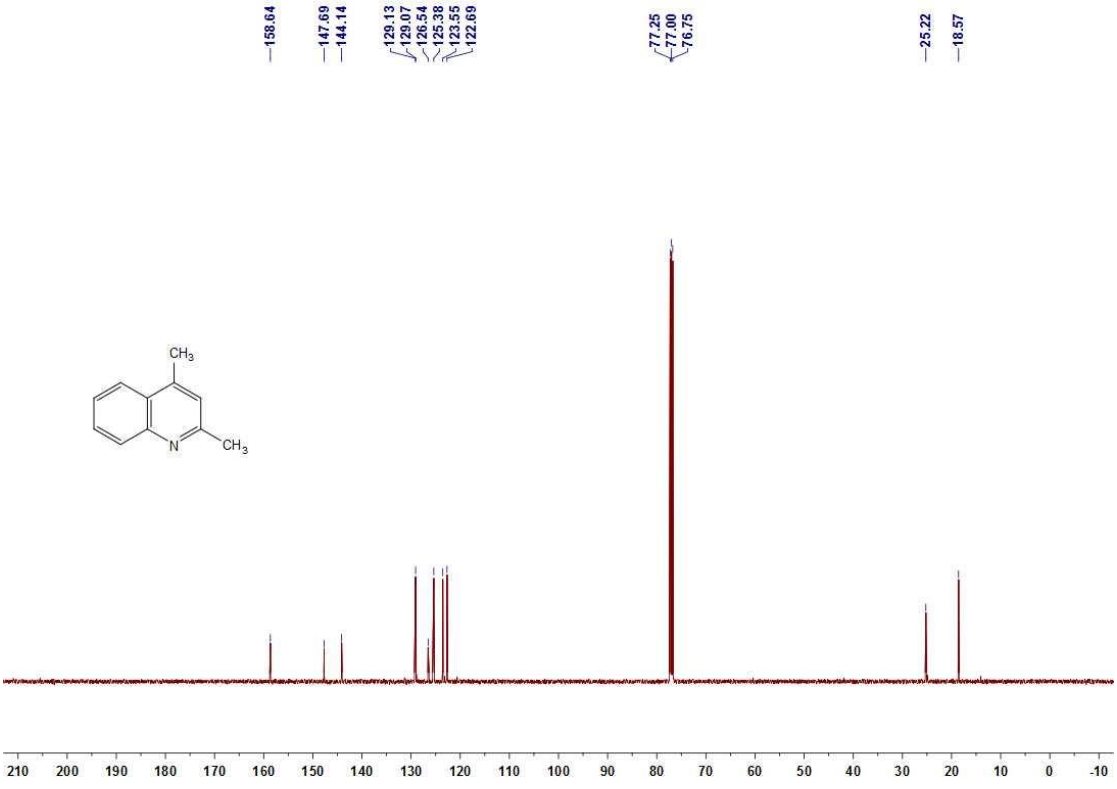

Figure S39. ^{1}H NMR spectrum of compound **1,2,4-trimethylbenzene (3v),** related to **Table 2.**

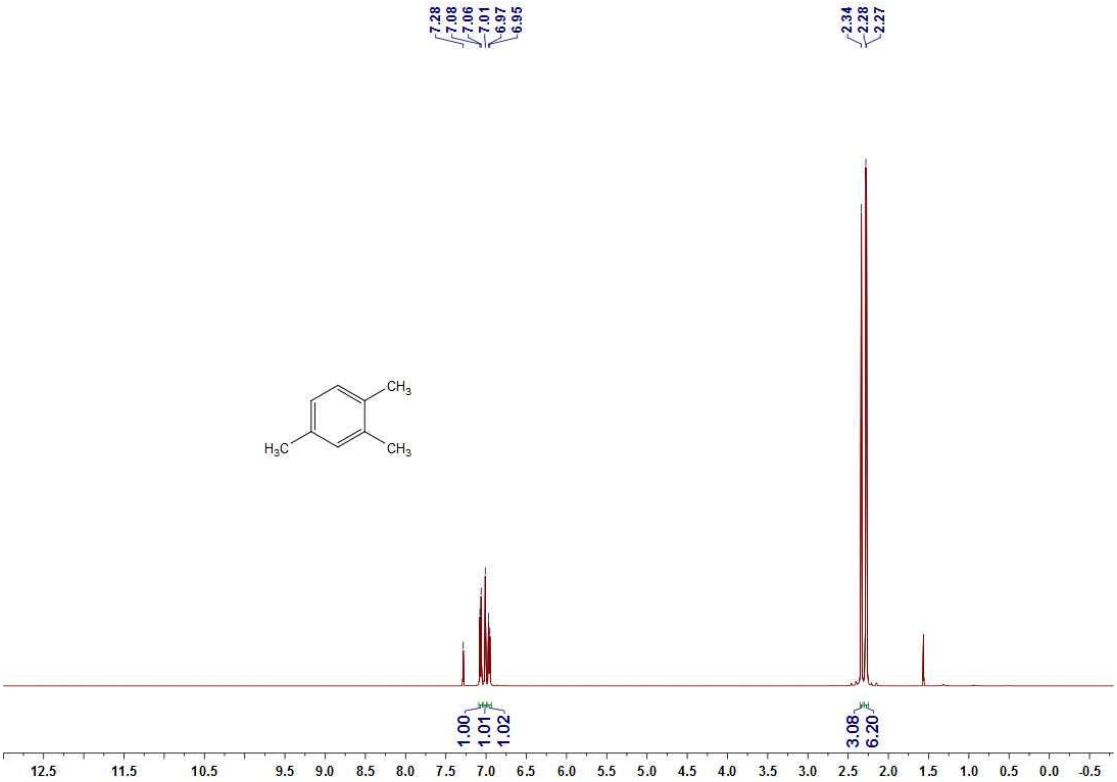

Figure S40. ^{13}C NMR spectrum of compound **1,2,4-trimethylbenzene (3v),** related to **Table 2.**

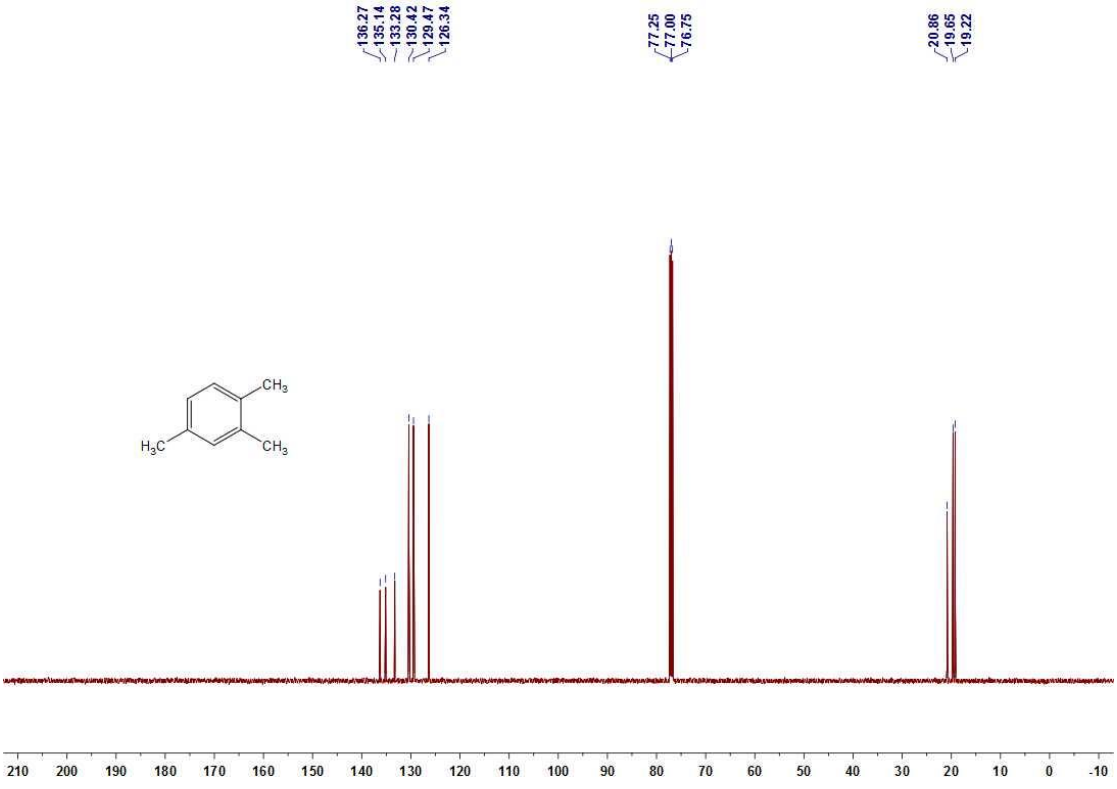

Figure S41. ^{1}H NMR spectrum of compound **1-ethyl-3-methoxybenzene (3aa),** related to **Table 2.**

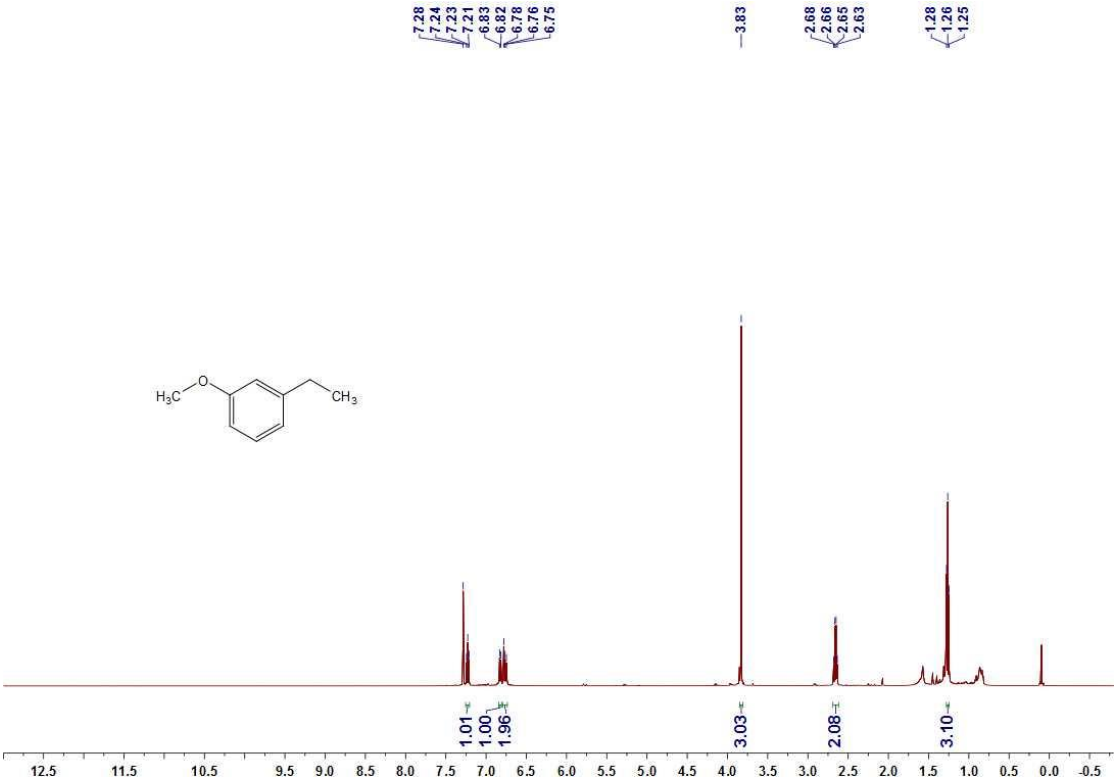

Figure S42. ^{13}C NMR spectrum of compound **1-ethyl-3-methoxybenzene (3aa),** related to **Table 2.**

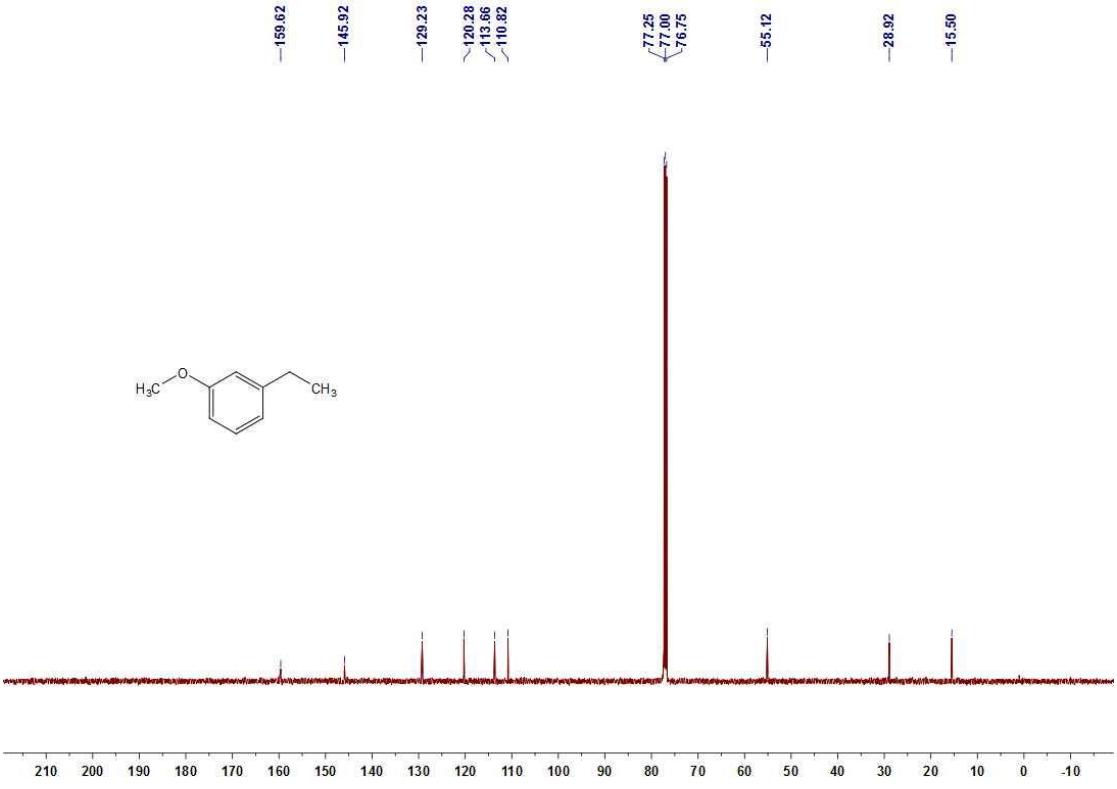

Figure S43. ^{1}H NMR spectrum of compound **1-ethyl-2-methoxybenzene (3ab),** related to **Table 2.**

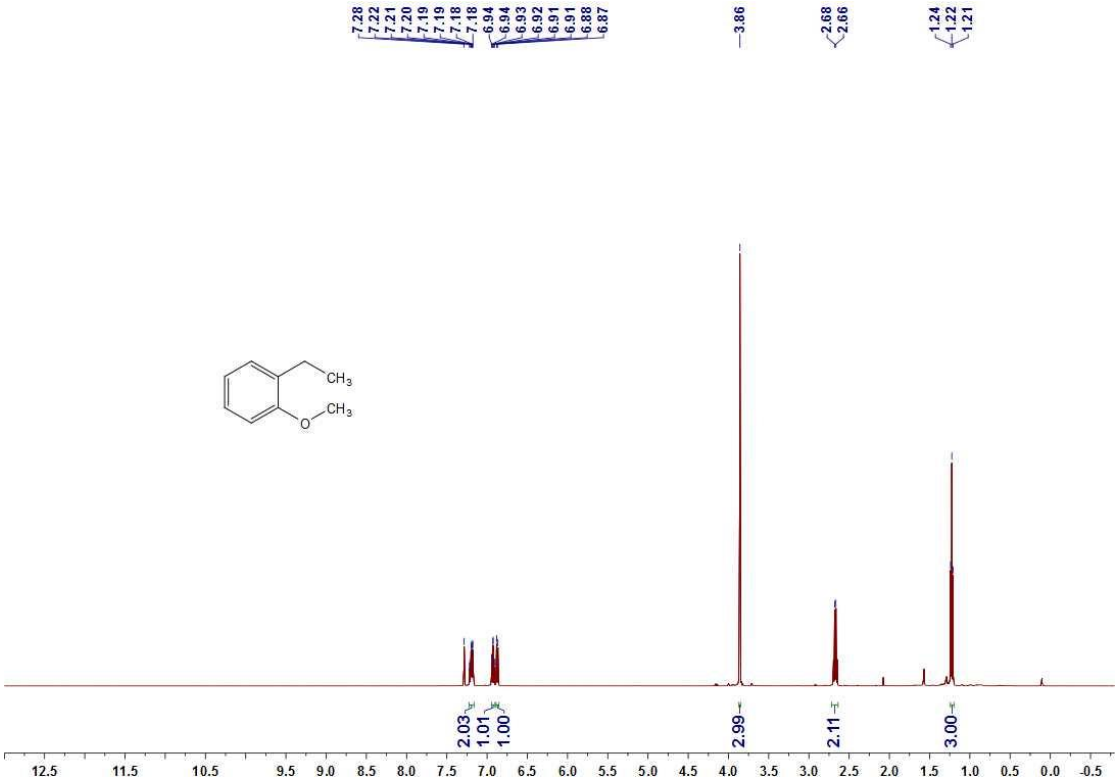

Figure S44. ^{13}C NMR spectrum of compound **1-ethyl-2-methoxybenzene (3ab),** related to **Table 2.**

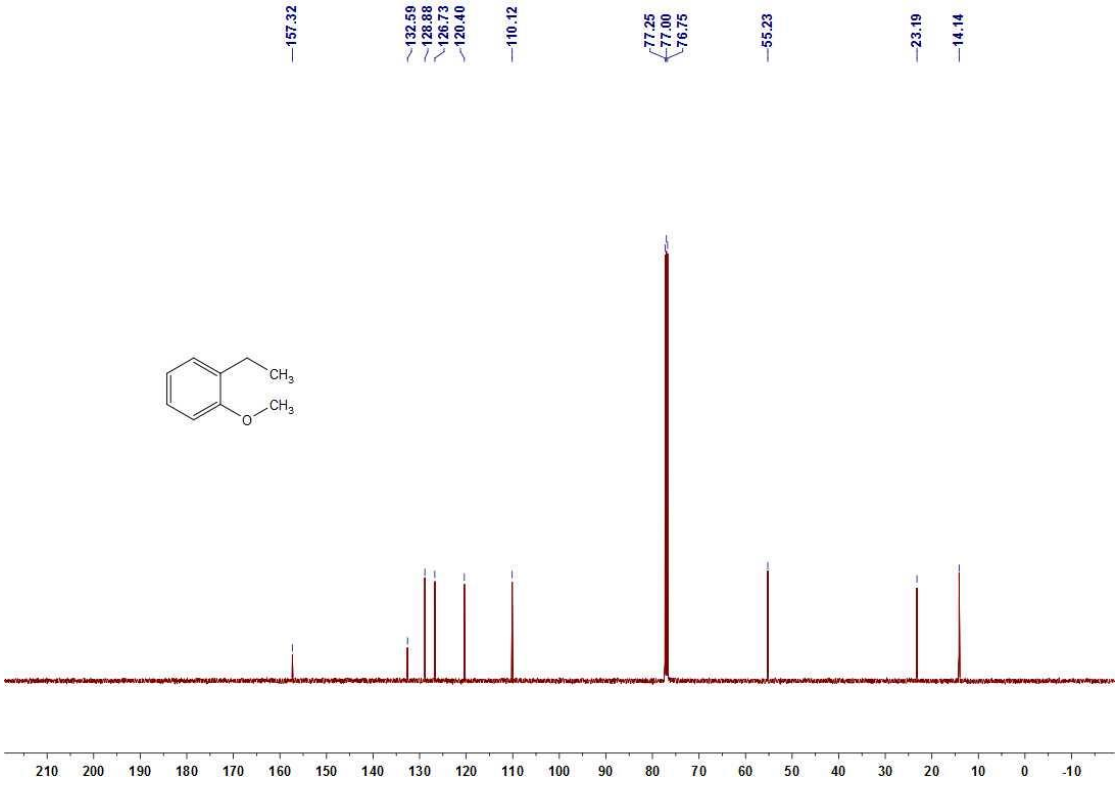

Figure S45. ^{1}H NMR spectrum of compound **hexylbenzene (3ac),** related to **Table 2, Table 5.**

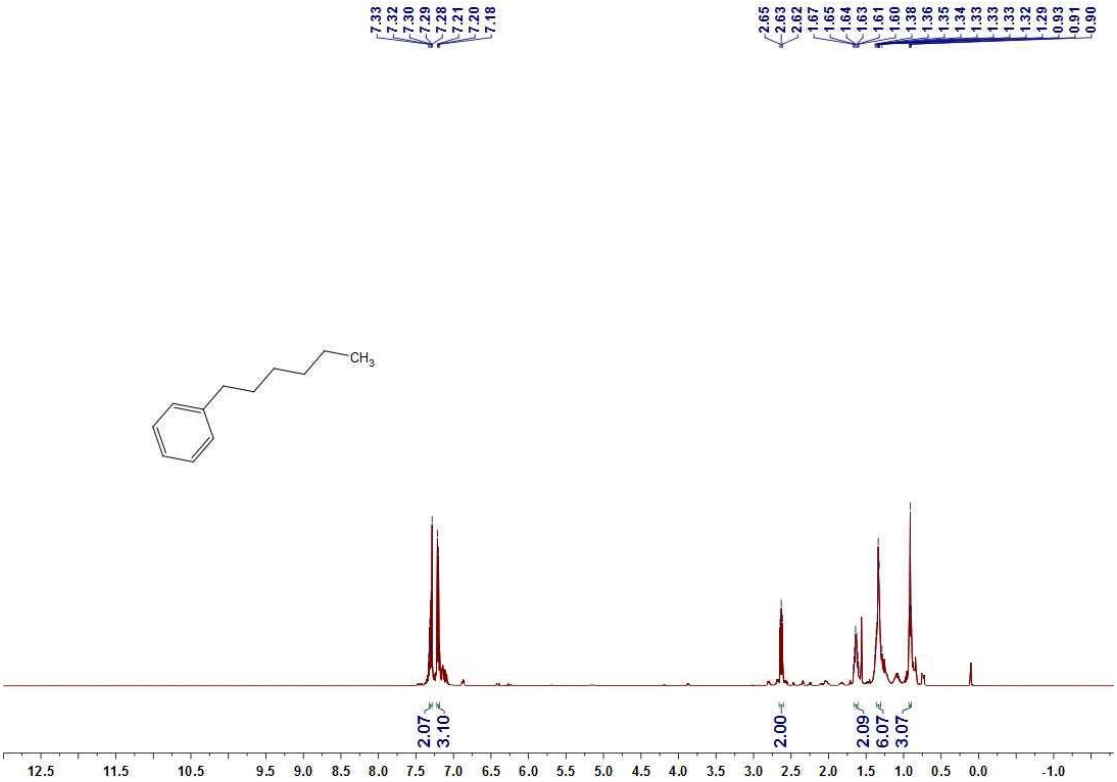

Figure S46. ^{13}C NMR spectrum of compound **hexylbenzene (3ac),** related to **Table 2, Table 5.**

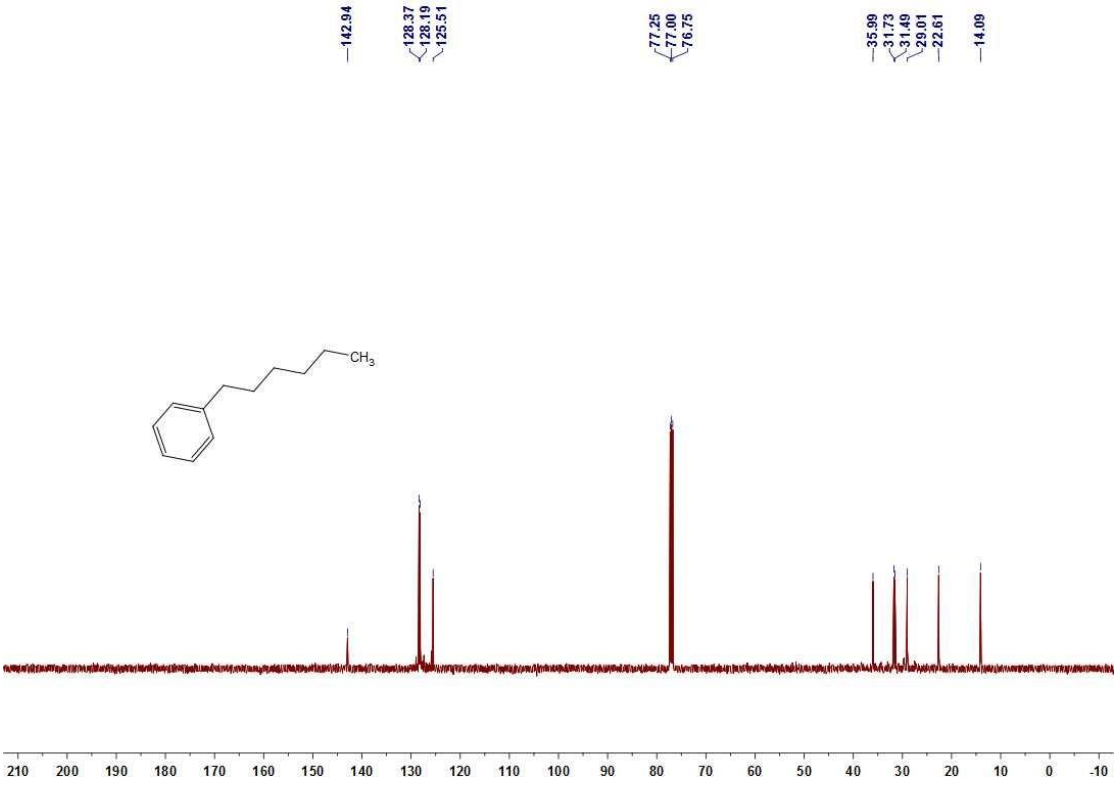

Figure S47. ^{1}H NMR spectrum of compound **1,2-diphenylethane (3ad),** related to **Table 2.**

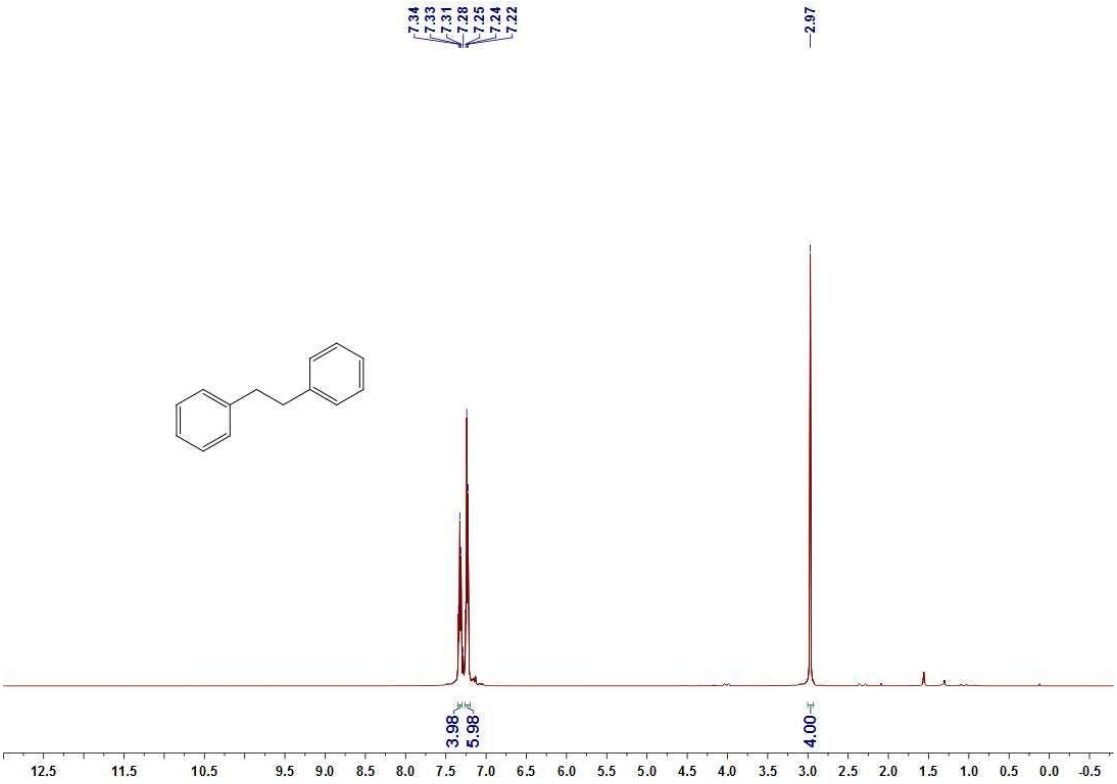

Figure S48. ^{13}C NMR spectrum of compound **1,2-diphenylethane (3ad),** related to **Table 2.**

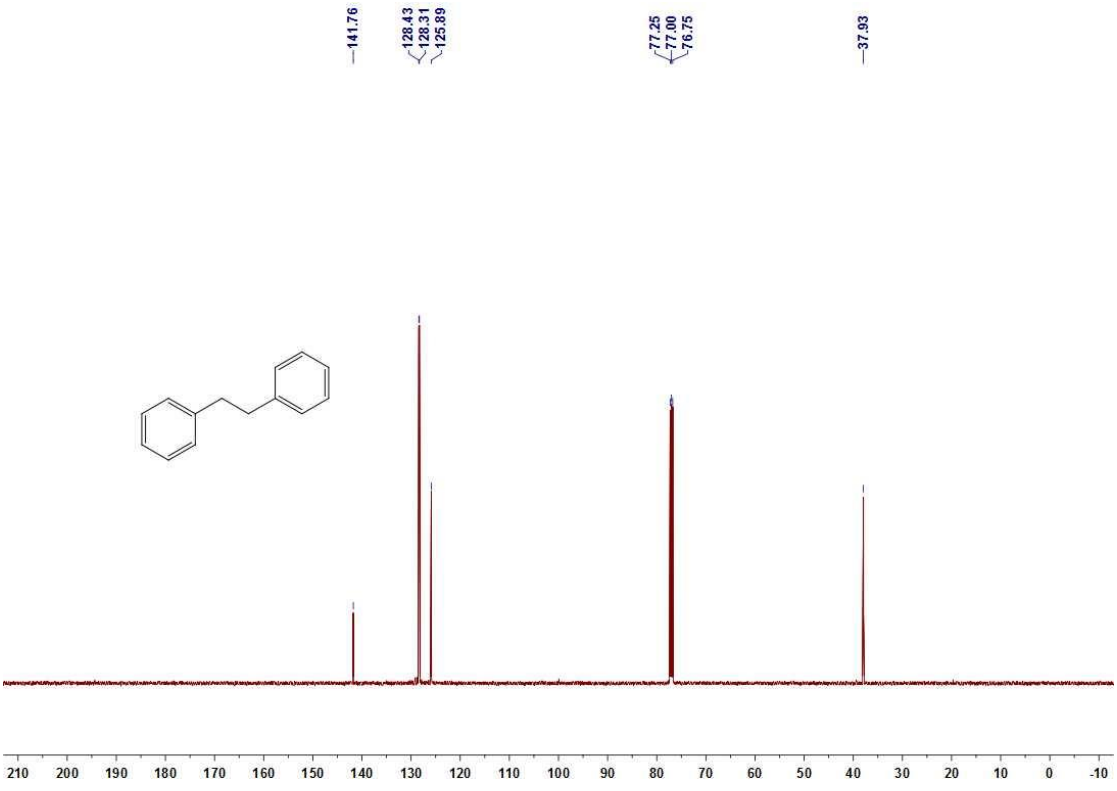

Figure S49. ^{1}H NMR spectrum of compound **diphenylmethane (3ae),** related to **Table 2.**

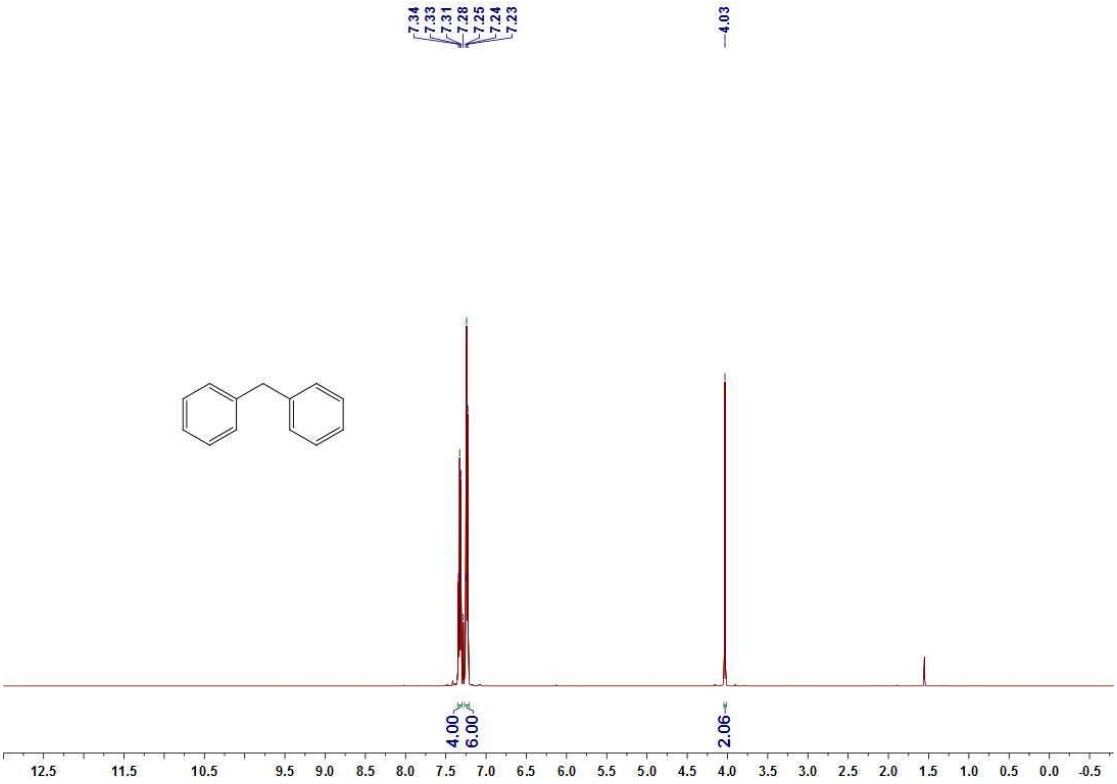

Figure S50. ^{13}C NMR spectrum of compound **diphenylmethane (3ae),** related to **Table 2.**

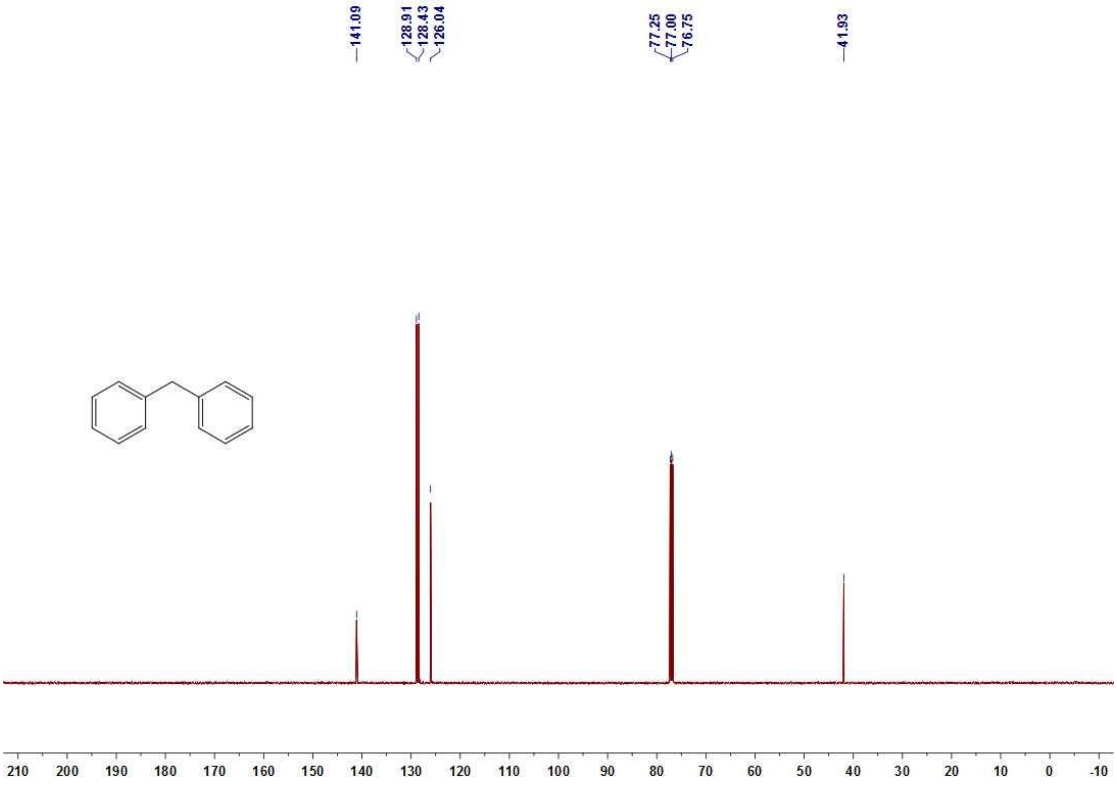

Figure S51. ^{1}H NMR spectrum of compound **di-*p*-tolylmethane (3af),** related to **Table 2, Table 5.**

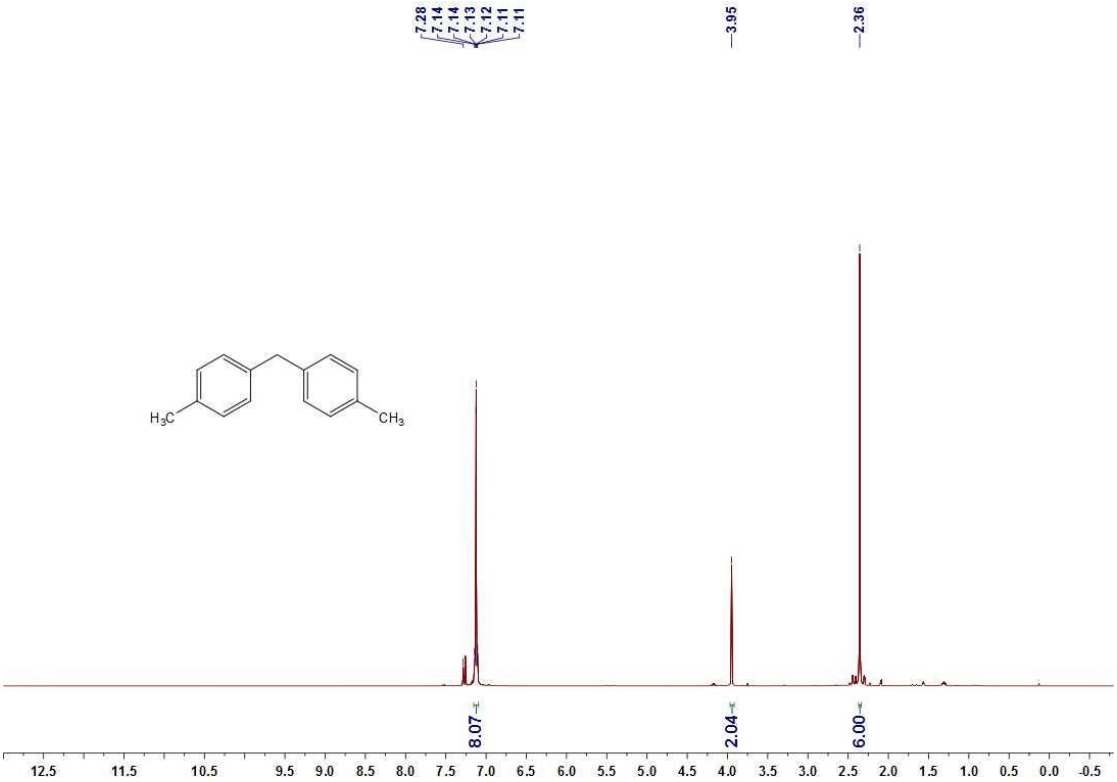

Figure S52. ^{13}C NMR spectrum of compound **di-*p*-tolylmethane (3af),** related to **Table 2, Table 5.**

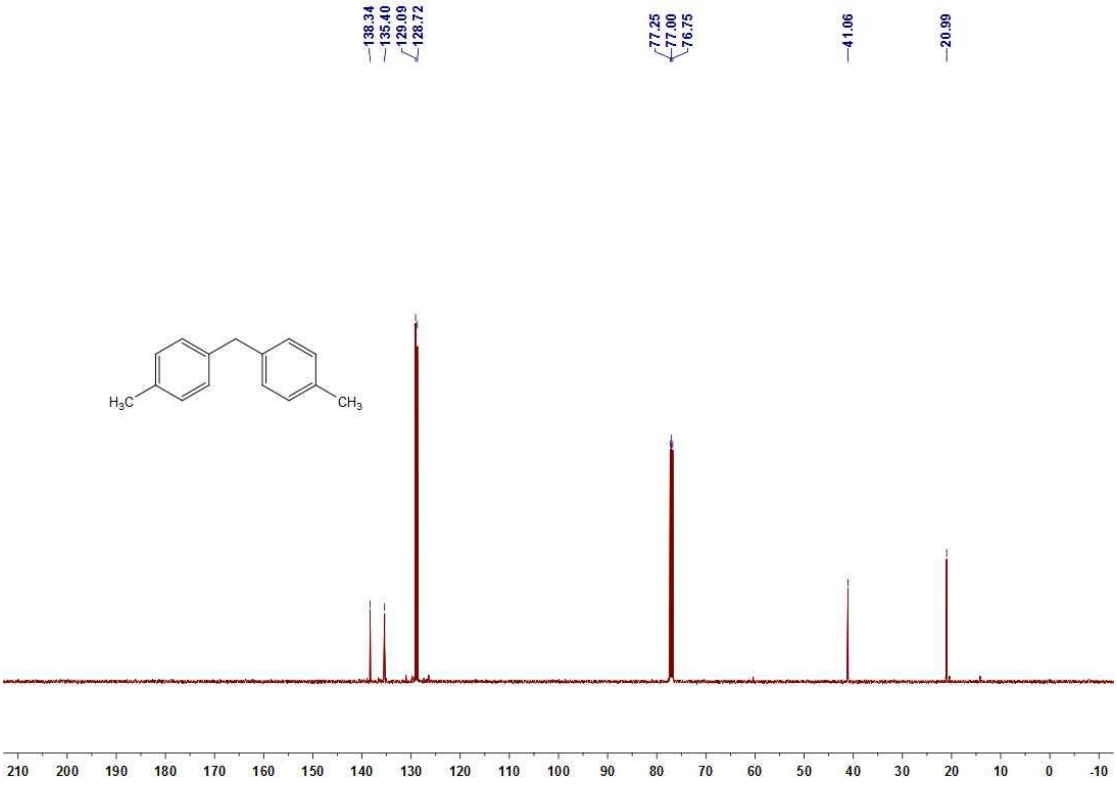

Figure S53. ^{1}H NMR spectrum of compound **1-benzyl-4-methylbenzene (3ag),** related to **Table 2.**

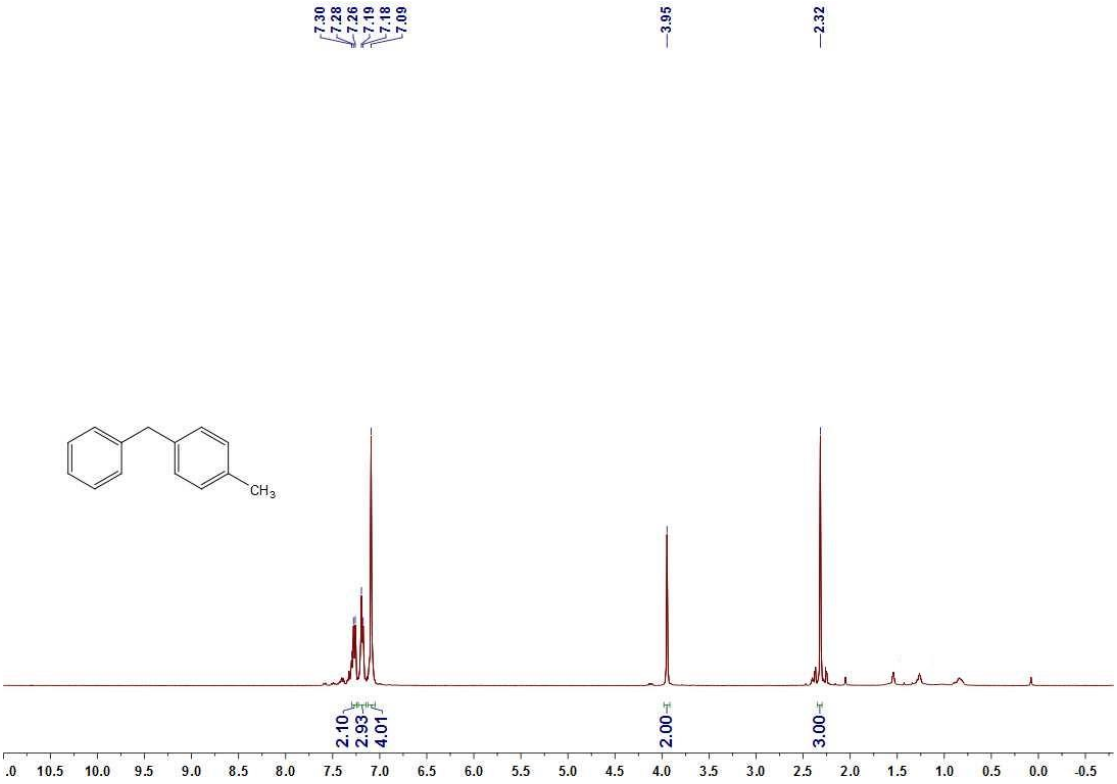

Figure S54. ^{13}C NMR spectrum of compound **1-benzyl-4-methylbenzene (3ag),** related to **Table 2.**

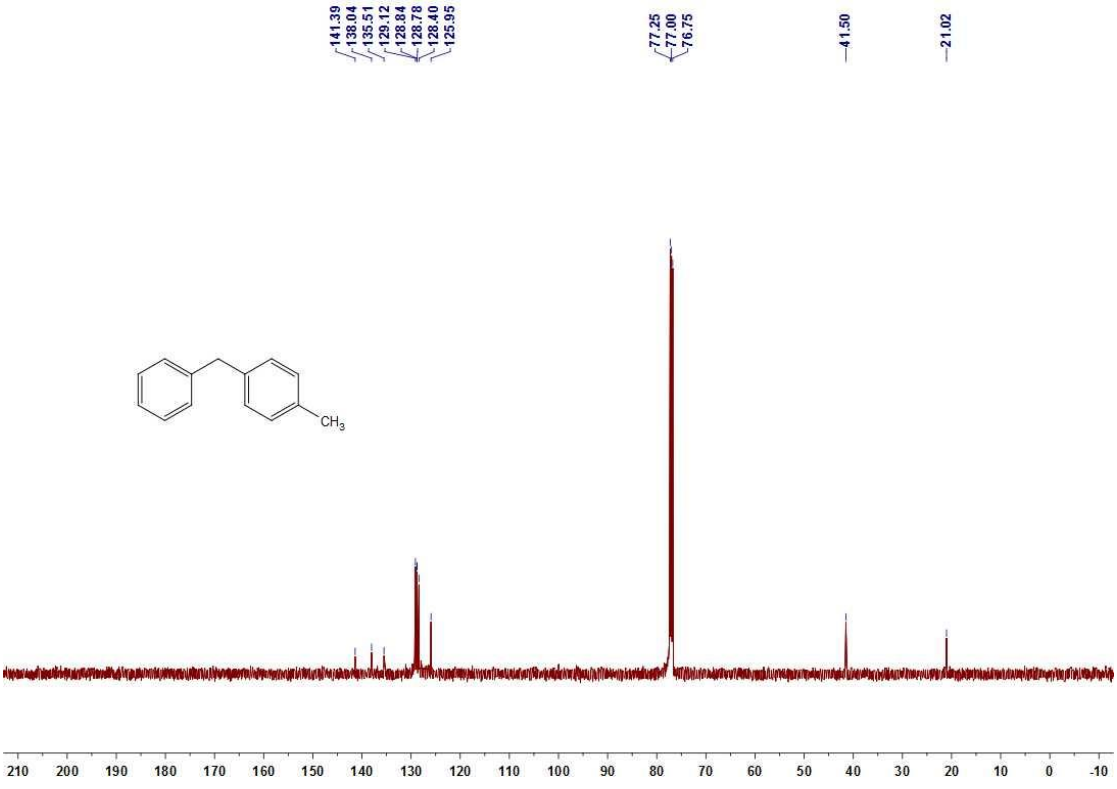

Figure S55. ^{1}H NMR spectrum of compound **2,3-dihydro-1*H*-indene (3ah),** related to **Table 2.**

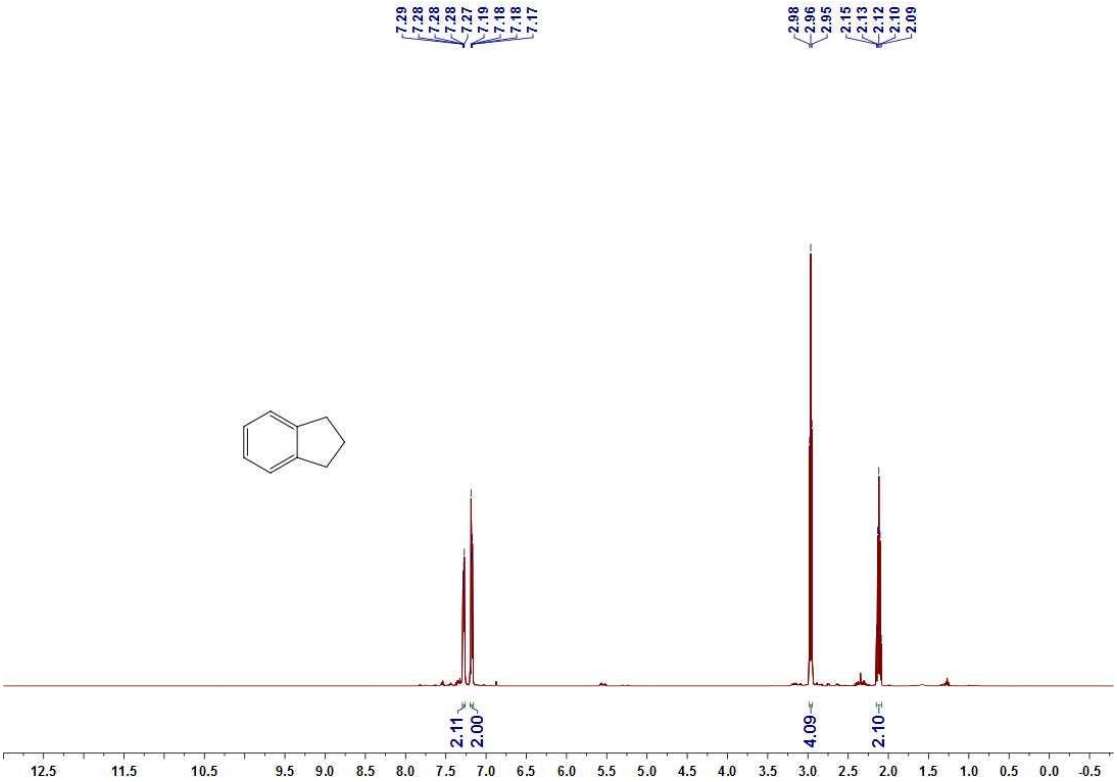

Figure S56. ^{13}C NMR spectrum of compound **2,3-dihydro-1*H*-indene (3ah),** related to **Table 2.**

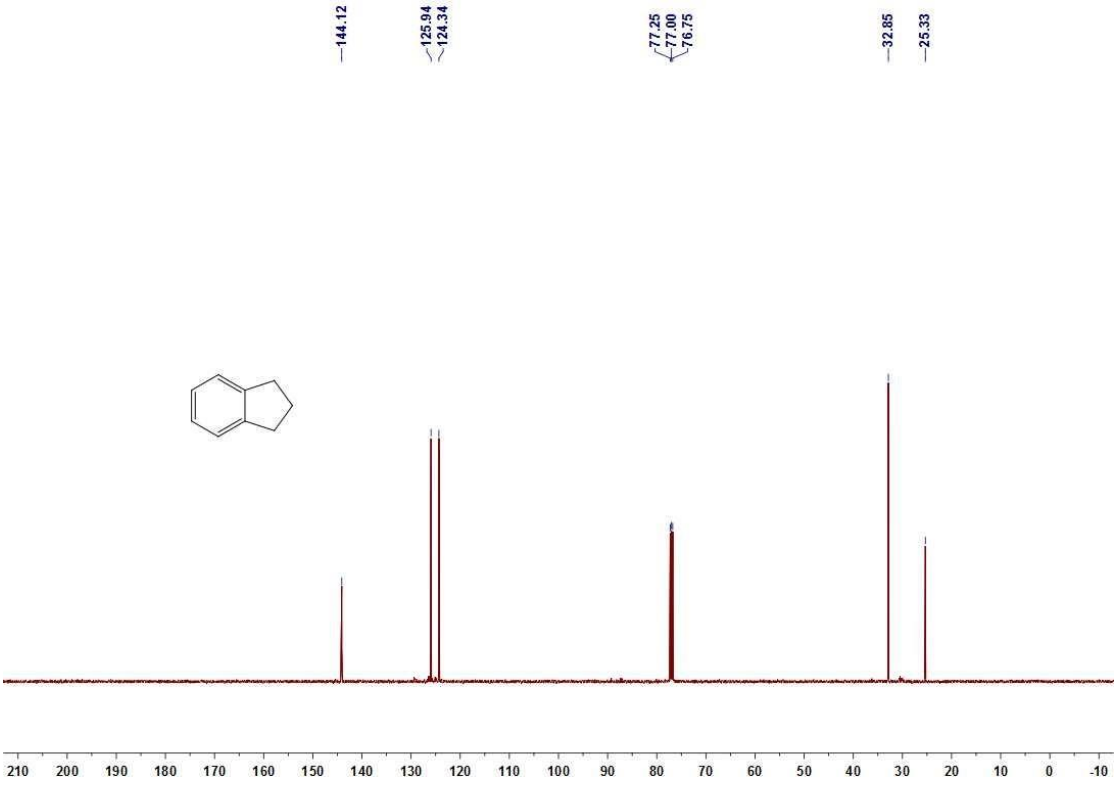

Figure S57. ^{1}H NMR spectrum of compound **chroman (3ai),** related to **Table 2, Table 5.**

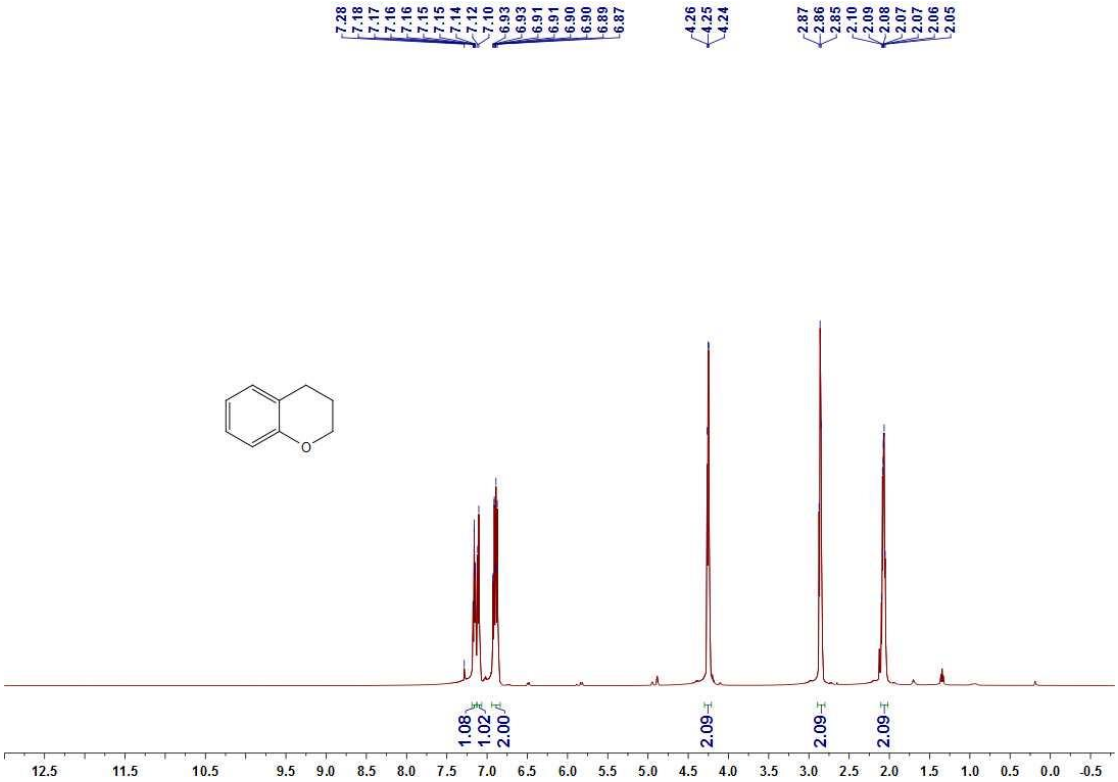

Figure S58. ^{13}C NMR spectrum of compound **chroman (3ai),** related to **Table 2, Table 5.**

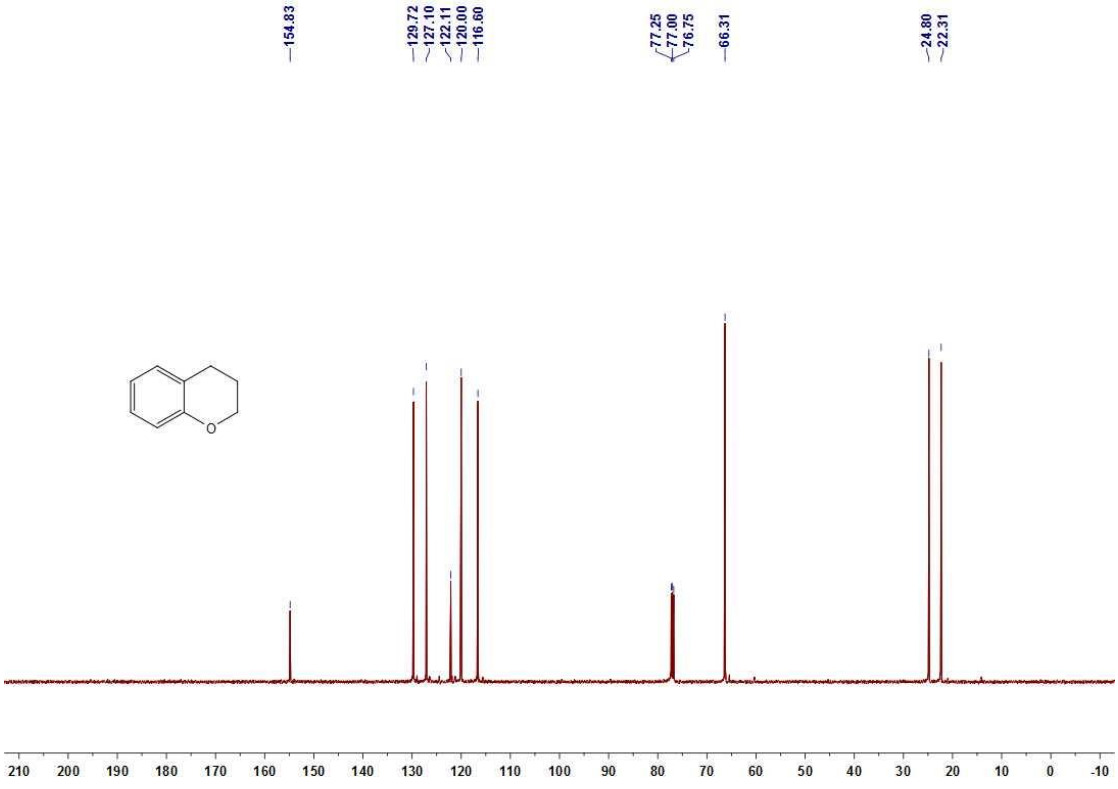

Figure S59. ^{1}H NMR spectrum of compound **9*H*-xanthene (3aj),** related to **Table 2.**

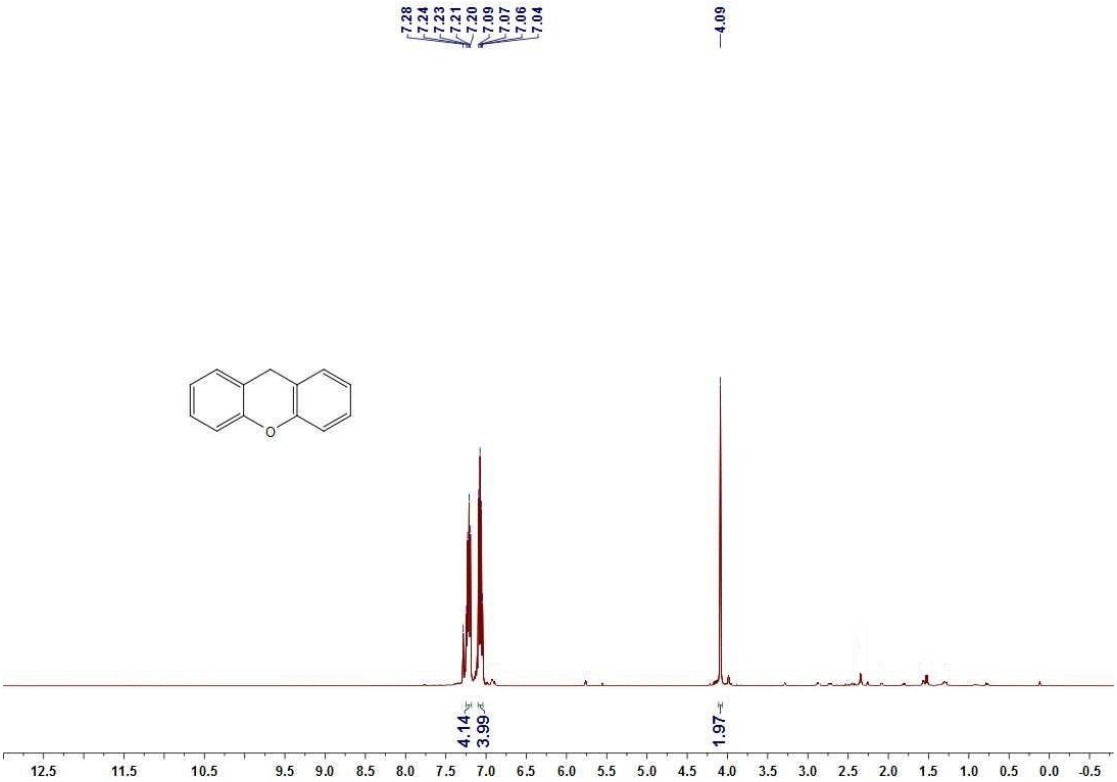

Figure S60. ^{13}C NMR spectrum of compound **9*H*-xanthene (3aj),** related to **Table 2.**

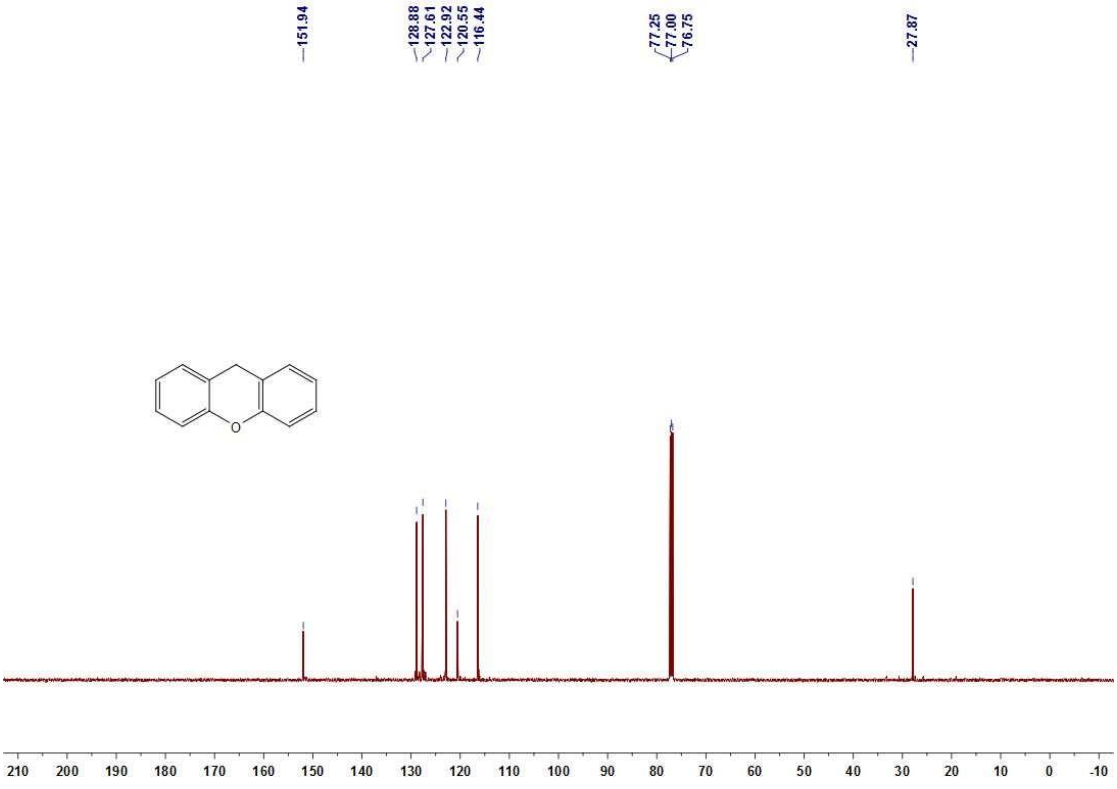

Figure S61. ^{1}H NMR spectrum of compound **2-phenylethanol (3ak),** related to **Table 3.**

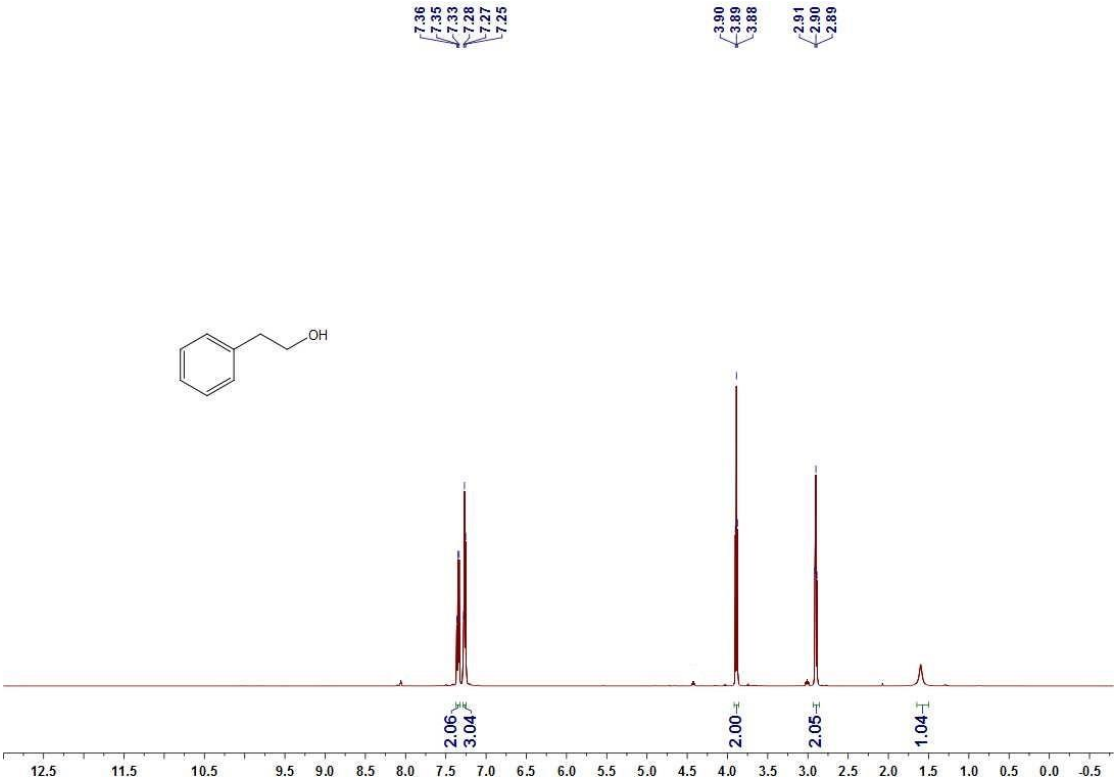

Figure S62. ^{13}C NMR spectrum of compound **2-phenylethanol (3ak),** related to **Table 3.**

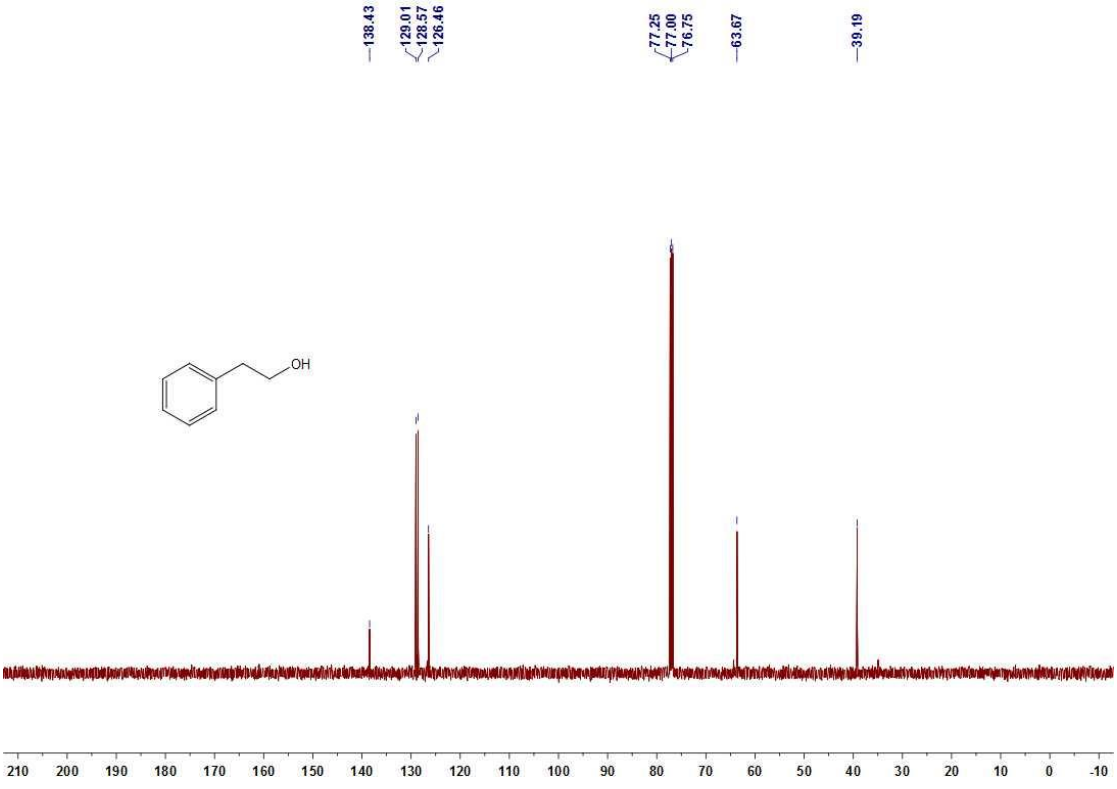

Figure S63. ^{1}H NMR spectrum of compound **1-methoxy-4-methylbenzene (3al),** related to **Table 3**, **Table 4.**

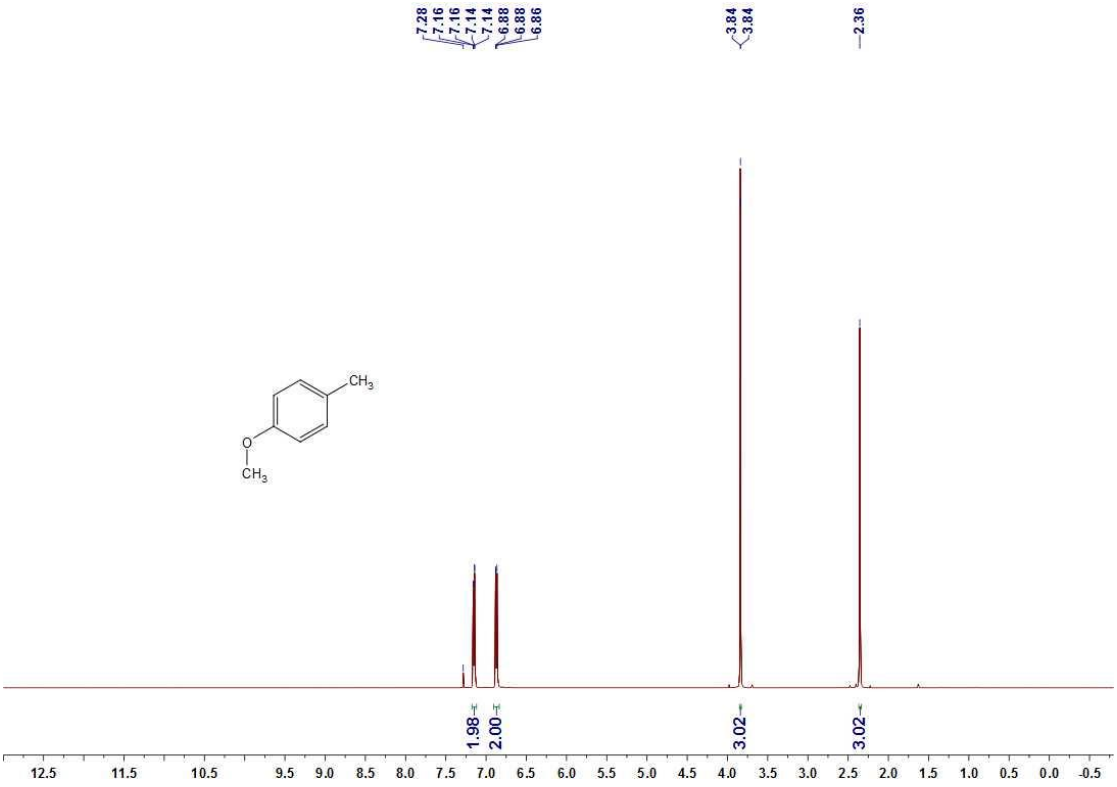

Figure S64. ^{13}C NMR spectrum of compound **1-methoxy-4-methylbenzene (3al),** related to **Table 3**, **Table 4.**

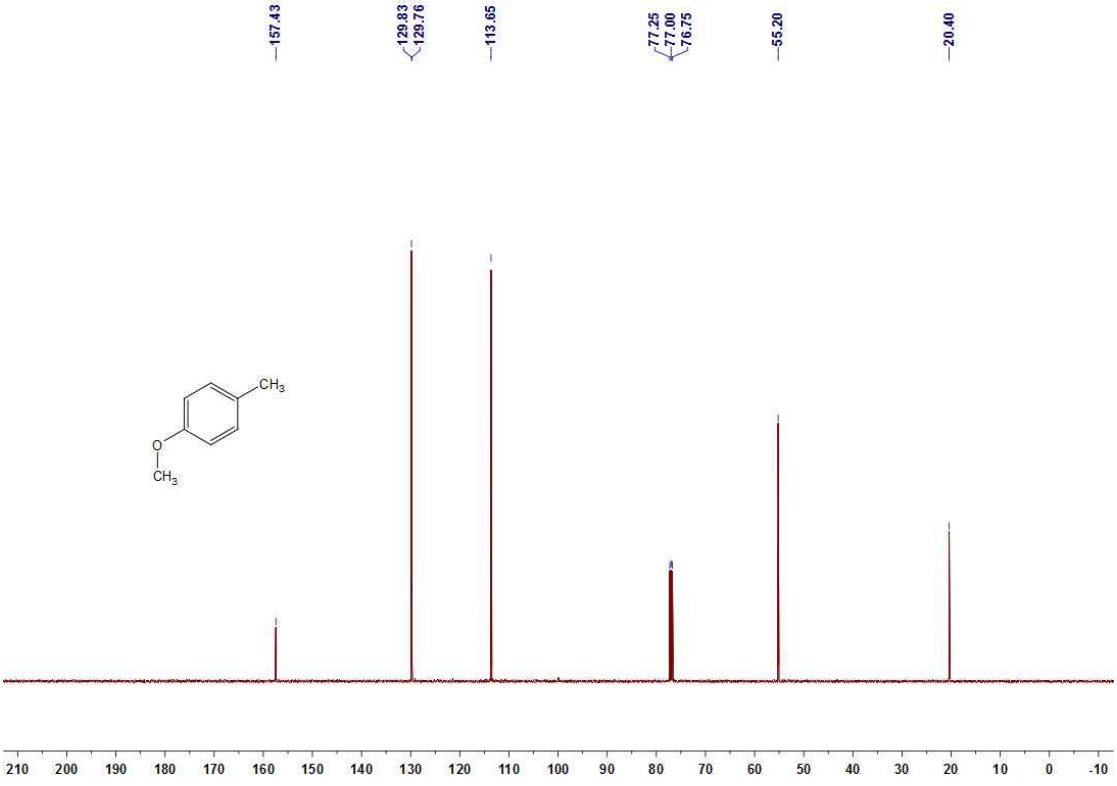

Figure S65. ^{1}H NMR spectrum of compound ***N,N,*4-trimethylaniline (3am),** related to **Table 3.**

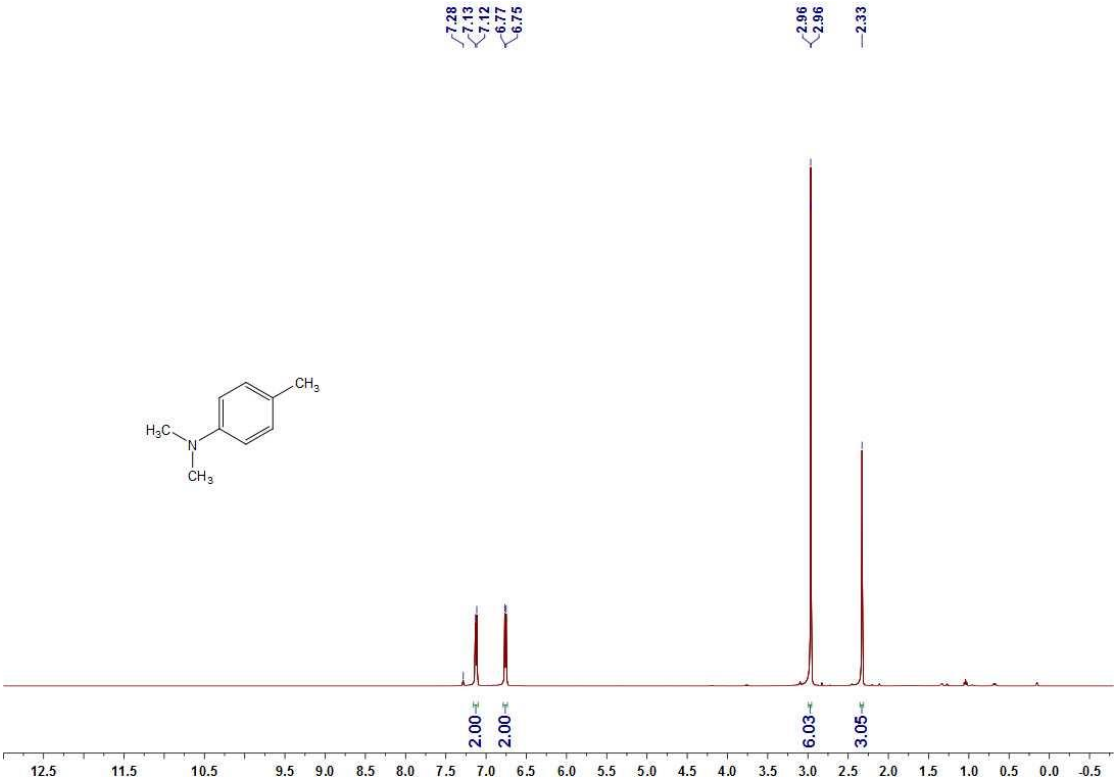

Figure S66. ^{13}C NMR spectrum of compound ***N,N,*4-trimethylaniline (3am),** related to **Table 3.**

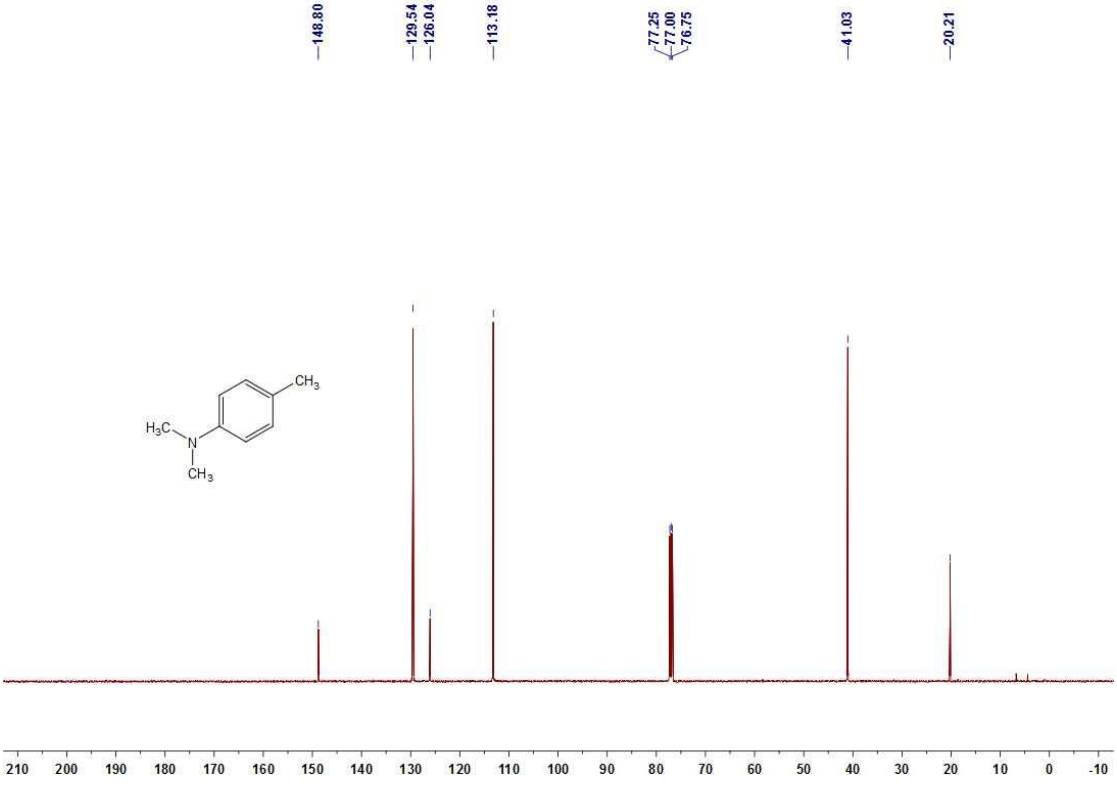

Figure S67. ^{1}H NMR spectrum of compound **1-ethyl-4-methoxybenzene (3an),** related to **Table 4.**

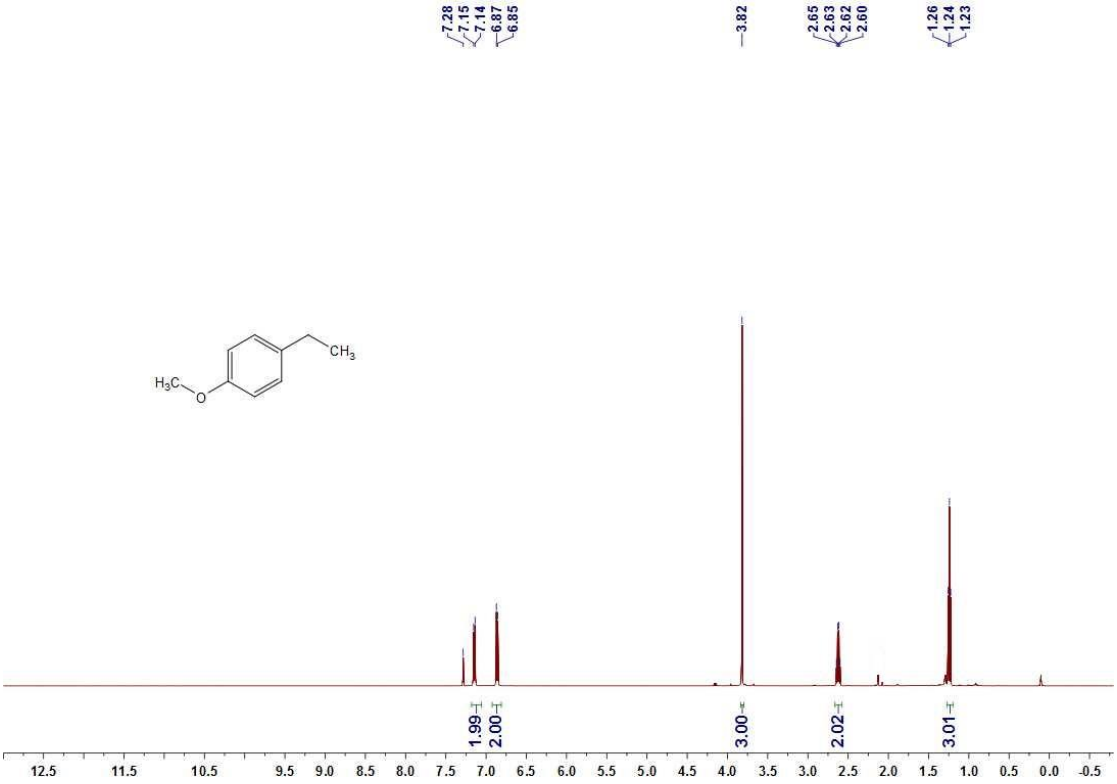

Figure S68. ^{13}C NMR spectrum of compound **1-ethyl-4-methoxybenzene (3an),** related to **Table 4.**

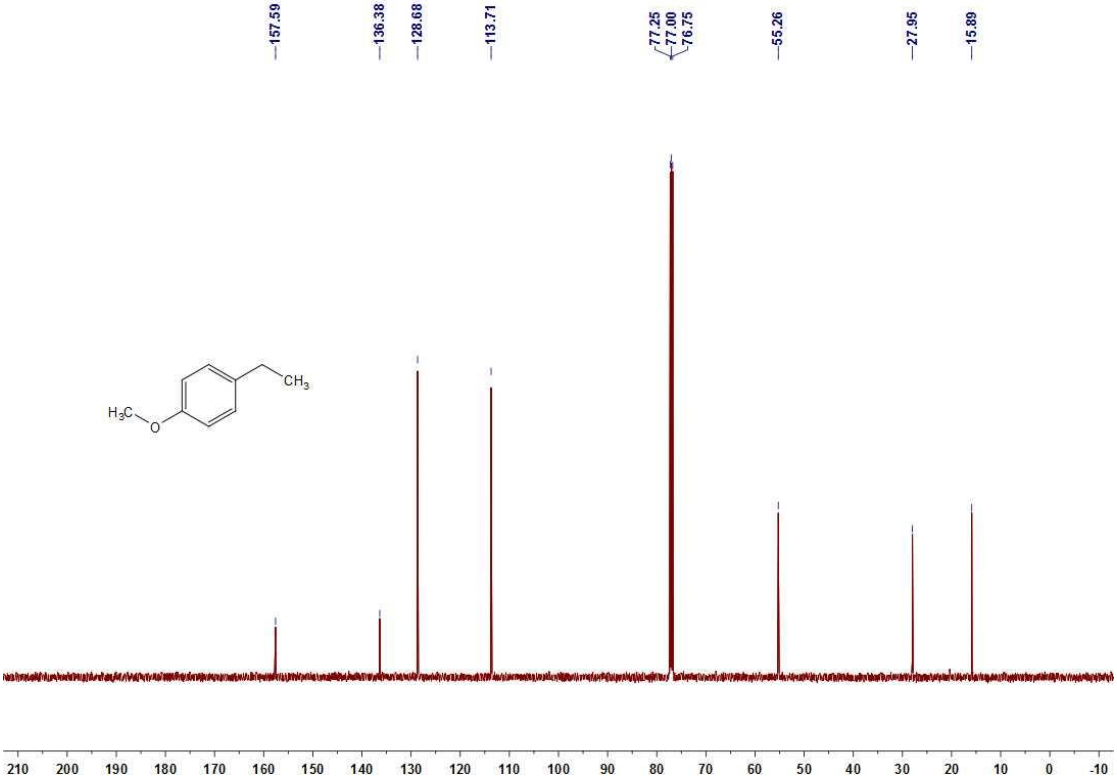

Figure S69. ^{1}H NMR spectrum of compound **phenol (4a),** related to **Table 4.**

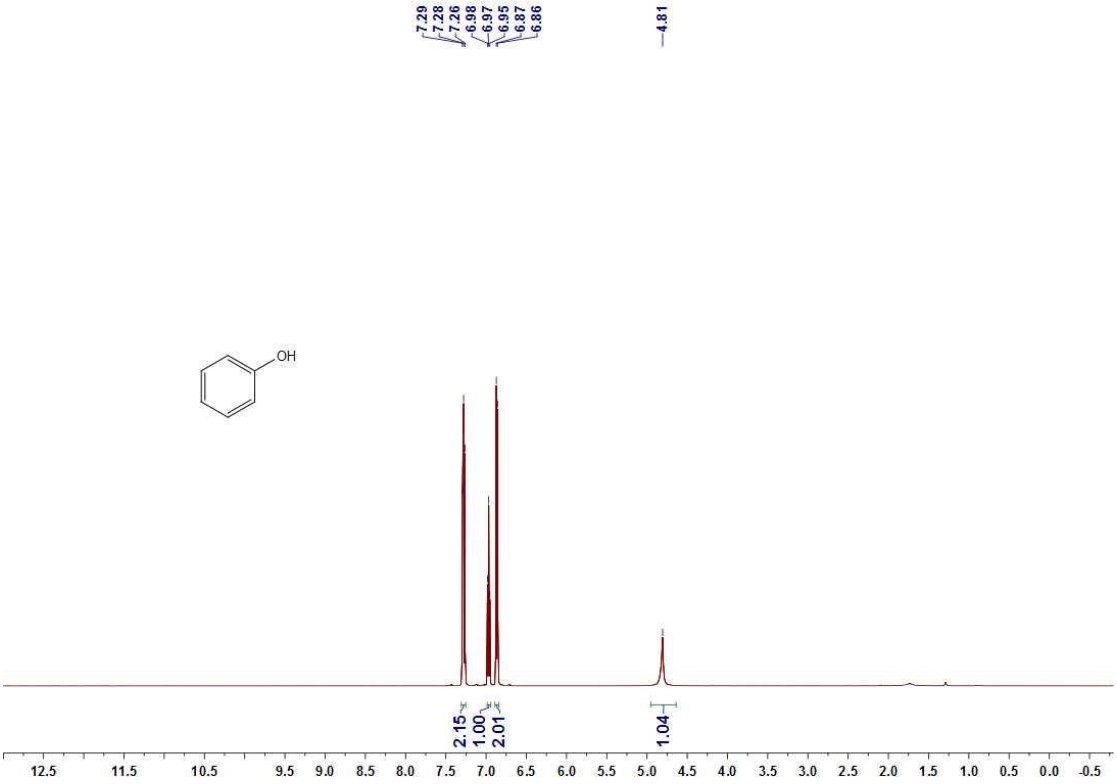

Figure S70. ^{13}C NMR spectrum of compound **phenol (4a),** related to **Table 4.**

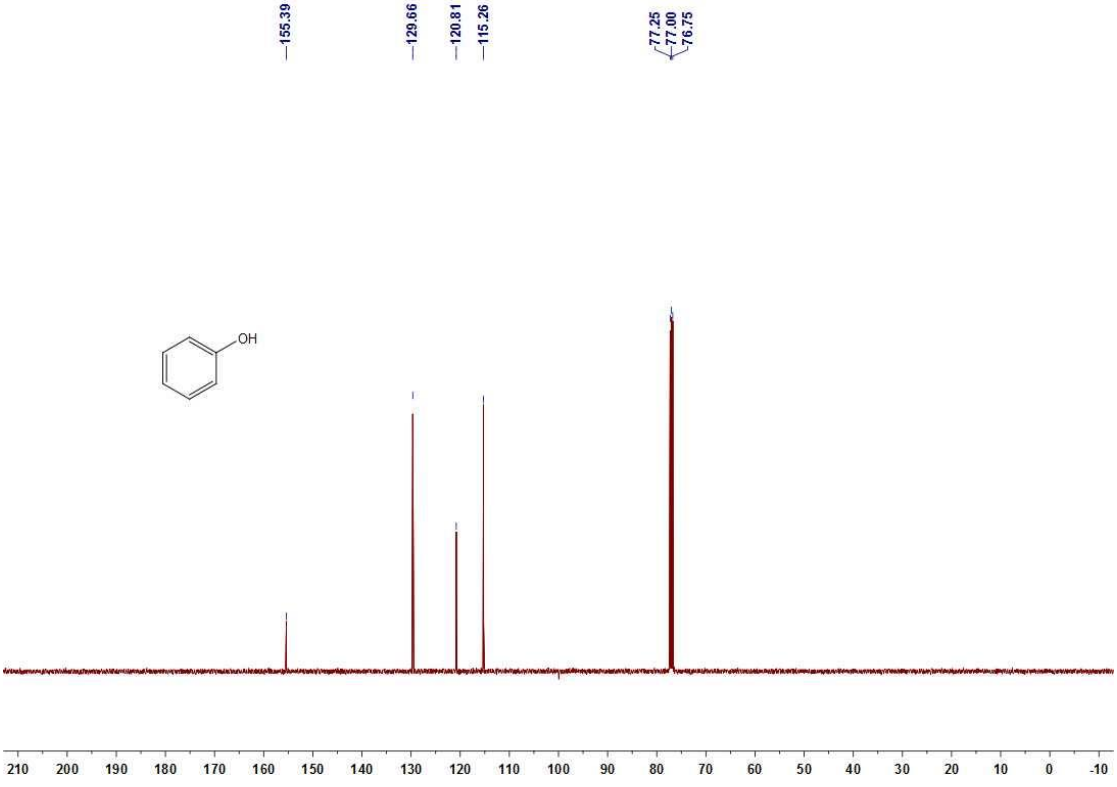

Figure S71. ^{1}H NMR spectrum of compound **4-methoxyphenol (4b),** related to **Table 4.**

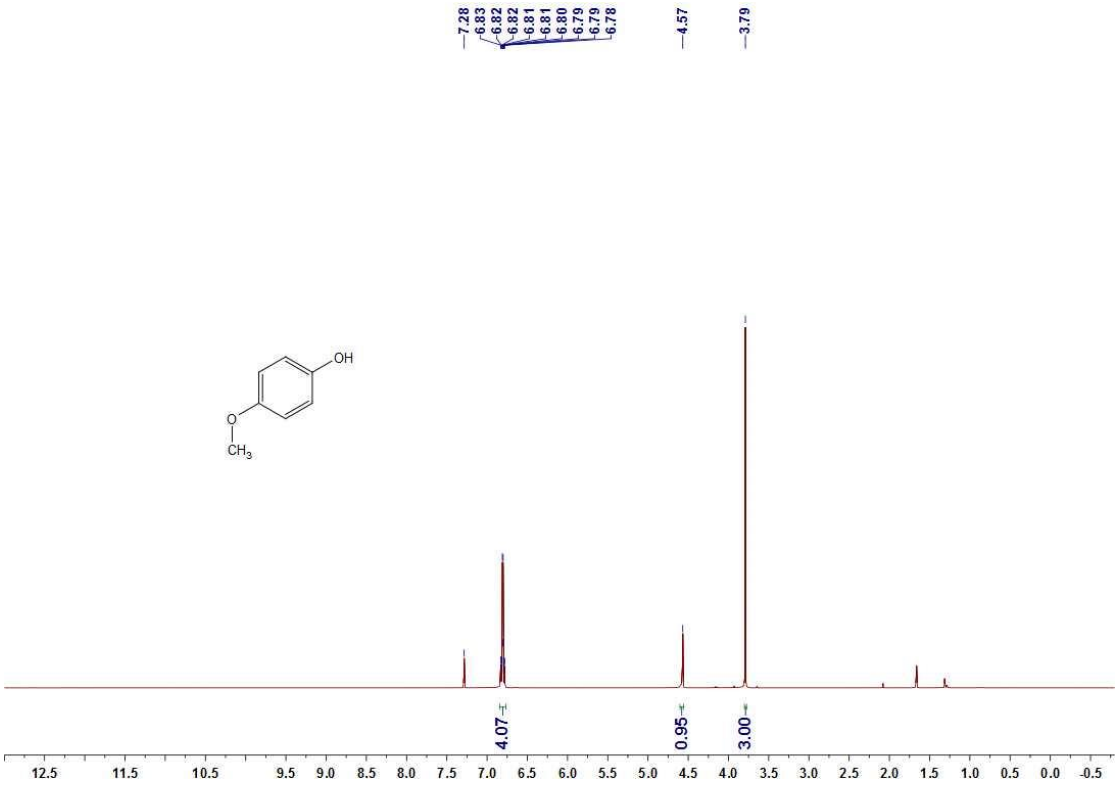

Figure S72. ^{13}C NMR spectrum of compound **4-methoxyphenol (4b),** related to **Table 4.**

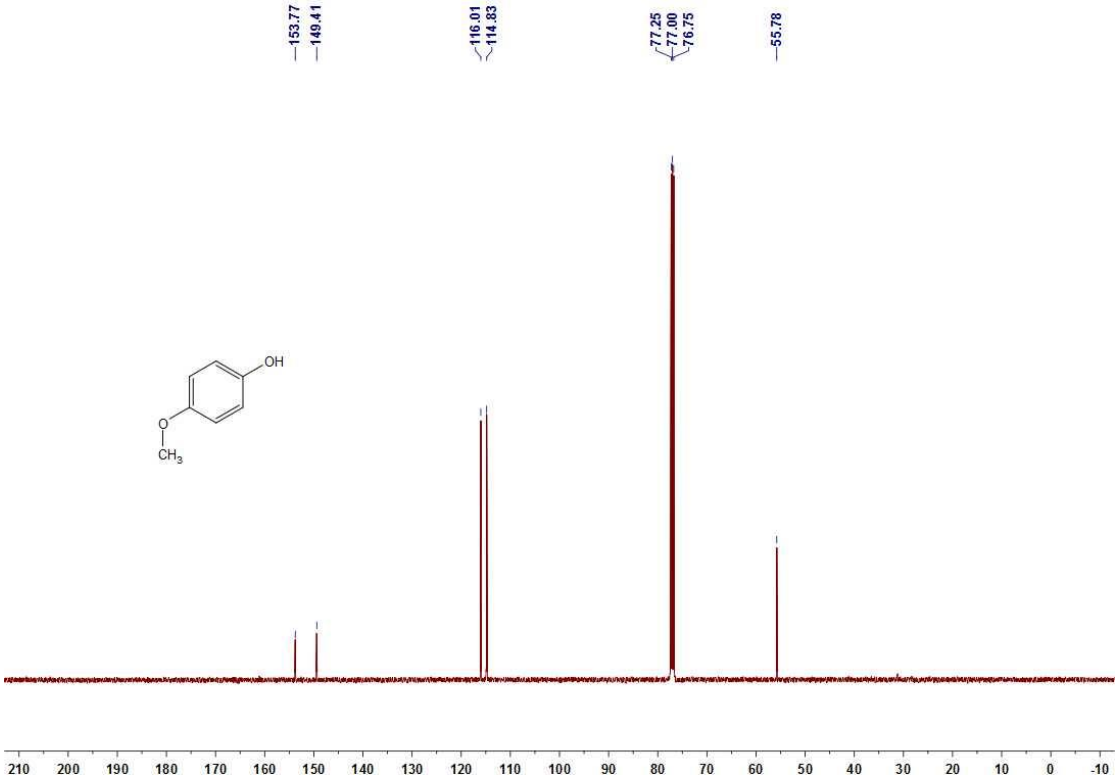

Figure S73. UV reactor, related to **Table 1-5** and **Scheme 1-3**.

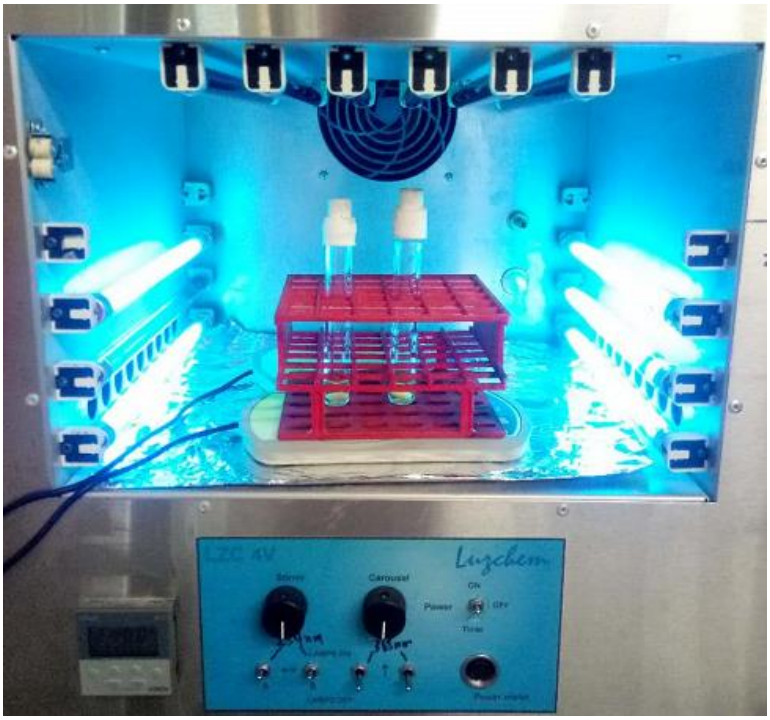

Transparent methods:

(1) General methods

All reagents and solvents were purchased from commercial sources (Alfa, Acros, Aldrich, TCI and Combi-Blocks) and used without further purification unless otherwise stated. ^{1}H, ^{19}F and ^{13}C NMR spectra were taken on Bruker 400 or 500 MHz spectrometer. Chemical shifts of ^{1}H NMR spectra were reported using either residual solvent signal of $CDCl_3$ (δ = 7.26 ppm) or TMS (δ = 0.00 ppm) as internal standard. Chemical shifts of ^{13}C NMR spectra were reported using residual solvent signal of $CDCl_3$ (δ = 77.16 ppm) as internal standard. The peak patterns are indicated as follows: s, singlet; d, doublet; dd, doublet of doublet; t, triplet; q, quartet; m, multiplet. The coupling constants, J, are reported in Hertz (Hz). All reactions were monitored by thin-layer chromatography (TLC). Column chromatography was performed on silica gel (200-300 mesh) and visualized with ultraviolet light. Hydrazine hydrate-d6 was purchased from Toronto Research Chemicals. EI-MS was obtained from the Agilent GC-MS system. All solvents were purified and dried by standard techniques.

(2) General experimental procedure and spectroscopic data of products

In 15 mL quartz tube was charged with a magnetic stir-bar, were added sequentially alcohol (0.1 mmol, 1 equiv), $N_2H_4•H_2O$ (0.4 mmol, 4 equiv) and DMSO (1 mL) under air. Then the tube was placed in a UV reactor (**Figure S73**) (Qiu et al., 2019) at room temperature and the mixture was stirred for 24 or 36 h. 10 mL water was added to quench reaction, and the mixture was extracted with EtOAc (5 mL × 4). The combined organic solvent was washed with brine, dried with anhydrous Na_2SO_4, and then concentrated under reduced pressure. The residues were purified by preparative TLC on silica gel eluting with hexane: EtOAc (300:1-20:1) to afford the product. Due to the volatility of most deoxygenated alkanes (**3a**,**3t**,**3w**), 1,3,5-trimethoxybenzene (16.8 mg, 0.1 mmol) was directly added into the reaction mixture as an internal standard upon completion of the reaction. A small amount of reaction mixture (roughly 20 μL) was filtered through a short plug made of neutral Al_2O_3 and anhydrous Na_2SO_4, flushed by $CDCl_3$ (0.7 mL), analyzed by GC-MS, and subjected to ^{1}H NMR for yield determination. (**Note**: Considering safety issues, the reaction can also be conducted as following: a short 1 mm diameter syringe needle pierced through the rubber cap of the reaction tube to keep the reaction mixture in contact with the atmosphere and prevent the rapid evaporation of the volatile compounds simultaneously. Thus, the reaction could proceed smoothly without safety problems).

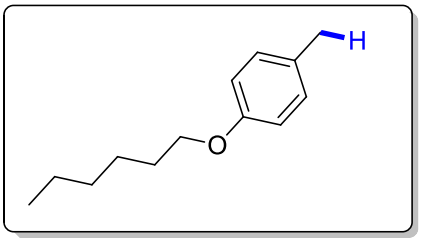

1-(Hexyloxy)-4-methylbenzene (3b) (CAS: 57792-40-2) (Sutter et al., 2013)

Yield: 86% (16.5 mg) using hydrazine as reducing reagent;

Yield: 83% (16.0 mg) using dimethyl sulfide as reducing reagent.

^{1}H NMR ($CDCl_3$, 500 MHz) δ: 7.10 (d, J = 8.2 Hz, 2H), 6.82 (d, J = 8.6 Hz, 2H), 3.95 (t, J = 6.6 Hz, 2H), 2.31 (s, 3H), 1.79 (dd, J = 8.2, 7.0 Hz, 2H), 1.48 (dd, J = 10.0, 4.9 Hz, 2H), 1.38 – 1.35 (m, 4H), 0.93 (dd, J = 9.2, 4.8 Hz, 3H).

^{13}C NMR ($CDCl_3$, 126 MHz) δ: 157.0, 129.8, 129.6, 114.3, 68.1, 31.6, 29.3, 25.7, 22.6, 20.4, 14.0.

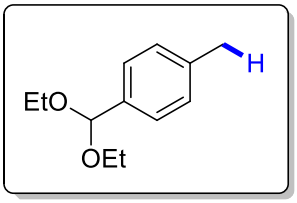

1-(Diethoxymethyl)-4-methylbenzene (3c) (CAS: 2403-59-0) (Ugarte et al., 2017)

Yield: 92% (17.9 mg) using hydrazine as reducing reagent;

Yield: 85% (16.5 mg) using dimethyl sulfide as reducing reagent.

^{1}H NMR ($CDCl_3$, 500 MHz) δ: 7.41 (d, J = 8.0 Hz, 2H), 7.21 (d, J = 7.9 Hz, 2H), 5.52 (s, 1H), 3.66 (dq, J = 9.4, 7.1 Hz, 2H), 3.60 – 3.53 (m, 2H), 2.39 (s, 3H), 1.28 (t, J = 7.1 Hz, 6H).

^{13}C NMR ($CDCl_3$, 126 MHz) δ: 137.9, 136.1, 128.8, 126.5, 101.5, 60.8, 21.1, 15.1.

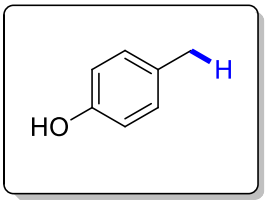

***p*-Cresol (3d) (CAS: 106-44-5)** (Wang et al., 2013)

Yield: 40% (4.3 mg).

^{1}H NMR ($CDCl_3$, 500 MHz) δ: 7.07 (d, J = 7.9 Hz, 2H), 6.77 (d, J = 8.4 Hz, 2H), 4.92 (s, 1H), 2.31 (s, 3H);

^{13}C NMR ($CDCl_3$, 126 MHz) δ: 153.1, 130.1, 130.0, 115.1, 20.4.

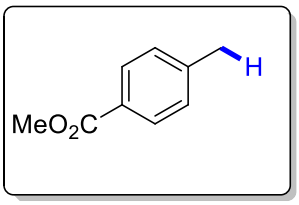

Methyl 4-methylbenzoate (3e) (CAS: 99-75-2) (Diéguez et al., 2010)

Yield: 45% (6.8 mg).

^{1}H NMR ($CDCl_3$, 500 MHz) δ: 7.94 (d, J = 8.2 Hz, 2H), 7.23 (dd, J = 7.9, 0.4 Hz, 2H), 3.90 (s, 3H), 2.39 (s, 3H).

^{13}C NMR ($CDCl_3$, 126 MHz) δ: 167.0, 143.4, 129.4, 128.9, 127.3, 51.7, 21.4.

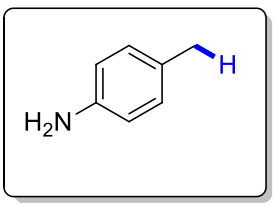

***p*-Toluidine (3f) (CAS: 106-49-0)** (Yan et al., 2020)

Yield: 55% (5.9 mg).

^{1}H NMR ($CDCl_3$, 500 MHz) δ: 7.00 (d, J = 8.0 Hz, 2H), 6.64 (d, J = 8.3 Hz, 2H), 3.55 (s, 2H), 2.28 (s, 3H).

^{13}C NMR ($CDCl_3$, 126 MHz) δ: 143.8, 129.7, 127.7, 115.2, 20.4.

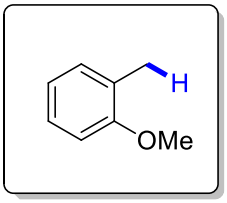

1-Methoxy-2-methylbenzene (3g) (CAS: 578-58-5) (Huang et al., 2013)

Yield: 68% (8.3 mg).

^{1}H NMR ($CDCl_3$, 500 MHz) δ: 7.23 – 7.16 (m, 2H), 6.90 (ddd, J = 13.7, 10.1, 4.5 Hz, 2H), 3.87 (s, 3H), 2.27 (s, 3H).

^{13}C NMR ($CDCl_3$, 126 MHz) δ: 157.7, 130.6, 126.8, 126.6, 120.2, 109.9, 55.2, 16.2.

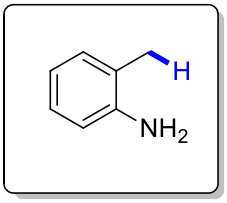

***o*-Toluidine (3h) (CAS: 95-53-4)** (Yan et al., 2020)

Yield: 92% (9.9 mg).

^{1}H NMR ($CDCl_3$, 500 MHz) δ: 7.13 (t, J = 7.7 Hz, 2H), 6.80 (t, J = 7.4 Hz, 1H), 6.75 (d, J = 7.7 Hz, 1H), 3.64 (s, 2H), 2.25 (s, 3H).

^{13}C NMR ($CDCl_3$, 126 MHz) δ: 144.5, 130.3, 126.8, 122.2, 118.5, 114.8, 17.2.

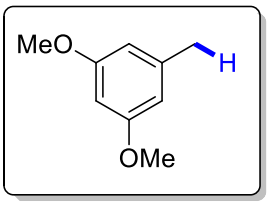

1,3-Dimethoxy-5-methylbenzene (3i) (CAS: 4179-19-5) (Xi et al., 2018)

Yield: 70% (10.7 mg).

^{1}H NMR ($CDCl_3$, 500 MHz) δ: 6.36 (s, 2H), 6.31 (s, 1H), 3.80 (s, 6H), 2.33 (s, 3H).

^{13}C NMR ($CDCl_3$, 126 MHz) δ: 160.7, 140.2, 107.1, 97.5, 55.2, 21.8.

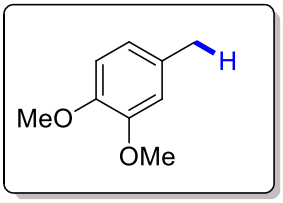

1,2-Dimethoxy-4-methylbenzene (3j) (CAS: 494-99-5) (Huang et al., 2013)

Yield: 72% (11.0 mg) using (3,4-dimethoxyphenyl)methanol as substrate;

Yield: 30% (4.6 mg) using 2-(3,4-dimethoxyphenyl)-1-(4-methoxyphenyl)propane-1,3-diol as substrate.

^{1}H NMR ($CDCl_3$, 500 MHz) δ: 6.79 (d, J = 8.5 Hz, 1H), 6.75 – 6.71 (m, 2H), 3.88 (s, 3H), 3.87 (s, 3H), 2.33 (s, 3H).

^{13}C NMR ($CDCl_3$, 126 MHz) δ: 148.6, 146.8, 130.3, 120.7, 112.3, 111.2, 55.8, 55.6, 20.9.

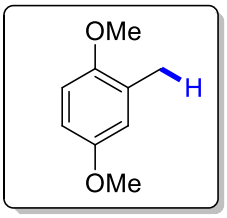

1,4-Dimethoxy-2-methylbenzene (3k) (CAS: 24599-58-4) (Jiang et al., 2014)

Yield: 92% (14.0 mg).

^{1}H NMR ($CDCl_3$, 500 MHz) δ: 6.77 (t, J = 5.9 Hz, 2H), 6.71 (dd, J = 8.7, 3.0 Hz, 1H), 3.81 (s, 3H), 3.79 (s, 3H), 2.24 (s, 3H).

^{13}C NMR ($CDCl_3$, 126 MHz) δ: 153.3, 152.0, 127.8, 117.0, 110. 9, 110.7, 55.9, 55.7, 16.4.

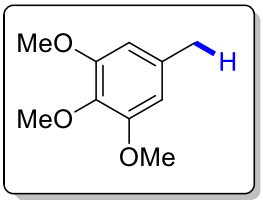

1,2,3-Trimethoxy-5-methylbenzene (3l) (CAS: 6443-69-2) (Diéguez et al., 2010)

Yield: 89% (16.2 mg) using hydrazine as reducing reagent;

Yield: 81% (14.8 mg) using dimethyl sulfide as reducing reagent.

^{1}H NMR ($CDCl_3$, 500 MHz) δ: 6.42 (s, 2H), 3.87 (s, 6H), 3.84 (s, 3H), 2.34 (s, 3H).

^{13}C NMR ($CDCl_3$, 126 MHz) δ: 153.0, 135.8, 133.6, 105.9, 60.9, 56.0, 21.8.

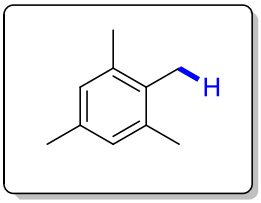

1,2,3,5-Tetramethylbenzene (3m) (CAS: 527-53-7) (Ding et al., 2019)

Yield: 62% (8.3 mg).

^{1}H NMR ($CDCl_3$, 500 MHz) δ: 6.86 (s, 2H), 2.28 (s, 9H), 2.16 (s, 3H).

^{13}C NMR ($CDCl_3$, 126 MHz) δ: 136.2, 134.5, 131.8, 128.3, 20.8, 20.4, 14.9.

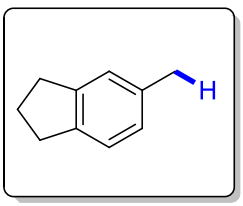

5-Methyl-2,3-dihydro-1*H*-indene (3n) (CAS: 874-35-1) (Adamczyk et al., 1984)

Yield: 86% (11.4 mg).

^{1}H NMR ($CDCl_3$, 500 MHz) δ: 7.15 (d, J = 7.5 Hz, 1H), 7.09 (s, 1H), 6.98 (d, J = 7.5 Hz, 1H), 2.90 (t, J = 7.3 Hz, 4H), 2.35 (s, 3H), 2.11 – 2.07 (m, 2H).

^{13}C NMR ($CDCl_3$, 126 MHz) δ: 144.3, 141.1, 135.5, 126.7, 125.1, 124.0, 32.8, 32.4, 25.6, 21.2.

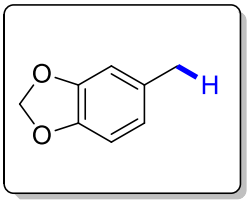

5-Methylbenzo[*d*][1,3]dioxole (3o) (CAS: 7145-99-5) (Huang et al., 2013)

Yield: 91% (12.4 mg) using hydrazine as reducing reagent;

Yield: 84% (11.4 mg) using dimethyl sulfide as reducing reagent.

^{1}H NMR ($CDCl_3$, 500 MHz) δ: 6.73 (d, J = 7.9 Hz, 1H), 6.69 (s, 1H), 6.64 (d, J = 7.9 Hz, 1H), 5.93 (s, 2H), 2.30 (s, 3H).

^{13}C NMR ($CDCl_3$, 126 MHz) δ: 147.4, 145.2, 131.5, 121.5, 109.6, 108.0, 100.7, 21.2.

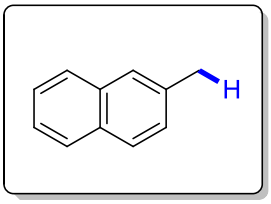

2-Methylnaphthalene (3p) (CAS: 91-57-6) (Zhu et al., 2018)

Yield: 82% (11.7 mg).

^{1}H NMR ($CDCl_3$, 500 MHz) δ: 7.82 (d, J = 7.8 Hz, 1H), 7.78 (dd, J = 8.0, 4.8 Hz, 2H), 7.64 (s, 1H), 7.45 (dtd, J = 14.6, 6.9, 1.3 Hz, 2H), 7.34 (dd, J = 8.4, 1.6 Hz, 1H), 2.54 (s, 3H).

^{13}C NMR ($CDCl_3$, 126 MHz) δ: 135.4, 133.6, 131.7, 128.1, 127.7, 127.6, 127.2, 126.8, 125.8, 124.9, 21.7.

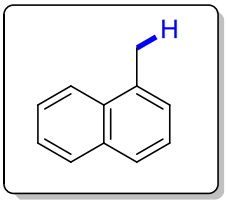

1-Methylnaphthalene (3q) (CAS: 90-12-0) (Zhu et al., 2018)

Yield: 61% (8.7 mg).

^{1}H NMR ($CDCl_3$, 500 MHz) δ: 8.09 – 8.04 (m, 1H), 7.91 (dd, J = 8.3, 1.0 Hz, 1H), 7.78 (d, J = 8.1 Hz, 1H), 7.57 (dddd, J = 18.1, 8.0, 6.8, 1.4 Hz, 2H), 7.47 – 7.41 (m, 1H), 7.39 (d, J = 6.9 Hz, 1H), 2.77 (s, 3H).

^{13}C NMR ($CDCl_3$, 126 MHz) δ: 134.2, 133.5, 132.6, 128.5, 126.5, 126.3, 125.7, 125.5 (2C), 124.1, 19.6.

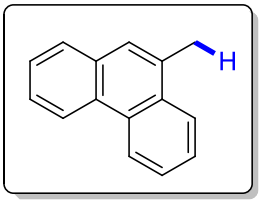

9-Methylphenanthrene (3r) (CAS: 883-20-5) (Zhu et al., 2018)

Yield: 60% (11.5 mg).

^{1}H NMR ($CDCl_3$, 500 MHz) δ: 8.78 – 8.75 (m, 1H), 8.69 (d, J = 8.0 Hz, 1H), 8.10 (dd, J = 7.0, 2.4 Hz, 1H), 7.87 – 7.82 (m, 1H), 7.72 – 7.66 (m, 2H), 7.66 – 7.59 (m, 3H), 2.78 (s, 3H).

^{13}C NMR ($CDCl_3$, 126 MHz) δ: 132.5, 132.1, 132.0, 130.4, 129.7, 127.8, 126.7, 126.6, 126.5, 126.2, 125.8, 124.7, 123.0, 122.4, 20.0.

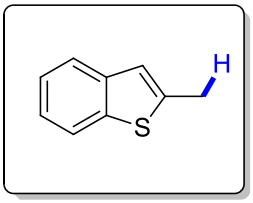

2-Methylbenzo[*b*]thiophene (3s) (CAS: 1195-14-8) (Urban et al., 2012)

Yield: 95% (14.1 mg) using hydrazine as reducing reagent;

Yield: 88% (13.0 mg) using dimethyl sulfide as reducing reagent.

^{1}H NMR ($CDCl_3$, 500 MHz) δ: 7.77 (d, J = 8.0 Hz, 1H), 7.67 (d, J = 7.8 Hz, 1H), 7.32 (td, J = 7.6, 1.1 Hz, 1H), 7.29 – 7.25 (m, 1H), 7.00 (s, 1H), 2.62 (s, 3H).

^{13}C NMR ($CDCl_3$, 126 MHz) δ: 140.8, 140.4, 139.7, 124.0, 123.3, 122.5, 122.0, 121.6, 16.1.

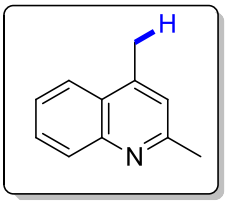

2,4-Dimethylquinoline (3u) (CAS: 1198-37-4) (Jin et al., 2015)

Yield: 96% (15.1 mg) using hydrazine as reducing reagent;

Yield: 76% (11.9 mg) using dimethyl sulfide as reducing reagent.

^{1}H NMR ($CDCl_3$, 500 MHz) δ: 8.04 (d, J = 8.4 Hz, 1H), 7.97 (d, J = 8.3 Hz, 1H), 7.71 – 7.67 (m, 1H), 7.54 – 7.50 (m, 1H), 7.16 (s, 1H), 2.72 (s, 3H), 2.69 (s, 3H).

^{13}C NMR ($CDCl_3$, 126 MHz) δ: 158.6, 147.7, 144.1, 129.1, 129.1, 126.5, 125.4, 123.6, 122.7, 25.2, 18.6.

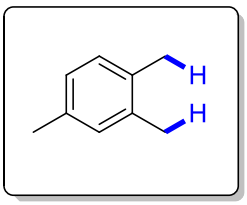

1,2,4-Trimethylbenzene (3v) (CAS: 95-63-6) (Dalling et al., 1977)

Yield: 62% (7.5 mg).

^{1}H NMR ($CDCl_3$, 500 MHz) δ: 7.07 (d, J = 7.6 Hz, 1H), 7.01 (s, 1H), 6.96 (d, J = 7.6 Hz, 1H), 2.34 (s, 3H), 2.28 (d, J = 3.9 Hz, 6H).

^{13}C NMR ($CDCl_3$, 126 MHz) δ: 136.3, 135.1, 133.3, 130.4, 129.5, 126.3, 20.9, 19.7, 19.2.

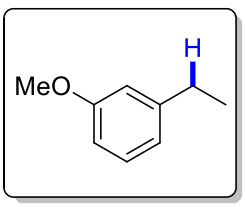

1-Ethyl-3-methoxybenzene (3aa) (CAS: 10568-38-4) (Tietze et al., 2009)

Yield: 62% (8.4 mg).

^{1}H NMR ($CDCl_3$, 500 MHz) δ: 7.23 (t, J = 7.8 Hz, 1H), 6.82 (d, J = 7.5 Hz, 1H), 6.79 – 6.74 (m, 2H), 3.83 (s, 3H), 2.66 (q, J = 7.6 Hz, 2H), 1.26 (t, J = 7.6 Hz, 3H).

^{13}C NMR ($CDCl_3$, 126 MHz) δ: 159.6, 145.9, 129.2, 120.3, 113.7, 110.8, 55.1, 28.9, 15.5.

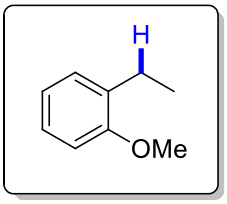

1-Ethyl-2-methoxybenzene (3ab) (CAS: 14804-32-1) (Wang et al., 2013)

Yield: 36% (4.9 mg).

^{1}H NMR ($CDCl_3$, 500 MHz) δ: 7.22 – 7.16 (m, 2H), 6.93 (td, J = 7.4, 0.8 Hz, 1H), 6.87 (d, J = 8.1 Hz, 1H), 3.86 (s, 3H), 2.67 (d, J = 7.5 Hz, 2H), 1.22 (t, J = 7.5 Hz, 3H).

^{13}C NMR ($CDCl_3$, 126 MHz) δ: 157.3, 132.6, 128.9, 126.7, 120.4, 110.1, 55.2, 23.2, 14.1.

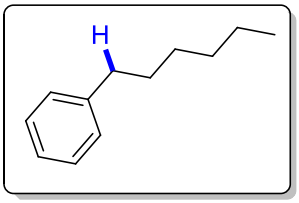

Hexylbenzene (3ac) (CAS: 1077-16-3) (Hu et al., 2019)

Yield: 93% (15.1 mg) using hydrazine as reducing reagent;

Yield: 81% (13.1 mg) using dimethyl sulfide as reducing reagent.

^{1}H NMR ($CDCl_3$, 500 MHz) δ: 7.33 – 7.28 (m, 2H), 7.21 – 7.18 (m, 3H), 2.63 (d, J = 10.2, 2H), 1.67 – 1.60 (m, 2H), 1.38 – 1.29 (m, 6H), 0.91 (t, J = 6.8 Hz, 3H).

^{13}C NMR ($CDCl_3$, 126 MHz) δ: 142.9, 128.4, 128.2, 125.5, 36.0, 31.7, 31.5, 29.0, 22.6, 14.1.

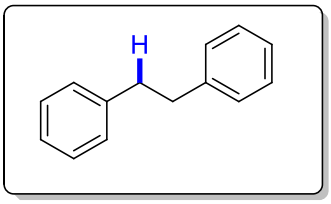

1,2-Diphenylethane (3ad) (CAS: 103-29-7) (Hu et al., 2019)

Yield: 96% (17.5 mg).

^{1}H NMR ($CDCl_3$, 500 MHz) δ: 7.33 (t, J = 7.5 Hz, 4H), 7.24 (t, J = 7.2 Hz, 6H), 2.97 (s, 4H).

^{13}C NMR ($CDCl_3$, 126 MHz) δ: 141.8, 128.4, 128.3, 125.9, 37.9.

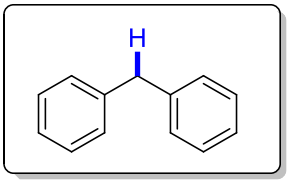

Diphenylmethane (3ae) (CAS: 101-81-5) (Wang et al., 2013)

Yield: 52% (8.7 mg) using diphenylmethanol as substrate;

Yield: 48% (8.1 mg) using (4-bromophenyl)(phenyl)methanol as substrate;

Yield: 160% (26.9 mg) using 1,1,2,2-tetraphenylethane-1,2-diol as substrate.

^{1}H NMR ($CDCl_3$, 500 MHz) δ: 7.35 – 7.30 (m, 4H), 7.24 (t, J = 6.7 Hz, 6H), 4.03 (s, 2H).

^{13}C NMR ($CDCl_3$, 126 MHz) δ: 141.1, 128.9, 128.4, 126.0, 41.9.

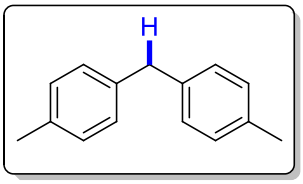

Di-*p*-tolylmethane (3af) (CAS: 4957-14-6) (Wang et al., 2013)

Yield: 95% (18.6 mg) using hydrazine as reducing reagent;

Yield: 83% (16.3 mg) using dimethyl sulfide as reducing reagent.

^{1}H NMR ($CDCl_3$, 500 MHz) δ: 7.15 – 7.09 (m, 8H), 3.95 (s, 2H), 2.36 (s, 6H).

^{13}C NMR ($CDCl_3$, 126 MHz) δ: 138.3, 135.4, 129.1, 128.7, 41.1, 21.0.

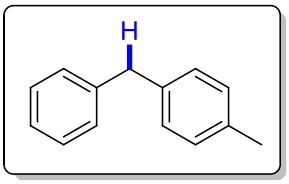

1-Benzyl-4-methylbenzene (3ag) (CAS: 620-83-7) (Guan et al., 2014)

Yield: 90% (16.4 mg).

^{1}H NMR ($CDCl_3$, 500 MHz) δ: 7.27 (d, J = 7.6 Hz, 2H), 7.18 (d, J = 7.5 Hz, 3H), 7.09 (s, 4H), 3.95 (s, 2H), 2.32 (s, 3H).

^{13}C NMR ($CDCl_3$, 126 MHz) δ: 141.4, 138.0, 135.5, 129.1, 128.8, 128.8, 128.4, 126.0, 41.5, 21.0.

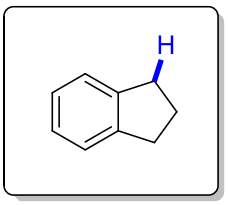

2,3-Dihydro-1*H*-indene (3ah) (CAS: 496-11-7) (Huang et al., 2013)

Yield: 57% (6.7 mg).

^{1}H NMR ($CDCl_3$, 500 MHz) δ: 7.30 – 7.26 (m, 2H), 7.18 (dd, J = 5.5, 3.2 Hz, 2H), 2.96 (t, J = 7.4 Hz, 4H), 2.15 – 2.08 (m, 2H).

^{13}C NMR ($CDCl_3$, 126 MHz) δ: 144.1, 125.9, 124.3, 32.9, 25.3.

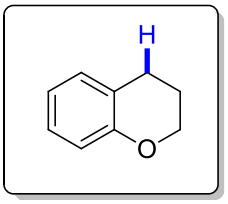

Chroman (3ai) (CAS: 493-08-3) (Meng et al., 2019)

Yield: 89% (11.9 mg) using hydrazine as reducing reagent;

Yield: 80% (10.7 mg) using dimethyl sulfide as reducing reagent.

^{1}H NMR ($CDCl_3$, 500 MHz) δ: 7.19 – 7.13 (m, 1H), 7.11 (d, J = 7.5 Hz, 1H), 6.90 (ddd, J = 12.4, 9.4, 4.6 Hz, 2H), 4.30 – 4.21 (m, 2H), 2.86 (t, J = 6.5 Hz, 2H), 2.11 – 2.02 (m, 2H).
^{13}C NMR ($CDCl_3$, 126 MHz) δ: 154.8, 129.7, 127.1, 122.1, 120.0, 116.6, 66.3, 24.8, 22.3.

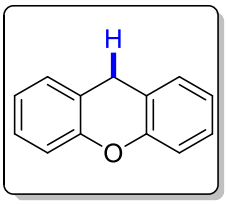

9*H*-xanthene (3aj) (CAS: 92-83-1) (Sousa et al., 2016)
Yield: 62% (11.3 mg).
^{1}H NMR ($CDCl_3$, 500 MHz) δ: 7.22 (dd, J = 16.5, 7.8 Hz, 4H), 7.07 (dd, J = 15.7, 7.9 Hz, 4H), 4.09 (s, 2H).
^{13}C NMR ($CDCl_3$, 126 MHz) δ: 151.9, 128.9, 127.6, 122.9, 120.6, 116.4, 27.9.

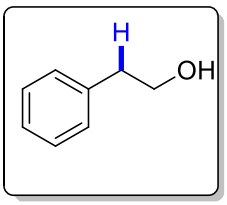

2-Phenylethanol (3ak) (CAS: 60-12-8) (Behera et al., 2020)
Yield: 76% (9.3 mg).
^{1}H NMR ($CDCl_3$, 500 MHz) δ: 7.37 – 7.32 (m, 2H), 7.27 (t, J = 6.3 Hz, 3H), 3.89 (t, J = 6.6 Hz, 2H), 2.90 (t, J = 6.6 Hz, 2H), 1.60 (s, 1H).
^{13}C NMR ($CDCl_3$, 126 MHz) δ: 138.4, 129.0, 128.6, 126.5, 63.7, 39.2.

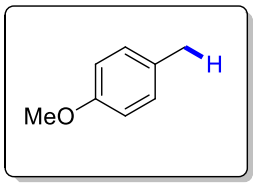

1-Methoxy-4-methylbenzene (3al) (CAS: 104-93-8) (Huang et al., 2013)
Yield: 126% (15.4 mg) using 1,2-bis(4-methoxyphenyl)ethane-1,2-diol as substrate.
Yield: 86% (10.5 mg) using (1R,2R)-1,2-bis(4-methoxyphenyl)propane-1,3-diol as substrate;
Yield: 45% (5.5 mg) using (1R,2R)-2-(3,4-dimethoxyphenyl)-1-(4-methoxyphenyl)propane-1,3-diol as substrate;
Yield: 32% (3.9 mg) using 2-(4-methoxyphenoxy)-1-(4-methoxyphenyl)propane-1,3-diol as substrate.
^{1}H NMR ($CDCl_3$, 500 MHz) δ: 7.15 (dd, J = 8.0, 0.5 Hz, 2H), 6.87 (dd, J = 8.0, 0.5 Hz, 2H), 3.84 (s, 3H), 2.36 (s, 3H).
^{13}C NMR ($CDCl_3$, 126 MHz) δ: 157.4, 129.8, 129.8, 113.7, 55.2, 20.4.

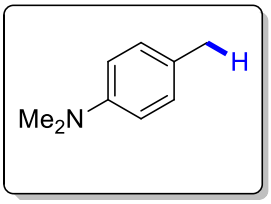

***N,N*,4-Trimethylaniline (3am) (CAS: 99-97-8)** (Yang et al., 2018)

Yield: 122% (16.5 mg).

^{1}H NMR ($CDCl_3$, 500 MHz) δ: 7.12 (d, J = 8.1 Hz, 2H), 6.76 (d, J = 8.4 Hz, 2H), 2.96 (d, J = 0.7 Hz, 6H), 2.33 (s, 3H).

^{13}C NMR ($CDCl_3$, 126 MHz) δ: 148.8, 129.5, 126.0, 113.2, 41.0, 20.2.

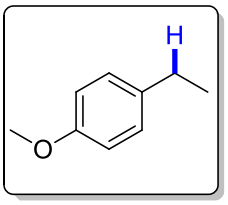

1-Ethyl-4-methoxybenzene (3an) (CAS: 1515-95-3) (Huang et al., 2013)

Yield: 43% (5.9 mg).

^{1}H NMR ($CDCl_3$, 500 MHz) δ: 7.15 (d, J = 8.7 Hz, 2H), 6.86 (d, J = 8.6 Hz, 2H), 3.82 (s, 3H), 2.62 (q, J = 7.6 Hz, 2H), 1.24 (t, J = 7.6 Hz, 3H).

^{13}C NMR ($CDCl_3$, 126 MHz) δ: 157.6, 136.4, 128.7, 113.7, 55.3, 28.0, 15.9.

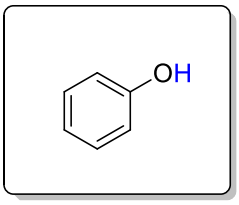

Phenol (4a) (CAS: 108-95-2) (Sun et al., 2019)

Yield: 46% (4.3 mg) using 2-phenoxy-1-phenylethanol as substrate;

Yield: 47% (4.4 mg) using 1-(4-methoxyphenyl)-2-phenoxyethanol as substrate.

^{1}H NMR ($CDCl_3$, 500 MHz) δ: 7.31 – 7.25 (m, 2H), 6.97 (t, J = 7.4 Hz, 1H), 6.87 (d, J = 7.6 Hz, 2H), 4.81 (s, 1H).

^{13}C NMR ($CDCl_3$, 126 MHz) δ: 155.4, 129.7, 120.8, 115.3.

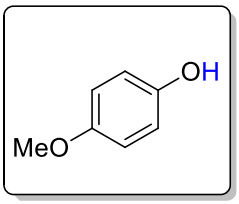

4-Methoxyphenol (4b) (CAS: 150-76-5) (Sun et al., 2019)

Yield: 44% (5.5 mg).

^{1}H NMR ($CDCl_3$, 500 MHz) δ: 6.84 – 6.77 (m, 4H), 4.57 (s, 1H), 3.79 (s, 3H).

^{13}C NMR ($CDCl_3$, 126 MHz) δ: 153.8, 149.4, 116.0, 114.8, 55.8.

References

Qiu, Z.; Pham, H. D. M.; Li, J.; Li, C.-C.; Castillo-Pazos, D. J.; Khaliullin, R. Z.; Li, C.-J. (2019). Light-enabled metal-free pinacol coupling by hydrazine. Chem. Sci. *10*, 10937-10943.

Sutter, M.; Lafon, R.; Raoul, Y.; Métay, E.; Lemaire, M. (2013). Heterogeneous Palladium-Catalyzed Synthesis of Aromatic Ethers by Solvent-Free Dehydrogenative Aromatization: Mechanism, Scope, and Limitations Under Aerobic and Non-Aerobic Conditions. Eur. J. Org. Chem. *2013*, 5902-5916.

Ugarte, R. A.; Hudnall, T. W. (2017). Antimony(v) catalyzed acetalisation of aldehydes: an efficient, solvent-free, and recyclable process. Green Chem. *19*, 1990-1998.

Wang, H.; Li, L.; Bai, X.-F.; Shang, J.-Y.; Yang, K.-F.; Xu, L.-W. (2013). Efficient Palladium-Catalyzed C–O Hydrogenolysis of Benzylic Alcohols and Aromatic Ketones with Polymethylhydrosiloxane. Adv. Synth. Catal. *355*, 341-347.

Diéguez, H. R.; López, A.; Domingo, V.; Arteaga, J. F.; Dobado, J. A.; Herrador, M. M.; Quílez del Moral, J. F.; Barrero, A. F. (2010). Weakening C–O Bonds: Ti(III), a New Reagent for Alcohol Deoxygenation and Carbonyl Coupling Olefination. J. Am. Chem. Soc. *132*, 254-259.

Yan, Z.; Xie, X.; Song, Q.; Ma, F.; Sui, X.; Huo, Z.; Ma, M. (2020). Tandem selective reduction of nitroarenes catalyzed by palladium nanoclusters. Green Chem. *22*, 1301-1307.

Huang, J.-L.; Dai, X.-J.; Li, C.-J. (2013). Iridium-Catalyzed Direct Dehydroxylation of Alcohols. Eur. J. Org. Chem. *2013*, 6496-6500.

Xi, X.; Chen, T.; Zhang, J.-S.; Han, L.-B. (2018). Efficient and selective hydrogenation of C–O bonds with a simple sodium formate catalyzed by nickel. Chem. Commun. *54*, 1521-1524.

Jiang, J.-A.; Chen, C.; Guo, Y.; Liao, D.-H.; Pan, X.-D.; Ji, Y.-F. (2014). A highly efficient approach to vanillin starting from 4-cresol. Green Chem. *16*, 2807-2814.

Ding, Y.; Luo, S.; Ma, L.; An, J. (2019). Reductive Cleavage of Unactivated Carbon–Cyano Bonds under Ammonia-Free Birch Conditions. J. Org. Chem. *84*, 15827-15833.

Adamczyk, M.; Watt, D. S.; Netzel, D. A. (1984). Synthesis of biological markers in fossil fuels. 2. Synthesis and carbon-13 NMR studies of substituted indans and tetralins. J. Org. Chem. *49*, 4226-4237.

Zhu, D.; Shi, L. (2018). Ni-Catalyzed cross-coupling of aryl thioethers with alkyl Grignard reagents via C–S bond cleavage. Chem. Commun. *54*, 9313-9316.

Urban, S.; Beiring, B.; Ortega, N.; Paul, D.; Glorius, F. (2012). Asymmetric Hydrogenation of Thiophenes and Benzothiophenes. J. Am. Chem. Soc. *134*, 15241-15244.

Jin, J.; MacMillan, D. W. C. (2015). Alcohols as alkylating agents in heteroarene C–H functionalization. Nature, *525*, 87-90.

Dalling, D. K.; Ladner, K. H.; Grant, D. M.; Woolfenden, W. R. (1977). Carbon-13 magnetic resonance. 27.

The dependence of chemical shifts on methyl rotational conformations and dynamics in the methylated benzenes and naphthalenes. J. Am. Chem. Soc. *99*, 7142-7150.

Tietze, L.; Vock, C.; Krimmelbein, I.; Nacke, L. (2009). Synthesis of Novel Structurally Simplified Estrogen Analogues with Electron-Donating Groups in Ring A. Synthesis, *2009*, 2040-2060.

Hu, X.; Wang, G.; Qin, C.; Xie, X.; Zhang, C.; Xu, W.; Liu, Y. (2019). Ligandless nickel-catalyzed transfer hydrogenation of alkenes and alkynes using water as the hydrogen donor. Org. Chem. Front. *6*, 2619-2623.

Guan, Z.; Li, B.; Hai, G.; Yang, X.; Li, T.; Tan, B. (2014). A highly efficient catalyst for Suzuki–Miyaura coupling reaction of benzyl chloride under mild conditions. RSC Adv. *4*, 36437-36443.

Meng, Q.-Y.; Schirmer, T. E.; Berger, A. L.; Donabauer, K.; König, B. (2019). Photocarboxylation of Benzylic C–H Bonds. J. Am. Chem. Soc. *141* (29), 11393-11397.

Sousa, S. C. A.; Fernandes, T. A.; Fernandes, A. C. (2016). Highly Efficient Deoxygenation of Aryl Ketones to Arylalkanes Catalyzed by Dioxidomolybdenum Complexes. Eur. J. Org. Chem. *2016*, 3109-3112.

Behera, R. R.; Ghosh, R.; Panda, S.; Khamari, S.; Bagh, B. (2020). Hydrosilylation of Esters Catalyzed by Bisphosphine Manganese(I) Complex: Selective Transformation of Esters to Alcohols. Org. Lett. *22*, 3642-3648.

Yang, S.; Tang, W.; Yang, Z.; Xu, J. (2018). Iridium-Catalyzed Highly Efficient and Site-Selective Deoxygenation of Alcohols. ACS Catal. *8*, 9320-9326.

Sun, N.; Wang, C.; Wang, H.; Yang, L.; Jin, P.; Zhang, W.; Jiang, J. (2019). Multifunctional Tubular Organic Cage-Supported Ultrafine Palladium Nanoparticles for Sequential Catalysis. Angew. Chem. Int. Ed. *58*, 18011-18016.